

# **The Impact of Organic Aerosol Volatility on Particle Microphysics and Global Climate**

**Yuchao Gao**

Submitted in partial fulfillment of the  
requirements for the degree of  
Doctor of Philosophy  
in the Graduate School of Arts and Sciences

**COLUMBIA UNIVERSITY**

2019





# **ABSTRACT**

## **The Impact of Organic Aerosol Volatility on Particle Microphysics and Global Climate**

**Yuchao Gao**

Atmospheric aerosols are tiny particles suspended in the atmosphere. They affect global air quality, public health and climate (Boucher et al., 2013; Myhre et al., 2013; Seinfeld and Pandis, 2016), thus playing a key role in the Earth system. However, due to the complexity of aerosol processes and climate change feedbacks, our understanding of aerosols in a changing world is still limited (Boucher et al., 2013). To understand the impact of organic aerosol volatility on particle microphysics and global climate, I developed a new aerosol microphysics scheme, MATRIX-VBS, and its evaluation and application are presented in this dissertation.

MATRIX-VBS couples the volatility-basis set (VBS, Donahue et al., 2006) framework with the aerosol microphysical scheme MATRIX (Multiconfiguration Aerosol TRacker of mIXing state, Bauer et al., 2008) that resolves aerosol mass and number concentrations, size, and mixing state. With the inclusion of organic partitioning and photochemical aging of semi-volatile organic aerosols, aerosols are able to grow via organic condensation, a process previously not available in the original model MATRIX, where organic aerosols were treated as nonvolatile. Both MATRIX and MATRIX-VBS can be used as stand-alone box models or within a global model. After the development of MATRIX-VBS in the box model framework, both model's simulations were performed and assessed on the box and global scales.

On the box model scale, idealized experiments were designed to simulate different environments, clean, polluted, urban, and rural. I investigated the evolution of organic aerosol mass concentration and volatility distribution among gas and aerosol phases, and results show that semi-volatile primary organic aerosols evaporate almost completely in the intermediate-volatility range and stay in the particle phase in the low volatility range. I also concluded that the volatility distribution of organics relies on emission, oxidation, and temperature, and the inclusion of organic aerosol volatility changes aerosol mixing state. Comparing against parallel simulations with the original model MATRIX, which treats organic aerosols as nonvolatile, I assessed the effect of gas-particle partitioning and photochemical aging of semi-volatile organics on particle growth, composition, size distribution and mixing state. Results also show that the new model produces different mixing states, increased number concentrations and decreased aerosol sizes for organic-containing aerosol populations.

Monte-Carlo type experiments were performed and they offered a more in-depth look at the impact of organic aerosol volatility on activated number concentration, which is the number concentration of aerosols that are activated but has not yet formed into a cloud droplet. By testing multiple parameters such as aerosol composition, mass concentration and number concentration, as well as particle size, I examined the impact of partitioning organic aerosols on activated aerosol number concentration. I found that the new model MATRIX-VBS produces fewer activated particles compared to the original model MATRIX, except in environments with low cloud updrafts, in clean regions at above freezing temperatures, and in polluted areas at high temperature (310K) and extremely low humidity conditions. I concluded that such change is caused by the differences in aerosol number concentration and size between the two models, which would determine how many particles could activate.

On the global scale, MATRIX-VBS was implemented in the NASA GISS ModelE Earth systems model. I assessed and evaluated the new model by comparing aerosol mass and number concentrations, activated cloud number concentration, and AOD against output from the original MATRIX model. Further, I evaluate the two models against observations of organic aerosol mass concentration from the aircraft campaign ATom (Atmospheric Tomography Mission), and aerosol optical depth from ground measurement stations from AERONET (Aerosol Robotic Network) as well as satellite retrievals from MODIS (MODerate resolution Imaging Spectroradiometer) and CALIPSO (Cloud-Aerosol Lidar and Infrared Pathfinder Satellite Observations).

Results show that organics in MATRIX-VBS experience more distant long-range transport, and their mass concentration increase aloft and decrease at the surface as compared to those in MATRIX. There are still underestimations in the vertical profiles of mass concentration in both models, especially in the high latitudes in the Northern Hemisphere and South Pacific Ocean basin, possibly due to the application of universal distribution of mass-based emission factors among different volatilities that perhaps is not realistic in all climate zones, thus affecting organic aerosol lifetime and transport. Just as the box model results, there are more particles and generally more activated ones (except for rare cases such as the highly polluted Eastern China) in MATRIX-VBS than in MATRIX. As for AOD comparisons, MATRIX-VBS have generally lower AOD than MATRIX, which can be due to smaller aerosols and different aerosol composition in the new model, which is also underestimating biomass burning in the Amazon and Congo basins. Compared to satellite retrievals from MODIS and ground measurements from AERONET, both models overestimate aerosol optical depth over anthropogenic polluted regions and biomass regions such as central Africa. Overall, both models also underestimate AOD as compared to AERONET in the winter (DJF), whereas they generally overestimate or estimate it well in other seasons.

Even though during its initial evaluation, MATRIX-VBS does not seem to have improved from MATRIX on the global scale in representing the real world, it made the first key step in improving our understanding of organic aerosols on the process level. Changes in mass, number concentration, size distribution, and mixing state (composition) have great implications and impact on climate. Further studies are needed in examining and improving factors linked to the new representation of semi-volatiles in an aerosol microphysics model, including but not limited to the treatment of mass-based emission factor distribution among different organic volatilities and the size distribution of tiny organic particles that have evaporated but not completely. Challenges in evaluations of organic aerosol against measurements remain in that remote regions of significant interest lack available measurements, and additional field campaigns will be important for us to better understand real world conditions and shed light on model performance.

# TABLE OF CONTENTS

<b>List of Figures and Tables</b> .....	iv
<b>Acknowledgments</b> .....	ix
<b>Dedication</b> .....	xiii
<b>Chapter 1: Introduction</b> .....	1
1.1. Aerosol basics.....	1
1.2. Aerosol microphysics and mixing state.....	2
1.3. Organic aerosol and its volatility.....	7
1.4. Relating organic volatility to aerosol microphysics.....	10
1.5. Applications on clouds and climate.....	13
<b>Part I: Box-Modeling</b> .....	17
<b>Chapter 2: MATRIX-VBS (v1.0): implementing an evolving organic aerosol volatility in an aerosol microphysics model</b> .....	18
Abstract.....	18
2.1. Introduction.....	19
2.2. Model description.....	22
2.2.1. MATRIX box model.....	22
2.2.2. VBS framework.....	25
2.3. Model development.....	26
2.4. Simulations.....	28
2.5. Results and discussion.....	30
2.5.1. Winter.....	30
2.5.2. Summer.....	34
2.5.3. Mixing state.....	36

2.5.4. Size distribution.....	39
2.6. Conclusion.....	44
<b>Chapter 3: Can semi-volatile organic aerosols lead to fewer cloud particles?.....</b>	<b>45</b>
Abstract.....	45
3.1. Introduction.....	46
3.2. Methods.....	48
3.2.1. Model Description.....	48
3.2.2. Simulations.....	49
3.3. Results and discussion.....	50
3.4. Conclusion.....	58
<b>Part II: Global Modeling.....</b>	<b>61</b>
<b>Chapter 4: The global impact of organic aerosol volatility on particle microphysics.....</b>	<b>62</b>
Abstract.....	62
4.1. Introduction.....	63
4.2. Model description.....	66
4.2.1. GISS ModelE.....	66
4.2.2. MATRIX-VBS.....	66
4.3. Methodology.....	67
4.4. Results and discussion.....	69
4.4.1. Organic aerosol mass .....	69
4.4.1.1 Model version comparison.....	69
4.4.1.2 Evaluation.....	72
4.4.2. Aerosol number concentration.....	79
4.4.3. Activated number concentration.....	81

4.4.4. Aerosol optical depth.....	84
4.5. Conclusions.....	95
<b>Part III: Concluding Material .....</b>	<b>98</b>
<b>Chapter 5: Synthesis and future work.....</b>	<b>99</b>
<b>Part IV: Bibliography .....</b>	<b>103</b>

# LIST OF FIGURES AND TABLES

## Chapter 1 Introduction

<b>Figure 1.1:</b> Illustrations of aerosol microphysics: formation via nucleation, growth via condensation and coagulation, and growth via both condensation and coagulation .....	3
<b>Figure 1.2:</b> Simple schematic of the coagulation process among some aerosol populations in MATRIX.....	6
<b>Figure 1.3:</b> Illustration of the volatility-basis set (VBS). .....	9
<b>Figure 1.4:</b> Simple schematic of MATRIX-VBS .....	12

## Part I: Box-Modeling

**Chapter 2:** MATRIX-VBS (v1.0): implementing an evolving organic aerosol volatility in an aerosol microphysics model

<b>Table 2.1:</b> Aerosol population chemical composition in MATRIX.....	23
<b>Table 2.2:</b> Naming convention and parameters used in the VBS implementation.....	25
<b>Table 2.3:</b> Conditions of each location used in the simulations, taken from the GISS ModelE for January and July 2006.....	29
<b>Figure 2.1:</b> Schematic showing coagulation pathways among organics-containing aerosol populations.....	24
<b>Figure 2.2:</b> Temporal evolution of the mass concentration of semi-volatile organics in the gas phase, aerosol phase and total using the new scheme for January.....	32
<b>Figure 2.3:</b> Temporal evolution of the mass concentration of semi-volatile organics in the gas phase, aerosol phase and total using the new scheme for July.....	35
<b>Figure 2.4:</b> Temporal evolution of organic aerosol mass concentration in each organics-containing population from the new scheme and the old scheme.....	37



<b>Figure 2.5:</b> Temporal evolution of organic aerosol mass concentration fraction in each organics-containing population from the new scheme and the old scheme. ....	38
<b>Figure 2.6:</b> Organics-containing aerosol populations (except MXX) and AKK (Aitken mode sulfate) size distributions for Mexico City in January .....	41
<b>Figure 2.7:</b> Organics-containing aerosol populations (except MXX) and AKK (Aitken mode sulfate) size distributions for Centreville in January .....	43
<b>Chapter 3: Can semi-volatile organic aerosols lead to fewer cloud particles?</b>	
<b>Table 3.1:</b> Hygroscopicity $\kappa$ used for each organic aerosol volatility bin.....	49
<b>Table 3.2:</b> Parameters used in the Monte-Carlo simulations.....	50
<b>Table 3.3:</b> Minimum and maximum of fractional change in average activated number concentration over the last 24 hours between the two models with low, medium and high level emissions at updraft velocities of 0.5, 1 and 2 m/s.....	53
<b>Table 3.4:</b> Minimum and maximum of average activated number concentration over the last 24 hours of MATRIX and MATRIX-VBS with low, medium and high level emissions at updraft velocities of 0.5, 1 and 2 m/s.....	54
<b>Figure 3.1:</b> Activated number concentration of aerosol populations for MATRIX and MATRIX-VBS for 290 K and 40% RH at 30°N latitude with medium emission levels and 0.5 m/s updraft velocity.....	51
<b>Figure 3.2:</b> Fractional change of average activated number concentration over the last 24 hours of a 5-day simulation between the two models with low, medium and high level emissions at updraft velocities of 0.5, 1, and 2 m/s.....	52
<b>Figure 3.3:</b> Average activated number concentration during the last 24 hours of a 5-day simulation in MATRIX and MATRIX-VBS with low, medium and high emission levels at updraft velocities of 0.5, 1, and 2 m/s. Note difference in scales per column.....	55

**Figure 3.4:** Number concentration (left column) and dry particle diameter (right column) by mode (color lines) for MATRIX (dashed lines) and MATRIX-VBS (solid lines) for the experiments with the same conditions as Figure 1.....56

## **Part II: Global Modeling**

### **Chapter 4: The global impact of organic aerosol volatility on particle microphysics and climate**

**Table 4.1:** Mean, standard deviation and correlation coefficient for seasonal mean AOD from MATRIX and MATRIX-VBS data against MODIS.....86

**Table 4.2:** Mean, standard deviation and correlation coefficient for seasonal mean AOD from MATRIX and MATRIX-VBS data against AERONET.....90

**Figure 4.4.1:** Annual mean mass load of organic aerosol in MATRIX and MATRIX-VBS.....69

**Figure 4.1.2:** Difference in annual mean organic aerosol mass loads between MATRIX- VBS and MATRIX.....70

**Figure 4.1.3:** Annual mean zonal organic aerosol mass concentration in MATRIX-VBS and MATRIX.....72

**Figure 4.1.4:** Difference in the annual mean zonal organic aerosol mass concentrations between MATRIX and MATRIX-VBS.....72

**Figure 4.1.5:** Difference in monthly mean spatial and zonal organic aerosol mass loads between MATRIX and MATRIX-VBS for August 2016.....73

**Figure 4.1.6:** Vertical profiles of organic aerosol mass concentration for MATRIX, MATRIX-VBS for August 2016 and Atom-1 measurements.....75

**Figure 4.1.7:** Difference in monthly mean spatial and zonal organic aerosol mass loads between MATRIX and MATRIX-VBS for February 2017.....76

<b>Figure 4.1.8:</b> Vertical profiles of organic aerosol mass concentration for MATRIX, MATRIX-VBS for February 2017 and Atom-1 measurements.....	78
<b>Figure 4.2.1:</b> Total surface number concentration of organic-containing populations in MATRIX and MATRIX-VBS.....	79
<b>Figure 4.2.2:</b> Difference in annual mean surface and zonal number concentrations of organic-containing aerosol populations between the two models.....	80
<b>Figure 4.2.3:</b> Annual mean surface number concentration differences in individual organic-containing aerosol populations.....	81
<b>Figure 4.3.1:</b> Annual mean total surface activated number concentration of organic-containing populations in MATRIX and MATRIX-VBS.....	82
<b>Figure 4.3.2:</b> Difference in total annual mean total surface activated number concentration for the two models.....	82
<b>Figure 4.3.3:</b> Annual mean surface activated number concentration differences in major organic-containing aerosol populations.....	83
<b>Figure 4.4.1:</b> Annual mean total aerosol optical depth in MATRIX and MATRIX-VBS.....	84
<b>Figure 4.4.2:</b> Difference in total aerosol optical depth between MATRIX and MATRIX-VBS.....	85
<b>Figure 4.4.3:</b> Difference in seasonal aerosol optical depth between MATRIX and MATRIX-VBS.....	85
<b>Figure 4.4.4:</b> Seasonal column aerosol optical depth from MODIS.....	87
<b>Figure 4.4.5:</b> Seasonal aerosol optical depth for MATRIX and MATRIX-VBS with AERONET measurements over-plotted.....	88

<b>Figure 4.4.6:</b> Seasonal difference in aerosol optical depth between the two models and AERONET measurements.....	89
<b>Figure 4.4.7:</b> Difference in total annual clear sky AOD between the two models, showing green boxes over regions studied for CALIPSO and yellow circles over AERONET stations Bonanza Creek in Alaska and Ascension Island off the coast of Central Africa.....	92
<b>Figure 4.4.8:</b> Height profile plots of aerosol extinction from CALIPSO and the two models.....	93
<b>Figure 4.4.9:</b> Timeseries of AOD from AERONET stations Ascension Island and Bonanza Creek for MATRIX, MATRIX-VBS, MODIS, CALIPSO, AERONET.....	94
<b>Figure 4.4.10:</b> Size distributions of aerosols in Ascension Island and Bonanza Creek for MATRIX and MATRIX-VBS.....	95

# ACKNOWLEDGMENTS

I lived in a university located in a rural town until I was eight. One of the most distinct memories from my kindergarten years is how much I loved lying on the grass to watch clouds change, and how excited I was every time an airplane flew by. I would immediately jump up and down, waving frantically towards the plane, and yell, “airplane, airplane, take me away!” until it was out of sight or I ran out of breath. Another memory I have is from first grade. It was raining during recess, my friends excitedly tried to catch raindrops with their heads tilted back and mouths wide open. I was the only one skeptical about the venture and warned them that the rain might not be as clean as it seemed. Everyone was too happy to care, but I was so convinced that the air was filled with dirty, tiny particles, and the rain washed them down. In a way, these two stories manifested my path onto the field of atmospheric chemistry and where I am today.

Of the 10 schools I have attended in my life, Columbia is the longest residency I have taken. It would not have been such a wonderful ride if it were not for my advisors, family, and friends. First and foremost, I want to thank Dr. Susanne Bauer and Dr. Kostas Tsigaridis. It does not escape me for a second that I am beyond lucky to have them as my advisors. Susanne, you are absolutely one of the most brilliant women I know, and you taught me how to grow gracefully as a woman scientist. You are a constant reminder that I should always think about “the big picture” - about science and about everything. I will always remember the importance of not calling my own questions “stupid questions.” Kostas, I do not know what I did to deserve all the time and patience you gave me, for that I can only say “thank you” times infinity, and it would not be enough. Intentionally or not, you also taught me the value of work-life balance, which I found deeply important. I am so glad to have gathered this realization early in my life. I might not always remember all the scientific knowledge or technical skills you two passed on to me through the

years, but I find great comfort in knowing that your ways of thinking and positive mentality will stay with me and help me in years to come. I am eternally grateful to you both for your guidance, patience, and encouragements. Thank you both for believing in me and for helping shape my values. I grew up both professionally and personally.

I am very fortunate to have other mentors who helped or inspired me immensely. Dr. Arlene Fiore is an absolute role model for what I have always imagined a perfect professor would be. She is kind, humble, thoughtful, and very proactive in mentoring and guiding her students. I remember and treasure each and every piece of advice and feedback she gave me. Dr. Faye McNeill is another big inspiration for me, I remember during the introduction of her atmospheric aerosols class, she said, "... this is atmospheric aerosols, it's what I do, it's my thing." I aspire to be as passionate and confident about my own research. Dr. Ron Miller is one of the most dedicated researchers/professors I have met, and perhaps the only professor who would 1) give 14 pages of homework and carefully corrects 14 pages of our answers with detailed comments, and 2) stop me in the hallway to discuss a tiny comment I made in a seminar a week prior and share a thorough response. Such dedication is beyond admirable. Dr. Gavin Schmidt is wonderfully full of wit, an inspiring leader, and has always offered some of the best perspectives on science and how to think about the world.

My academic sister Keren, one of my best friends, is a constant source of inspiration and positivity. I feel incredibly lucky that Susanne and Kostas picked the two of us to form our little work family. There are no words to articulate what her friendship means to me for the past five years. I can only wish for a lifetime of friendship.

I also want to express my huge gratitude to all the GISS researchers and staff. Every single one of them has treated me with kindness, from offering to escort me around the building to sharing

science insights, I feel so included and so fortunate to be part of this family. Thank you, Sabrina, Reto, Angel, Nestor, Jesse, Michael, Tony, Allegra, Ann, Robert, Max, Hyunho, Wasim, Lilly, Richard, Damian, Dan, and all the security guards. As well as past GISS friends Zach McGraw, Maria Sand, Parker Case, David Amundsen, and Kaoru Kakinuma.

I am in an environment where almost everyone has won a prestigious fellowship or award, and sometimes it gives me the false sense that these awards are “easily deserved.” But they are not, it is just that my cohorts are diligent and best in the field. I admire them so much and expect them to become world-renowned scientists. I want to thank Sage Li for being a great friend and sharing her reality checks with me whenever I am being too idealistic; Mukund Rao for being the kindest friend and the most patient listener since the day I met him. I would not have survived some of the hardest courses we have taken or TA’ed for together without his help and constant support; Olivia Clifton for telling me “you’re not going to get 100% of the position you don’t apply to!” and urging me to take a chance and move forward, when I spent too much time thinking than doing; Hyewon Kim for being cheerfully supportive, sometimes I think about how many hours she works and it always inspires me to work harder; Logan Brenner for being an excellent peer mentor who is always actively offering her help, she inspires me to pay it forward and give back to the community.

The emotional support I received outside of work and school is a huge part of the motivation for me to finish this dissertation. Albee’s friendship is paramount to me and I feel extremely lucky that our Ph.D. years overlapped; I thank her for being my person through and through. A thank-you list of all my friends’ names would make a dry read. Therefore, in an effort to keep the list short, I am including here only those who have 1) encouraged and motivated me to finish this dissertation, and 2) been there for the entire duration of this journey. Here goes: Yolanda,

Sophie, Ling, Baiyang, Zeyu, Xinyang, Yaqiong, Linbi, Yixuan, Fanghuizi, Bo, Yang, Aitong, and Dakai. Thank you for fighting dragons and sipping tea with me.

To quote Steve Jobs, I had “Good times, hard times, but never bad times.” During some of the most challenging times when my usual support system was not enough, Dr. Motoni Fong-Hodges helped me go through things that seemed overwhelming and impossible. I thank her for providing me a safe haven and helping me see light through dark tunnels.

Lastly and most importantly, I am grateful for my family. Mom, dad, and Andrew, you are my everything. Thank you for loving me.

To some extent, I am still that little girl waving at airplanes wanting to go places, and wondering what’s in the air, where did the rain come from, and whether clouds had stories to tell. Just very grateful to those there for the guidance and company.



To God,  
*for the footprints in the sand.*

To my brother Andrew,  
*for giving me a reason to love, live, and be better.*

To Mom and Dad,  
*for everything.*

*Thank you and I love you.*

# CHAPTER 1

## Introduction

### 1.1 Aerosol basics

The atmosphere consists of the anthroposphere, the part of the environment that is inhabited and impacted by humans, and the natural biosphere, the part of the environment occupied by other natural living organisms, which is also influenced by anthropogenic activity. Sources from the two spheres emit both gases and particles. These emitted particles are also called aerosols, which are defined as liquid or solid particles suspended in air (Seinfeld and Pandis, 2016).

Aerosols influence human lives in many ways, most notably their effects on air quality and climate. In epidemiology, particulate matter can cause harm to our cardiovascular and respiratory systems, and they are particularly damaging, even deadly, to patients with heart and lung complications (Dockery et al., 1993; Samet et al., 2000; Wichmann and Peters, 2000; Stieb et al., 2002). Aside from health impacts, aerosols adversely influence air quality by scattering light, creating haze, thus reducing visibility in both urban areas and remote regions (Cabada et al., 2004). Additionally, aerosols can also act as an agent in acid and nutrient depositions in the biogeochemical cycles of our ecosystems (Boucher et al., 2013; Seinfeld and Pandis, 2016). Lastly, and most relevant to this work, aerosols influence climate directly by absorbing and scattering solar radiation (aerosol–radiation interactions; Charlson et al., 1992) and indirectly by impacting

---

clouds (aerosol–cloud interactions, Twomey, 1974; Albrecht, 1989), which alters cloud microphysics by activating and acting as seeds for cloud formation (Myhre et al., 2013; Seinfeld and Pandis, 2016).

Sources of aerosols can be natural or anthropogenic in origin and deliver aerosols in two pathways: primary, which means direct emissions of particles, or secondary, which means formation from the oxidation of gaseous precursors (Boucher et al., 2013; Seinfeld and Pandis, 2016). Natural aerosols include, for instance, mineral dust, black carbon, and organic aerosols from biomass burning, volcanic aerosols from volcanic eruptions, biogenic organics from trees, seasalt from sea spray. Man-made aerosols from anthropogenic sources include, primary emissions of black carbon and organic aerosol from fossil fuel combustion and biomass burning in agricultural practices (Rogge et al., 1993), as well as secondary formation of sulfates, nitrates, and organics from the oxidation of their precursor gases (Seinfeld and Pandis, 2016).

## **1.2 Aerosol microphysics and mixing state**

Not all aerosol precursor gases get oxidized, some form gas clusters and nucleate to form particles directly (Aitken, 1897; Kulmala et al., 2004). For the scope of this dissertation, I am not investigating the formation of particles known as nucleation (Figure 1.1a) but diving deep with the growth of particles via condensation (Figure 1.1b), when gases are deposited onto particles, and coagulation (Figure 1.1c), when particles collide with each other to form a bigger particle (Seinfeld and Pandis, 2016). These processes, the formation and growth of aerosols, are collectively called aerosol microphysics. It is of vital importance to understand aerosol growth mechanisms, since it affects the chemical composition and microphysical properties, such as size, composition, hygroscopicity, scattering and absorption of particles and in turn affects how they interact with

climate, via cloud activation or interacting with solar radiation. To advance our understanding of these processes in the climate system, we need to investigate how to accurately represent the microphysical processes in global climate systems.

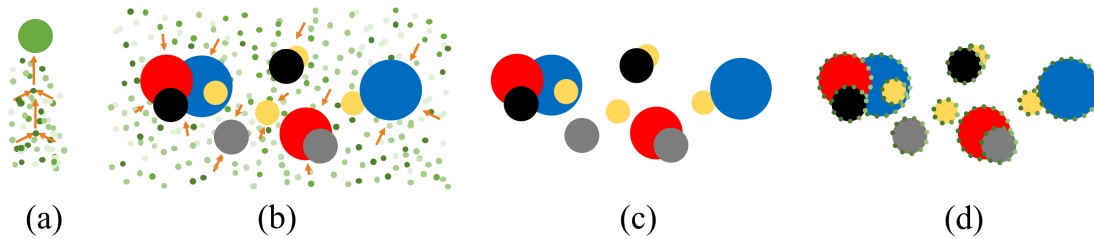


Figure 1.1 Illustrations of aerosol microphysics: formation via nucleation (a), growth via condensation (b) and coagulation (c), and growth via both condensation and coagulation (d).

When we look at aerosols under the microscope, every single aerosol takes different shape and size. Measurements have shown great variation in aerosol composition (Schwarz et al. 2008; Moffet et al. 2009; Liu et al. 2013; Healy et al. 2014). However, resolving single particle composition in large-scale chemical transport or climate models is not feasible (primarily due to expensive computations), and as an alternative, models resolve aerosol mixing state as simple representations of particle composition (Fierce et al., 2014). Mixing state describes the mean chemical composition of different aerosol populations, how much of each chemical specie is present in a representative aerosol mixture. The components that make up an aerosol population influence the overall aerosol radiative effect because each component can have different radiative effects. For instance, an aerosol population that contains mostly light-scattering components can have a cooling effect on the climate, and those that contain light-absorbing components can have a warming effect on the climate (Fierce et al., 2014).

---

The chemical composition, size distribution, and mixing state of aerosols both directly affect their optical properties, such as scattering, absorption and extinction coefficients (Boucher et al., 2013), and indirectly affect their hygroscopicity. Aerosol activation as CCN is vital to the evolution and microphysics of clouds (Reutter et al., 2009). However, with the large discrepancy between measurements and models, there is large uncertainty in the CCN and cloud droplet number concentration (CDNC) calculated in models. Furthermore, the relationship between aerosol mixing state and cloud microphysical properties leads to even more uncertainties in aerosol-cloud interactions and climate impact (Ghan et al., 1998; McFiggans et al., 2006; Ervens et al., 2007; Gibson et al., 2007; Medina et al., 2007; Cubison et al., 2008; Anttila, 2010).

An increasing number of aerosol schemes have been developed to resolve the microphysics of aerosols. Models also track the evolution of aerosol size distribution, and they are usually sorted into two types: sectional and modal (Mann et al., 2014). Sectional models simulate particles in different size bins and assume that within each bin, the composition of particles is the same, and they have been used on both regional and global scales (e.g., Wexler et al., 1994; Jacobson, 1997a, b; Lurmann et al., 1997; Jacobson, 2001; Adams and Seinfeld, 2002; Spracklen et al., 2005; Yu and Luo, 2009; Lee and Adams, 2010; Bergman et al., 2012). Most modal models sort particles by size regimes (e.g. Aitken mode, accumulation mode and coarse mode), without differentiating composition of particles (e.g., Ghan et al., 2001a, b). The modal model used in this dissertation, on the other hand, includes aerosol mixing state; it simulates different modes (or populations), and assumes that within each mode, the composition of particles is the same (Bauer et al., 2008). Modal schemes have also been implemented both regionally and globally (e.g. Binkowski and Shankar, 1995; Ghan et al., 2001a, b; Wilson et al., 2001; Stier et al., 2005; Liu et al., 2005, 2012; Bauer et al., 2008; Mann et al., 2010; Aan de Brugh et al., 2011; Zhang et al., 2012; Bellouin et al., 2013).

---

By simulating the evolution of aerosol size distribution, microphysics models are able to determine aerosol optical properties and cloud condensation nuclei (CCN) concentrations, thus representing aerosol-radiation and aerosol-cloud interactions based on key aerosol processes (Mann et al., 2014).

The aerosol microphysics model used in this study is MATRIX (Multiconfiguration Aerosol TRacker of mIXing state, Bauer et al., 2008), which resolves aerosol microphysical processes that include new particle formation, condensation and coagulation, as well as their mixing state and size distribution. MATRIX offers up to 18 different aerosol populations, or modes. Each aerosol population is defined by their mixing state, and their number concentration and mass concentration are tracked as tracers. For mass concentration, each aerosol population is tracked by their composition of sulfate, nitrate, ammonium, aerosol water, black carbon, organic carbon, mineral dust, and sea salt. Note that all aerosol populations include sulfate, nitrate, ammonium, aerosol water, and populations are defined by their other major component(s). Aerosol populations may be primary (from particle emissions), secondary (from coagulation among primary aerosol populations or condensation of gaseous components onto primary particles), or mixed (for particles that do not belong to primary or secondary populations). When particles from two populations coagulate to form a particle that does not match the mixing state of the parent populations, the particle is placed into a new population that describes its mixing state or the mixed population.

MATRIX can be used both as a standalone box model and within the NASA GISS ModelE2 Earth System Model. GISS ModelE has been used extensively in aerosol and climate related studies: climate forcing (Hansen et al., 2005), CMIP5 historical (Miller et al., 2014a), present day (Schmidt et al., 2014), and future (Nazarenko et al., 2015) climate simulations, as well

as atmospheric composition and its effect on climate (Bauer et al., 2010; Koch et al., 2011; Menon and Rotstayn, 2006; Miller et al., 2014b; Shindell et al., 2007; Tsigaridis et al., 2013).

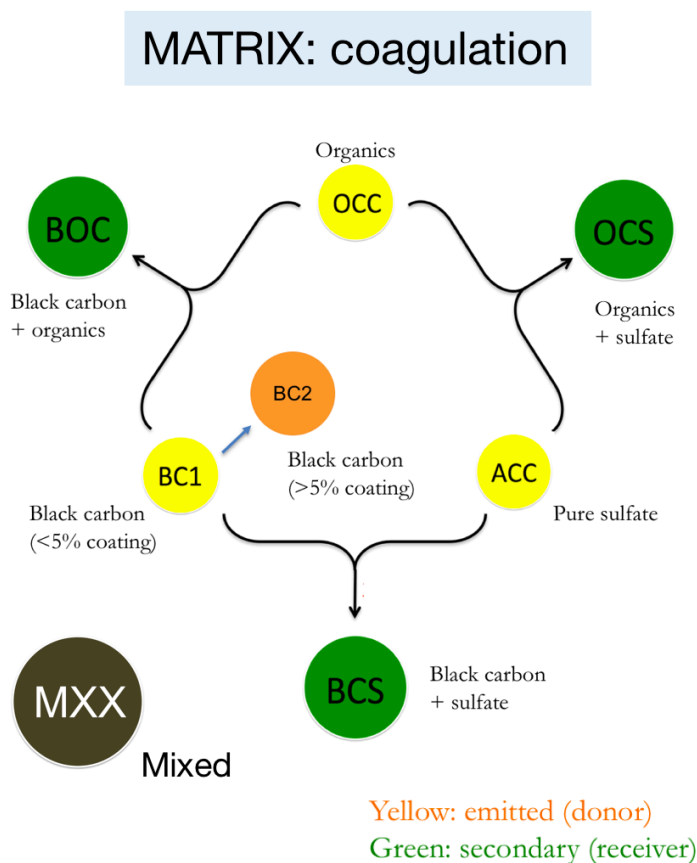


Figure 1.2 Simple schematic of the coagulation process among some aerosol populations in MATRIX, note that all aerosol populations can include sulfate, nitrate, ammonium, and aerosol water.

The original MATRIX scheme (Bauer et al., 2008) treats organic aerosols as non-volatile. Particles can only grow, not contract over time, via coagulation with other aerosols or condensation of secondary inorganic aerosols. Descriptions of the aerosol populations in MATRIX are listed in Table 2.1. Illustrated in Figure 1.2 (just showing a subsection of populations for illustration), the emitted organics aerosols are represented in population OCC, and via coagulation with black carbon population BC1 or BC2, it can become a new population BOC, which is a mixture of black

---

carbon and organics. Via coagulation with the accumulation sulfate population ACC, organics from OCC population can become population OCS, which is a mixture of organics and sulfate. Similarly, BC1 and ACC can coagulate to form BCS, which is a mixture of black carbon and sulfate. All aerosol population can receive coatings via condensation. A new population can also be formed if condensational processes change mixing state (e.g., BC1 to BC2, DD1 to DS1, AKK to ACC, etc.). Any aerosol mixture that does not fall into any aerosol population description, which will be thoroughly shown in Chapter 2, will be sorted into MXX, the “end-zone” population.

### 1.3 Organic aerosol and its volatility

To examine the composition of fine atmospheric particles, Zhang et al. (2007) performed a comprehensive study measuring fine aerosols in three different types of environments: urban, urban downwind and remote regions. Their study showed that organic aerosols are ubiquitous and a major component of the atmosphere. Jimenez et al. (2009) took a step further in investigating these measurement data, they examined the evolution of the organics and sorted organic aerosols into categories based on their oxidation state and volatility. They found that the more aged the organics are, they more oxidized and less volatile they are.

Organic volatility describes the tendency of an organic compound to vaporize and is related to the compound's vapor pressure, which is the pressure at which its condensed phase is in equilibrium with its gas phase. At a given temperature, a compound with a higher vapor pressure (more volatile) tend to evaporate more readily than one with a lower vapor pressure (less volatile). The most volatile organics are in the gas phase. They include aromatic compounds from anthropogenic sources (Odum et al., 1996, 1997), hydrocarbons such as monoterpenes (Hoffmann et al., 1997) and isoprene (Kanakidou et al., 2005) from biogenic sources, and other volatile



organic compounds (VOCs) from vegetation (Griffin et al., 1999). These gas phase organics are precursors to secondary organic aerosols and can be oxidized in the atmosphere (Shrivastava et al., 2017; Tsigaridis and Kanakidou, 2018). As the volatility of these organics change, they can partition between the gas and particle phase. Depending on how volatile they are, organic particles and these oxidized organic gases can condense onto other particles or evaporate from other particles.

Under steady state, during which the number of evaporating and condensing molecules per unit time is the same, dynamic equilibrium is reached and the equilibrium vapor pressure depends solely on temperature. The Clausius-Clapeyron equation describe the relationship between vapor pressure and temperature as a linear function,

$$\ln P = \frac{-\Delta H_{vap}}{R} \left( \frac{1}{T} \right) + C$$

which calculates the enthalpy of vaporization from measured vapor pressures at different temperatures. The phase partitioning thermodynamics of semi-volatile organic aerosols has been discussed in past studies (Pankow, 1994; Odum et al., 1996; Marcolli et al., 2004; Donahue et al., 2006). By converting an organic compound's saturation vapor pressure into mass concentration units and multiplying the inverse of the partition coefficient ( $K_{p,i} = 1/C_i^*$ ), they are able to show its effective saturation concentration  $C_i^*$ . For the total organics in the condensed and vapor phases, the equilibrium fraction  $\xi_i$  of a compound in the condensed phase can then be expressed as

$$\xi_i = \left( 1 + \frac{C_i^*}{C_{OA}} \right)^{-1}$$

where  $C_{OA}$  is the total concentration of the condensed-phase organic aerosol. With this equation, when  $C_i^* = 10 * C_{OA}$ , there will be ~10% of condensed-phase organics, and when  $C_i^* = 0.1 * C_{OA}$ , there will be ~90% of condensed-phase organics.

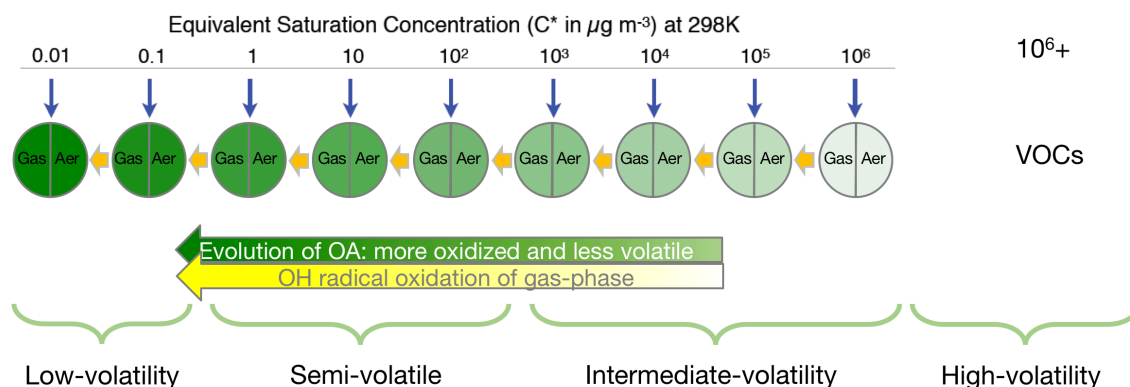


Figure 1.3 Illustration of the volatility-basis set (VBS).

Using an empirical approach based on the phase partitioning thermodynamics theory, Donahue et al. (2006) created the volatility-basis set (VBS). As illustrated in Figure 1.3, as they are emitted (blue arrows), organics are separated logarithmically into 9 bins based on their saturation concentration, and they can partition between the gas phase (notated as “Gas”) and the aerosol phase (notated as “Aer”) within their volatility bin. The gas from each bin can become oxidized by OH radicals, and their volatility can decrease. As their volatility decreases, they can move to a lower volatility bin to the left (yellow arrows) and partition in the new bin. From right to left, we follow the evolution of organic aerosols, they become more oxidized and less volatile. Based on their volatility, organics are also grouped into low-volatility, semi-volatile, intermediate-volatility and high-volatility groups as shown in Figure 1.3.

VBS is useful in improving organic aerosol representation in climate models, especially since measurements show that organic aerosols are underestimated in models (Tsigaridis et al., 2014). Measurements imply that missing sources of secondary organic aerosols are the main cause of this underestimation, and aerosol formation rates, especially those for organic aerosols, should be at least an order of magnitude higher in models, especially aloft (Heald et al., 2005; Volkamer et al., 2006; Hodzic et al., 2010; Spracklen et al., 2011). Robinson et al. (2007) suggested that

including semi-volatile primary organic aerosols (POA) and the intermediate volatility organic compounds (IVOC) as secondary organic aerosol (SOA) precursors may help bridge the observed gap.

Recent studies used VBS to fill this gap and included semi-volatile organic aerosols in their regional or global models (Lane et al., 2008; Shrivastava et al., 2008; Murphy and Pandis, 2009; Hodzic et al., 2010, 2016; Pye and Seinfeld, 2010; Tsimpidi et al., 2010, 2011, 2014, 2018; Jathar et al., 2011; Ahmadv et al., 2012; Athanasopoulou et al., 2013; Jo et al., 2013; Koo et al., 2014; Fountoukis et al., 2014; Ciarelli et al., 2017). However, the large number of tracers in VBS still makes it difficult to be implemented in a model. Donahue et al. (2011, 2012) introduced the two-dimensional VBS by adding the degree of oxidation of the organic compounds as an additional parameterized property, in addition to volatility. This new development created even more tracers to track, making the new approach extremely complex and difficult to implement in a global climate model. Nevertheless, VBS still helps our understanding of organic aerosols, since the organic matter to organic carbon ratio varies significantly in time and space (Turpin and Lim, 2001), a factor that most models currently overlook (Tsigaridis et al., 2014). Additionally, when semi-volatiles organics are included in models, they modify CCN formation rates (Petters et al., 2006; Riipenen et al., 2011; Scott et al., 2015) and particle hygroscopicity (Petters and Kreidenweis, 2007), as well as bulk aerosol mass, composition and size distribution.

#### **1.4 Relating organic volatility to aerosol microphysics**

The volatility of organic aerosols is not solely important for the bulk aerosol mass formation. Organic aerosols of different volatility contribute to the growth of particles differently depending on the size of the particles. This is where the chemistry part and the microphysics part

---

of my study meet: the larger the aerosol, the greater volatility ranges of organics it can take for condensation (Pierce et al., 2011; Yu, 2011). The condensation of high volatility organics is only important for large particles, but as the volatility of the organics decrease, the size range of particles that they can condense on increases, and low volatility organic compounds can condense on virtually all aerosol sizes. This phenomenon changes the aerosol chemical composition, number concentration, as well as CCN formation rates, thus affecting the size distribution of aerosols and their impact on climate (Paasonen et al., 2013).

However, the impact of organic partitioning on aerosols of different sizes as well as the impact of organic volatility on aerosol microphysics remain uncertain and unexplored. Given the ubiquitous presence of organic aerosols in the atmosphere (Zhang et al., 2007; Jimenez et al., 2009), and the increasing amounts of organic aerosol precursor vapors emitted in to the atmosphere in the future due to climate change (Sanderson et al., 2003; Kanakidou et al., 2005), it is essential that we include organic volatility and the partitioning process in our aerosol models, so that we can better understand their impacts on aerosol microphysics and climate.

To accomplish this goal, I developed a model called MATRIX-VBS, first of its kind to include representation of semi-volatile organics in an aerosol microphysical model, MATRIX. As VBS is coupled to MATRIX, the representation of organic aerosols is unique and more complicated. Organics in MATRIX-VBS are treated as semi-volatile and represented as VBS tracers, allowing them to condense and evaporate. Now particles can not only grow via coagulation and inorganic condensation, but also organic condensation (Figure 1.4), and this will be described and discussed thoroughly in Chapter 2. MATRIX-VBS is conveniently set up to be used as both a box model or a module within a global model. The improvement on the model makes it the most

sophisticated organic aerosol microphysics model of all the CMIP-class models, change the way organic aerosols are simulated on the global scale and their impact on particle microphysics and the climate system.

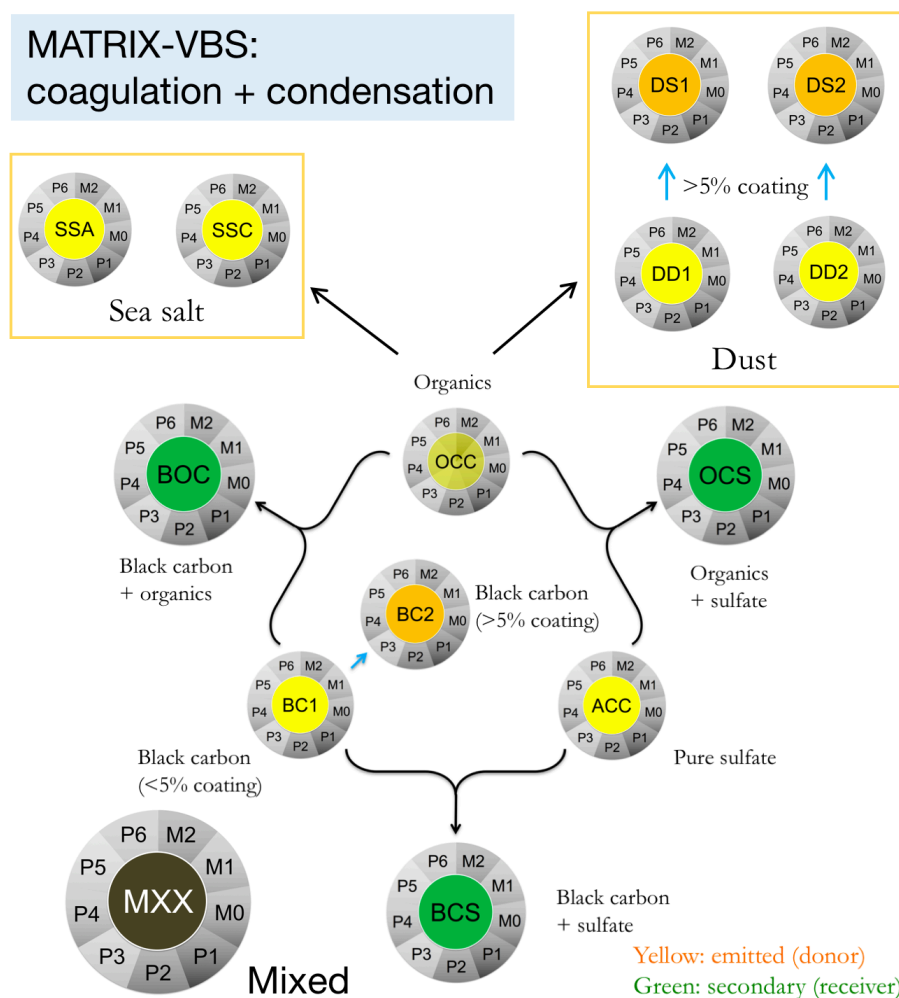


Figure 1.4 Simple schematic of MATRIX-VBS, with the condensation of organics shown as nine organic VBS species condensed as grey outer circles. OCC has a semi-transparent yellow core because it is actually emitted as the VBS species that can serve as condensation medium for gaseous VBS species, represented by the grey outer circles.

## 1.5 Applications on clouds and climate

Aerosol particles facilitate the condensation of water vapor to form clouds droplets. The Köhler theory is widely used to describe the activation of deliquesced aerosol particle into a cloud droplet by expressing the equilibrium vapor pressure of a droplet with a given radius. The theory combines two competing effects: the solute effect or Raoult's law, which describes the reduced equilibrium vapor pressure of a solution as compared to the saturation vapor pressure of pure water and depends on the inverse of the droplet radius cubed, and the curvature effect or Kelvin equation, which expresses that the equilibrium vapor pressure is greater over a curved droplet surface than over a flat surface and is inversely related to the droplet radius.

By accounting for these effects, the Köhler theory governs the CCN activation and hygroscopic growth of aerosol particles as a function of supersaturation: for a given dry particle diameter, we can calculate the critical supersaturation, which is the minimum supersaturation required for activation, or for an aqueous droplet to grow into a cloud droplet. The Köhler equation is as follows:

$$\ln\left(\frac{p_w(D_p)}{p^0}\right) = \frac{4M_w\sigma_w}{RT\rho_w D_p} - \frac{6n_s M_w}{\pi\rho_w D_p^3}$$

where  $D_p$  is the cloud droplet diameter,  $p_w$  is the droplet water vapor pressure,  $p^0$  is the saturation vapor pressure over a flat surface,  $M_w$  is the molecular weight of water,  $\sigma_w$  is the droplet surface tension,  $\rho_w$  is the density of water,  $n_s$  is the moles of solute.

Because the Köhler theory links equilibrium vapor pressure, which relates to volatility, and radius, which relates to aerosol microphysics in terms of size, the combination of organic volatility

---

and aerosol microphysics has an impact on aerosol activation and clouds. To investigate the difference VBS would make for activated particle number concentration, I tried to answer an intriguing and probing question: “Can semi-volatile organic aerosols lead to fewer cloud particles?” Some global climate models use physically based aerosol activation schemes (e.g., Abdul-Razzak and Ghan, 2000; Fountoukis and Nenes, 2005; Ming et al., 2006; Shipway and Abel, 2010), whose main governing parameters include aerosol number, size, hygroscopicity, updraft velocity, and critical supersaturation, to calculate CDNC. These governing parameters interact to activate particles, and Ghan et al. (1998) investigated the effect of sea salt particle on sulfate particle activation. They concluded that activated number concentration increases with increasing sea salt when sulfate is low and updraft is strong, and it decreases when sulfate is high and updraft is weak. This is due to a reduced maximum supersaturation, which introduced a competition effect between different aerosol types.

Reutter et al. (2009) found that size distribution is a more important factor for CDNC than particle hygroscopicity, and they discovered that aerosol number concentration and updraft velocity determines different CCN activation and cloud droplet formation regimes. Additionally, measurements at continental locations have shown that, compared to chemical composition, the size of the CCN is more important, since bigger particles require a lower critical supersaturation and are more readily activated than smaller particles (Dusek et al., 2006; Ervens et al., 2007). Yet other studies have found that chemical composition could be important for regions such as marine environments (Orellana et al., 2011; Ovadnevaite et al., 2011).

In a changing world, anthropogenic actions, such as increased pollution emissions, as well as byproducts of anthropogenic actions, namely climate change, also influence aerosols. Physical

---

(temperature, humidity, wind speed, precipitation, etc.), chemical (oxidant abundance), and biological changes (vegetation properties, etc.) derived from climate change drive changes in aerosols (Boucher et al., 2013). In turn, aerosol responds to climate change, creating a feedback loop to amplify or dampen the perturbation (Carslaw et al., 2010; Raes et al., 2010). Additionally, changes in aerosol concentration, life cycle, and properties from preindustrial times to present day conditions contribute to uncertainties in effective radiative forcing, from aerosol-radiation and aerosol-cloud interactions, which also leads to uncertainties in climate forcing (Shrivastava et al., 2017). Further, aerosols' effect on clouds and precipitation plays a major role in the uncertainties of net climate forcing, which makes it difficult for us to understand how anthropogenic activities affect the climate system and predict future changes (Stevens and Feingold, 2009; Stocker et al., 2013; Seinfeld et al., 2016). Studies agree that aerosols and their precursors' concentrations, emissions and properties can respond to climate change significantly, however, they cannot agree on its magnitude and sign, making aerosol radiative forcing highly uncertain (Boucher et al., 2013). Therefore, in order to reduce uncertainties in our projections of future changes in climate, it is essential that we improve models to better quantify aerosol properties (Andreae et al., 2005) and vital for us to investigate aerosols on the process level to better understand its evolution and impact on climate.

This dissertation follows my journey from the development of the box model in the first study (Chapter 2) to the evaluation of its performance in a global model in the last study (Chapter 4). Each study, or chapter, has a detailed introduction which includes more elaborate motivation and will not be repeated here. The storyline is linear yet distinctively divided in scale: from development and idealized experiments in the box model framework to implementation and evaluations on the global scale. Therefore, it is divided into Part I box modeling and Part II global



---

modeling, with a concluding Part III that summarizes the findings and offers insights into future research.

## **PART I**

### **Box-Modeling**

## CHAPTER 2

### **MATRIX-VBS (v1.0):**

### **implementing an evolving organic aerosol volatility in an aerosol microphysics model**

#### **Abstract**

The gas-particle partitioning and chemical aging of semi-volatile organic aerosol are presented in a newly developed box model scheme, where its effect on the growth, composition and mixing state of particles is examined. The volatility-basis set (VBS) framework is implemented into the aerosol microphysical scheme MATRIX (Multiconfiguration Aerosol Tracker of mIXing state), which resolves mass and number aerosol concentrations and in multiple mixing-state classes. The new scheme, MATRIX-VBS, has the potential to significantly advance the representation of organic aerosols in Earth system models by improving upon the conventional representation as non-volatile particulate organic matter, often also with an assumed fixed size distribution. We present results from idealized cases representing Beijing, Mexico City, a Finnish forest, and a Southeast U.S. forest, and investigate the evolution of mass concentrations and volatility distributions for organic species across the gas and particle phases, as well as assessing their mixing state among aerosol populations. Emitted semi-volatile primary organic aerosols

---

**Gao, C. Y.,** Tsigaridis, K., and Bauer, S. E.: MATRIX-VBS (v1.0): implementing an evolving organic aerosol volatility in an aerosol microphysics model, *Geosci. Model Dev.*, 10, 751-764, <https://doi.org/10.5194/gmd-10-751-2017>, 2017.

evaporate almost completely in the intermediate-volatility range, while they remain in the particle phase in the low volatility range. Their volatility distribution at any point in time depends on the applied emission factors, oxidation by OH radicals, and temperature. We also compare against parallel simulations with the original scheme, which represented only the particulate and non-volatile component of the organic aerosol, examining how differently the condensed-phase organic matter is distributed across the mixing states in the model. The results demonstrate the importance of representing organic aerosol as a semi-volatile aerosol, and explicitly calculating the partitioning of organic species between the gas and particulate phases.

## 2.1 Introduction

Atmospheric aerosols play a key role in the Earth system with great impacts on global air quality, public health and climate (Boucher et al., 2013; Myhre et al., 2013; Seinfeld and Pandis, 2016). One contribution to the large uncertainty in aerosol radiative forcing is organic aerosol (OA), which is ubiquitous in the atmosphere and contributes to a large portion of submicron particulate mass in various regions around the world (Zhang et al., 2007; Jimenez et al., 2009). Advancements in measurement techniques greatly improved our understanding of the evolution of OA and its lifetime in the atmosphere at the process level (Jimenez et al., 2009). However, OA processes in models still remain poorly constrained. Measurements imply that OA concentrations are potentially underestimated in current models (Tsigaridis et al., 2014). Such a discrepancy hints at large uncertainties in the prediction of aerosol-radiation interactions, their hygroscopicity, aerosol-cloud interactions and their overall impact on climate (Petters and Kreidenweis, 2007).

Missing sources of secondary organic aerosol (SOA) in models have been suggested to be the main cause of the underestimated OA formation (Heald et al., 2005; Volkamer et al., 2006;

Hodzic et al., 2010; Spracklen et al., 2011). More recently, studies have sought to investigate the underestimation of organic aerosol mass within more advanced model frameworks, which are capable of resolving semi-volatile primary organic aerosol (POA) and including secondary organic aerosol (SOA) from a wider set of precursors including intermediate-volatility organic compounds (IVOCs). The volatility-basis set (VBS) was developed (Donahue et al., 2006) to provide a relatively simple framework whereby models can represent the overall behavior of the myriad of compounds that constitute organic aerosol and their precursors. The approach involves considering OA as being composed of a number of representative species, each with a particular volatility, spanning a spectrum in vapor pressures from highly volatile (which essentially remains in the gas phase) to very low vapor pressure species which partition readily into the particle phase. VBS then captures the chemical aging of the organic species in the gas phase, with the hydroxyl radical oxidizing them and producing the adjacent lower-volatility class as a product. This method has been used extensively in regional studies (Robinson et al., 2007; Shrivastava et al., 2008; Murphy and Pandis, 2009; Tsimpidi et al., 2010; Hodzic et al., 2010; Fountoukis et al., 2011; Tsimpidi et al., 2011; Bergström et al., 2012; Athanasopoulou et al., 2013; Zhang et al., 2013; Fountoukis et al., 2014) but less so in global models (Pye and Seinfeld, 2010; Jathar et al., 2011; Jo et al., 2013; Tsimpidi et al., 2014; Hodzic et al., 2015). Other studies have used the 2-D VBS (Donahue et al., 2011; Murphy et al., 2011), an approach that in addition to the volatility space also resolves that of chemical composition, by tracking the amount of oxygenation in the representative organic compounds. However, the 2-D VBS is not implemented in global models, due to its large number of tracers and the large number of free parameters that are involved in the parameterization.

The inclusion of semi-volatile organics is important for accounting for the total mass of organics in the particulate phase, since an increase in particulate organic matter may not be the

result of chemically produced low-volatility species, but simply be reflecting a temperature-driven increase in the partitioning of semi-volatile organic aerosol into the particle phase. It has been established that the highly oxidized, very low volatility organics play a key role in particle formation (Metzger et al., 2010; Paasonen et al., 2013; Riccobono et al., 2014; Kirkby et al., 2016) and particle growth (Tröstl et al., 2016), while the range of volatilities contributing to aerosol growth increases with aerosol size (Pierce et al., 2011; Yu, 2011). Semi-volatile organics also affect aerosol size and mixing state, as well as their impact on climate, due to changes in cloud condensation nuclei (CCN) formation rates (Petters et al., 2006, Riipinen et al., 2011; Scott et al., 2015), hygroscopicity (Petters and Kreidenweis, 2007) and optical properties (Myhre et al., 2013). Since OA emissions are on the rise from developing countries (Lamarque et al., 2010) and no Earth system model considers anthropogenic OA as semi-volatile as measurements suggest, it is important to include and constrain semi-volatile organics to ultimately reduce uncertainties in aerosol radiative forcing and make climate model simulated aerosol changes more realistic.

The objective of this study is to further develop an aerosol microphysics model by including a more advanced representation of organic aerosol, including semi-volatile primary OA and an evolving OA volatility during chemical aging in the gas phase, in its calculations. This objective was achieved by implementing the VBS framework in the aerosol microphysical scheme MATRIX (Bauer et al., 2008), which represents major aerosol processes such as nucleation, condensation (excluding organics in its original version) and coagulation, and explicitly tracks the mixing state of different aerosol populations. As many traditional chemistry-climate models do (Tsigaridis et al., 2014), MATRIX treats POA and SOA as non-volatile (Bauer et al., 2008). By coupling MATRIX with VBS, POA are treated as condensable semi-volatile organic compounds. These can partition among different aerosol populations based on their volatility and aerosol

population size distribution, capturing particle growth via condensation of low-volatility organic vapors and thus providing a more physically based calculation of aerosol microphysics.

## 2.2 Model description

A box model is used for this study. The gas-phase chemical mechanism CBM-IV (carbon bond mechanism version IV; Gery et al., 1989), as used in the NASA GISS ModelE (Shindell et al., 2001; Shindell et al., 2003), is coupled to the MATRIX aerosol microphysics scheme, utilizing the Kinetic Pre-Processor KPP (Sandu and Sander, 2006) to solve the differential equations of the gas-phase chemistry scheme. A time step of 30 minutes is used, for consistency with the global model.

### 2.2.1 MATRIX box model

MATRIX (Bauer et al., 2008) is an aerosol microphysical model based on the quadrature-method-of-moments scheme (McGraw, 1997) in the NASA GISS ModelE Earth system model, which can be used either as a module within the global model or as a stand-alone box-model. Here, the stand-alone box model is used for development. The design of the code is such that the box-model code can be used as-is in the global model, without any changes, allowing for seamless transition and maximum portability. MATRIX is designed to resolve the aerosol temporal evolution and represent the mixing states of a user-selected set of aerosol populations, which are modes of different composition as listed in Table 2.1, tracking two moments each, number and mass, while keeping the width of the distribution fixed. It describes new particle formation, particle growth through condensation with explicit treatment of sulfuric acid condensation and lumped treatment of the  $\text{NH}_4\text{-NO}_3\text{-H}_2\text{O}$  system, as well as coagulation of particles among different

populations. Each aerosol population has its own set of aerosol components, which may be primary (from direct aerosol emissions), secondary (formed by nucleation or condensation of gas-phase components onto existing primary particles), or mixed (from any constituent, following condensation on primary aerosols or coagulation between primary, secondary, or mixed populations).

Table 2.1 Aerosol population chemical composition in MATRIX.

<b>Population abbreviation</b>	<b>Description</b>	<b>Composition</b> (constituents other than $\text{NH}_4^+$ , $\text{NO}_3^-$ , and $\text{H}_2\text{O}$ )
AKK	sulfate (Aitken mode)	$\text{SO}_4^{2-}$
ACC	sulfate (accumulation mode)	$\text{SO}_4^{2-}$
OCC	organic carbon	OC, $\text{SO}_4^{2-}$
BC1	fresh black carbon (<5% coating)	BC, $\text{SO}_4^{2-}$
BC2	aged (by condensation) black carbon (>5% coating)	BC, $\text{SO}_4^{2-}$
BCS	aged (by coagulation) black carbon	BC, $\text{SO}_4^{2-}$
BOC	black and organic carbon	BC, OC, $\text{SO}_4^{2-}$
OCS	organic carbon and sulfate	OC, $\text{SO}_4^{2-}$
SSA	sea salt (accumulation mode)	sea salt, $\text{SO}_4^{2-}$
SSC	sea salt (coarse mode)	sea salt, $\text{SO}_4^{2-}$
DD1	dust (accumulation mode; <5% coating)	mineral dust, $\text{SO}_4^{2-}$
DD2	dust (coarse mode; <5% coating)	mineral dust, $\text{SO}_4^{2-}$
DS1	dust (accumulation mode; >5% coating )	mineral dust, $\text{SO}_4^{2-}$
DS2	dust (coarse mode; >5% coating)	mineral dust, $\text{SO}_4^{2-}$
MXX	mixed (all components)	BC, OC, mineral dust, sea salt, $\text{SO}_4^{2-}$

\*The sigma values for all populations are 1.80, except for AKK, which has a sigma of 1.60, and for SSC and MXX, which both have a sigma of 2.00.



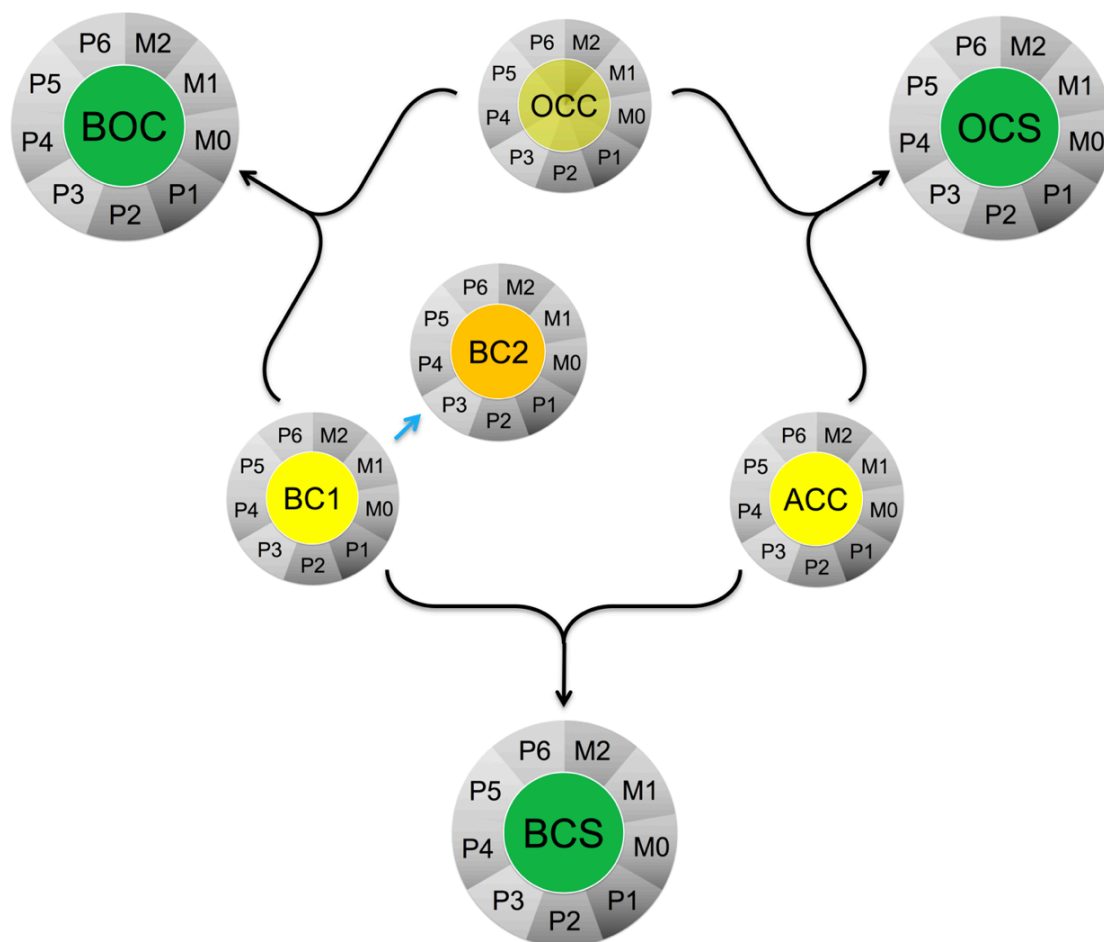


Figure 2.1. Schematic showing coagulation pathways among organics-containing aerosol populations as colored circles, with nine organic VBS species condensed as grey outer circles. In yellow are the emitted donor aerosol populations, and in green are the mixed recipient populations. OCC has a semi-transparent yellow core because it is actually emitted as the VBS species that can serve as condensation medium for gaseous VBS species, represented by the grey outer circles. In orange is population BC2, which contains a >5% coating of sulfate and organics, which is formed rapidly from the growth of population BC1, which has <5% sulfate and/or organics coating.

Black carbon is uniquely treated in MATRIX, in order to separate the coated (via condensation) from the mixed (via coagulation) populations. It is emitted in BC1, which can grow (blue arrow in Figure 2.1) with inorganic and organic coating, and as its coating volume fraction reaches 5%, it would be moved in the BC2 population (see Table 2.1 for a description), shown as the orange circle.

### 2.2.2 VBS framework

The volatility-basis set approach is introduced to the original model; it is an organic aerosol volatility parameterization that separates semi-volatile organic compounds into logarithmically spaced bins of effective saturation concentrations, which are used for gas-particle partitioning and photochemical aging (Donahue et al., 2006). The scheme groups organic compounds into nine surrogate VBS species according to their effective saturation concentrations ( $C^*$ ) at 298 K, which are separated by factors of 10, ranging from  $10^{-2}$  to  $10^6 \mu\text{g m}^{-3}$ .

Table 2.2. Naming convention and parameters used in the VBS implementation described here.

Parameter	9 Virtual VBS Species								
$C^* \mu\text{g m}^{-3}$ at 298K	$10^{-2}$	$10^{-1}$	$10^0$	$10^1$	$10^2$	$10^3$	$10^4$	$10^5$	$10^6$
Name of volatility bins	M2	M1	M0	P1	P2	P3	P4	P5	P6
Mass-based emission factors applied to POA emissions (Shrivastava et al., 2008)	0.03	0.06	0.09	0.14	0.18	0.30	0.40	0.50	0.80
Enthalpy of vaporization <sup>1</sup>	153	142	131	120	109	98	87	76	65

<sup>1</sup>: enthalpy of vaporization is calculated using Eqn.12 from Epstein et al. 2010.

We classify organics as Murphy et al., 2014 does: low-volatility organics are in bins  $10^{-2}$  to  $10^{-1} \mu\text{g m}^{-3}$  (M2 and M1 in Table 2.2), semi-volatile organics are in bins  $10^0$  to  $10^2 \mu\text{g m}^{-3}$  (M0, P1, P2), and intermediate-volatility organics are in bins  $10^3$  to  $10^6 \mu\text{g m}^{-3}$  (P3, P4, P5, and P6). Low-volatility organics partition almost exclusively to the particulate phase, the semi-volatile species are present in both the gas and aerosol phase, and intermediate-volatility organics are the most volatile ones in the framework and remain almost exclusively in the gas phase. Equilibrium partitioning is assumed for all volatility bins. Gas-phase organics can become chemically aged by the extremely reactive hydroxyl radicals ( $\bullet\text{OH}$ ) during daytime with a rate constant of  $10^{-11} \text{ cm}^3 \text{ s}^{-1}$ .

<sup>1</sup>, and as they become more oxidized, their volatility decreases, and they move down to the adjacent bin with a factor of 10 lower volatility (Donahue et al., 2006). Parameters and names used to represent them in this study are listed in Table 2.2.

The emission rates for the VBS species were derived from the POA emission rate in the global model for the corresponding grid box and month, which were distributed in the volatility space by using mass-based emission factors from Shrivastava et al. 2008 (Table 2.2). Adding up the 9 factors from each bin listed in Table 2.2, we obtain a total factor of 2.5, which means the new scheme's organics emission is 2.5 times that of the organics emissions in the original scheme. The additional multiplication factor of 1.5 is applied to the emission to account for missing sources of volatile organics in the IVOC volatility regime in the inventories (Shrivastava et al. 2008).

### 2.3 Model development

In the original version of the MATRIX model, organics only contribute to particle growth and mix with other aerosol species via coagulation. Primary organic aerosols are emitted only as non-volatile particulate organic matter, and do not exist in the gas phase or interact with other aerosol populations. Implementing the VBS scheme adds these missing processes. Before this development, there were eight alternative configurations of MATRIX available to the user, each representing a distinct set of aerosol populations whose number, composition and interactions by coagulation vary. A 9<sup>th</sup> configuration with 15 selected aerosol populations is created for this study (Table 2.1), in which eight of the 16 populations, ACC, OCC, BC1, BC2, OCS, BOC, BCS, and MXX, could contain organics as semi-volatile VBS species. We only included semi-volatile organics in 8 populations, so that we can examine the BC-OA-sulfate-nitrate system first, before adding them into the nucleation population AKK and the dust and sea salt populations (DD1, DS1,

DD2, DS2, SSA, SSC). Through coagulation, the 15 donor populations grow or mix and are placed into recipient populations, based on the donor population composition, as described in Bauer et al. (2008). In a future stage, organics will also be implemented in the AKK mode to present nanoparticle growth and we will include an additional nucleation scheme that considers the dependence of new particle formation that involve organics (Kirkby et al., 2016; Tröstl et al., 2016).

Previously, each aerosol population carried up to five tracers – sulfate, black carbon, non-volatile organics, dust and sea salt. Now each of the eight organic-containing populations carry nine additional semi-volatile VBS species listed in Table 2.2. Together with the 5 original tracers, we now have up to 14 available tracers per population, depending on whether they carry organic aerosols or not, with the original organics tracer (OCAR) representing the non-volatile biogenic OA, as it did in the original mechanism. This newly coupled model MATRIX-VBS treats POA as semi-volatile gas-phase species, which then partition into and out of the particulate phase. The amount of gas-phase species partitioned onto each aerosol population is based on the surface area of that population, in addition to the mass of that population and the volatility of species, and equilibrium partitioning is assumed.

The semi-volatile nature of biogenic SOA is not represented in the VBS framework in this work. Instead, biogenic SOA are treated as non-volatile, as in the original MATRIX version, and are produced with a 10% constant yield from terpenes emissions without any requirement for oxidation before the OA is formed (Lathi  re et al., 2005; Tsigaridis et al., 2014). The inclusion of semi-volatile biogenic SOA will be parameterized in the same way as in the VBS framework presented here in the future.

---

## 2.4 Simulations

To test the newly developed model's behavior, we simulated idealized cases representative of four different locations and environments: one very polluted city (Beijing), another cleaner yet still very polluted city at high altitude and closer to the tropics (Mexico City), a very clean Finnish forest (Hyytiälä), and an anthropogenically affected forest in southeast USA (Centreville, Alabama). The experiments are performed for a winter month (January) and a summer month (July) for 10 days, and initial conditions and emission rates for each location were extracted from a GISS ModelE simulation (similar setup as described in Mezuman et al., 2016) for the year 2006, listed in Table 2.3.

All parameters and emissions are held constant throughout the simulations. Here we do not include deposition and dilution, for simpler mass-balance calculations. Semi-volatile POA, sulfate in the accumulation mode, and black carbon, are emitted continuously in the OCC, ACC, and BC1 populations, respectively, shown in Figure 2.1 as yellow circles. Condensation of VBS species on BC1 can increase the non-absorbing shell of that population, leading to the formation of BC2, as described above. The four organics-containing populations described above can coagulate (black arrows in Figure 2.1) with themselves and each other and form three additional organics-containing mixed populations, BOC, OCS and BCS, shown as green circles. This schematic includes seven of the eight organics-containing populations in the model.

Table 2.3 Conditions of each location used in the simulations, taken from the GISS ModelE for January and July 2006.

January 2006		Units	Beijing	Centreville	Hyytiälä	Mexico City
<b>Fixed parameters</b>	Temperature	K	270	279	260	283
	Pressure	hPa	1007	996	1009	797
	RH	%	46.8	77.7	79.5	62.5
<b>Gaseous emissions</b>	NO <sub>x</sub>		216.5	92.4	169.7	148.7
	CO		6943.3	1199.3	557.3	2308.4
	Alkenes		4.3	0.3	0.1	1.3
	Paraffin	pptv/hr	8.2	2.1	0.6	10.5
	Terpenes		1.8	26.3	9.4	25.8
	Isoprene		1.3	23.8	0.0	0.0
	SO <sub>2</sub>		555.8	191.7	24.1	538.7
	NH <sub>3</sub>		181.3	24.2	50.7	63.3
<b>Aerosol emissions</b>	Sulfate		0.06	0.02	0.003	0.05
	Black carbon	μg/m <sup>3</sup> /hr	0.09	0.01	0.008	0.03
	Organics*		0.19	0.03	0.02	0.11

July 2006		Units	Beijing	Centreville	Hyytiälä	Mexico City
<b>Fixed parameters</b>	Temperature	K	304	303	292	289
	Pressure	hPa	986	995	998	800
	RH	%	59.8	61.8	77.8	83.1
<b>Gaseous emissions</b>	NO <sub>x</sub>		281.3	124.3	200.9	165.3
	CO		8111.9	1749.9	630.5	2276.1
	Alkenes		5.0	0.5	0.1	1.3
	Paraffin	pptv/hr	9.6	2.7	0.7	10.7
	Terpenes		36.9	145.4	87.6	44.9
	Isoprene		916.1	795.5	47.2	0.0
	SO <sub>2</sub>		653.7	206.5	26.8	549.5
	NH <sub>3</sub>		211.7	38.7	58.1	63.3
<b>Aerosol emissions</b>	Sulfate		0.06	0.02	0.002	0.05
	Black carbon	μg/m <sup>3</sup> /hr	0.10	0.01	0.01	0.03
	Organics*		0.21	0.03	0.07	0.11

---

## 2.5 Results and discussion

The temporal evolution of the total organics mass concentrations from the new scheme and the old scheme are presented in Figure 2.2 for January and Figure 2.3 for July in the four locations under study. They show large changes in organics concentrations between the old scheme (black line on the right column) and the new one (colors). The organics in the new scheme are represented and distributed by organics tracers of different volatility, whose saturation concentration  $C^*$  ranges from the least volatile  $10^{-2} \mu\text{g m}^{-3}$  (“M2” in Figures 2.2 and 2.3) to the most volatile  $10^6 \mu\text{g m}^{-3}$  (“P6” in Figures 2.2 and 2.3). They are distributed between the gas and aerosol phases by gas-particle partitioning, whereas the organics in the original scheme are only represented by one nonvolatile organic aerosol tracer (“OCAR”).

As mentioned in the model description, the emission rates for organics in each of the volatility bins in the new scheme were derived from the Shrivastava et al. (2008) mass-based emission factors. Consequently, since there is no deposition and dilution in the simulations, the new scheme’s organics total mass concentrations (shown in color in the right columns of Figures 2.2 and 2.3) always adds up to 2.5 times that of the old scheme (shown as dash-dotted lines) throughout the simulations in both January and July.

### 2.5.1 Winter

In January, the total mass concentration for organics in Beijing, Centreville, Hyytiälä and Mexico City at the end of 10 days are approximately  $115 \mu\text{g/m}^3$ ,  $16 \mu\text{g/m}^3$ ,  $13 \mu\text{g/m}^3$ , and  $65 \mu\text{g/m}^3$ , respectively. Organic VBS species partition between the gas and aerosol phases within their corresponding volatility bin. The more volatile the species, the more it partitions into the gas phase. The concentration evolution of VBS species in the gas phase from the four locations are shown in

the left column of Figure 2.2 for January. From top to bottom in each panel, volatility decreases from the most volatile species (“P6”) to the least volatile (“M2”). Although semi-volatile organics are emitted in the aerosol phase, in the intermediate-volatility range from P6 to P3 bins, the species are so volatile that they evaporate and partition into the gas phase almost completely.

In all four locations, almost all species in the intermediate-volatility range are in the gas phase, those in the semi-volatile range partition between the gas and aerosol phases, and those in the low volatility range are in the aerosol phase in January. This is especially true for Beijing and Hyytiälä, where the volatility distributions are very similar (in relative terms) and where the total concentration of gas-phase species is higher than the sum of all aerosol-phase species. In Centreville, the total amount of gas-phase species is approximately the same as that of the aerosol-phase species, whereas in Mexico City there are more species in the aerosol phase than in the gas phase. In Centreville and Mexico City, the species show a diurnal variability, which will be explained later.

Aging can help explain the similar volatility distributions in Beijing and Hyytiälä. The  $\cdot\text{OH}$  concentration in both locations are low in January: Beijing’s mean  $\cdot\text{OH}$  is approximately  $10^5$  molecules/cm<sup>3</sup> and Hyytiälä’s mean  $\cdot\text{OH}$  is approximately  $10^4$  molecules/cm<sup>3</sup>. Low  $\cdot\text{OH}$  concentrations limit the aging of intermediate-volatility organics and their ability to move to the lower volatility bins, thus the volatility distributions do not change drastically, something that is also evident by the lack of a daily cycle. On the other hand, much higher mean  $\cdot\text{OH}$  concentrations in Centreville ( $2 \cdot 10^6$  molecules/cm<sup>3</sup>) and Mexico City ( $5 \cdot 10^6$  molecules/cm<sup>3</sup>) provide more oxidation power, making oxidation a significant pathway in aerosol evolution.



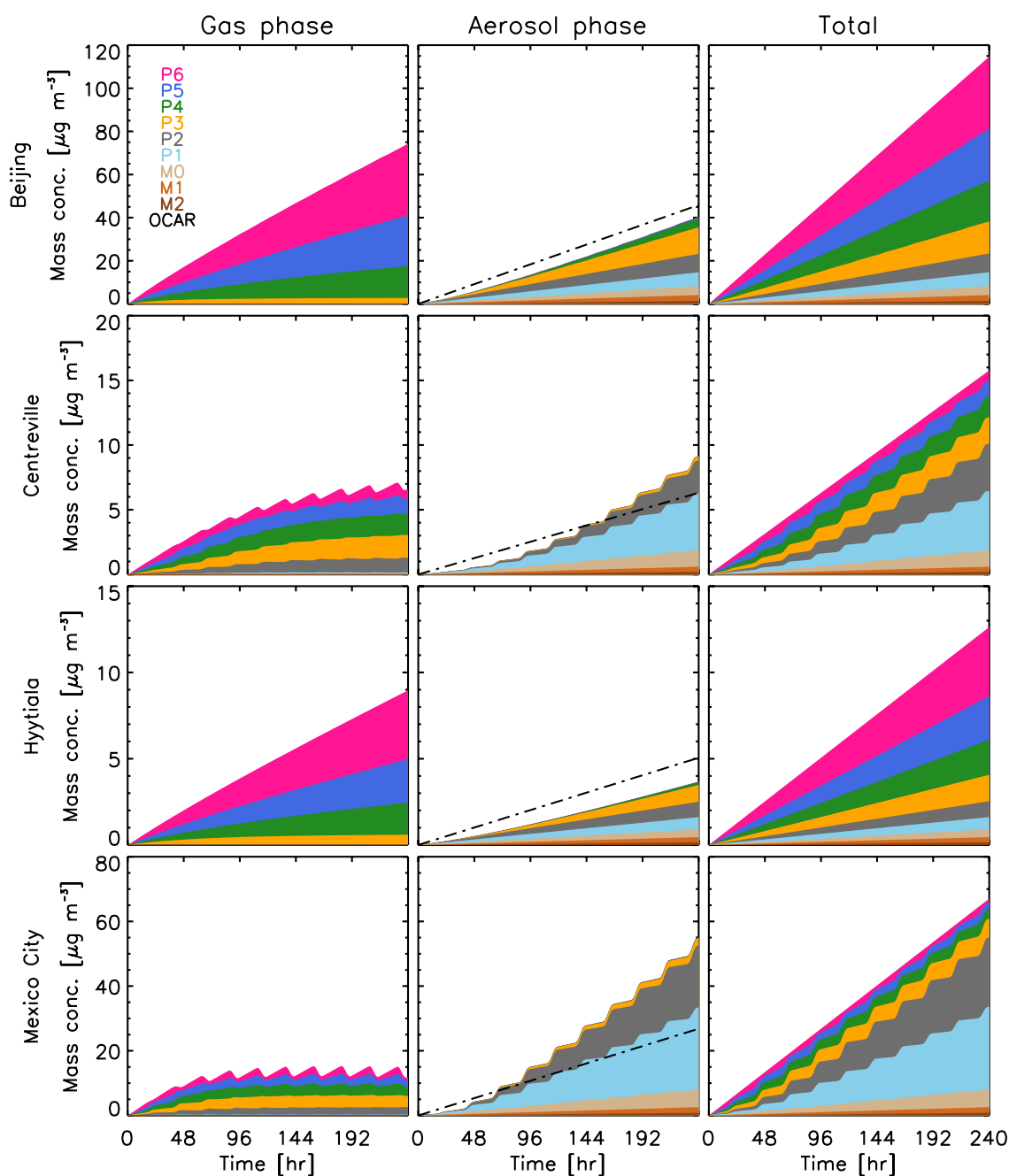


Figure 2.2 Temporal evolution of the mass concentration of semi-volatile organics in the gas phase (left column), aerosol phase (across all populations; middle column) and total (right column) using the new scheme (refer to Table 1.1 for legend) for January. The total of non-volatile organics from the original scheme (OCAR) is shown in black dash-dotted lines in the aerosol phase column (middle). OCAR from the old scheme is exactly 2.5 times smaller from the total organic species in the new scheme.

---

The higher mean  $\bullet\text{OH}$  concentrations also explain the diurnal variability of both gas-phase and aerosol-phase mass concentrations that we see in the two locations, because  $\bullet\text{OH}$  is only produced during daytime and has very low concentrations during the night. Since Mexico City has slightly higher  $\bullet\text{OH}$  concentration than Centreville, its total gas-phase concentration reaches a dynamic equilibrium after approximately 4 days, whereas Centreville's total gas phase continues to rise, approaching equilibrium at a slower pace.

Looking at the total of the organics (right column of Figure 2.2), it is not surprising that the very polluted Beijing has the highest concentration of total organics while the cleanest location, Hyytiälä, has the lowest; what is interesting, however, is that organics at these locations share similar volatility distributions. By the end of the 10-day simulations in the new scheme, the volatility distributions in Beijing and Hyytiälä are very similar to the emission factor distribution among the volatility, with factor differences of less than 0.1. This behavior is, again, a result of the low  $\bullet\text{OH}$  concentrations in the two locations, and the low oxidation rate that limits the change in volatility distribution. Volatility is also temperature dependent, which is also relevant to the total aerosols present. In Beijing, we would expect higher gas-phase concentration due to the higher temperatures. However, the larger amount of aerosols moves the partitioning point towards the aerosol phase, which offsets the temperature difference in the colder Hyytiälä case, and gives us similar results.

On the other hand, the volatility distributions in Centreville and Mexico City are very different from the applied emission factor distribution, except for the two bins in the low volatility range, M2 and M1. Due to the high concentrations of  $\bullet\text{OH}$ , both sites have low gas-phase organics concentrations because the intermediate-volatility gases are more efficiently oxidized and their

less volatile products partition into the aerosol phase. Therefore, the relative amount of organics from the intermediate-volatility range no longer resembles the applied emission factors. The organics in the intermediate-volatility range from P6 to P3, are totaling factors of approximately 0.38 and 0.15 in Centreville and Mexico City, respectively, which are in sharp contrast to the factors of 0.4, 0.5, and 0.8 applied to each of the respective bins.

### 2.5.2 Summer

The total mass concentration of organics in Beijing and Mexico City at the end of 10 days in July are approximately  $130 \mu\text{g}/\text{m}^3$  and  $67 \mu\text{g}/\text{m}^3$  respectively, very similar to the amounts in January. However, Centreville and Hyytiälä have higher concentrations of organics than they did in January, with  $90 \mu\text{g}/\text{m}^3$  and  $43 \mu\text{g}/\text{m}^3$  respectively. The volatility distributions for the four locations in July (Figure 2.3) are also very different from that of January.

Organics are all very low in the intermediate-volatility and semi-volatile ranges, and they are all high in the low volatility ranges, with less than 10% of the total organics in the gas phase in all four locations. This behavior means that at all locations' oxidation is very strong, stronger than any place during January. This sharp change in behavior is caused by the difference in  $\bullet\text{OH}$  concentrations during the 2 months. July's concentrations are much higher than those in January because  $\bullet\text{OH}$  production is increased due to increased photolysis in the summer. The mean  $\bullet\text{OH}$  concentration is approximately  $1.5 \cdot 10^7$  molecules/ $\text{cm}^3$  in Beijing and Hyytiälä, and it is approximately  $1 \cdot 10^7$  molecules/ $\text{cm}^3$  in Centreville and  $2 \cdot 10^7$  molecules/ $\text{cm}^3$  in Mexico City. More  $\bullet\text{OH}$  leads to faster oxidation of the gas-phase organics and the consequent partitioning of the less-volatile oxidation products into the aerosol phase. This is evident in Figure 2.3, where the gas-phase concentrations in all four locations are very low. In all cases, dynamic equilibrium was

reached after just 2 days. They also exhibit a strong diurnal variability, as expected from the fast  $\cdot\text{OH}$  oxidation, which decreases with decreasing volatility.

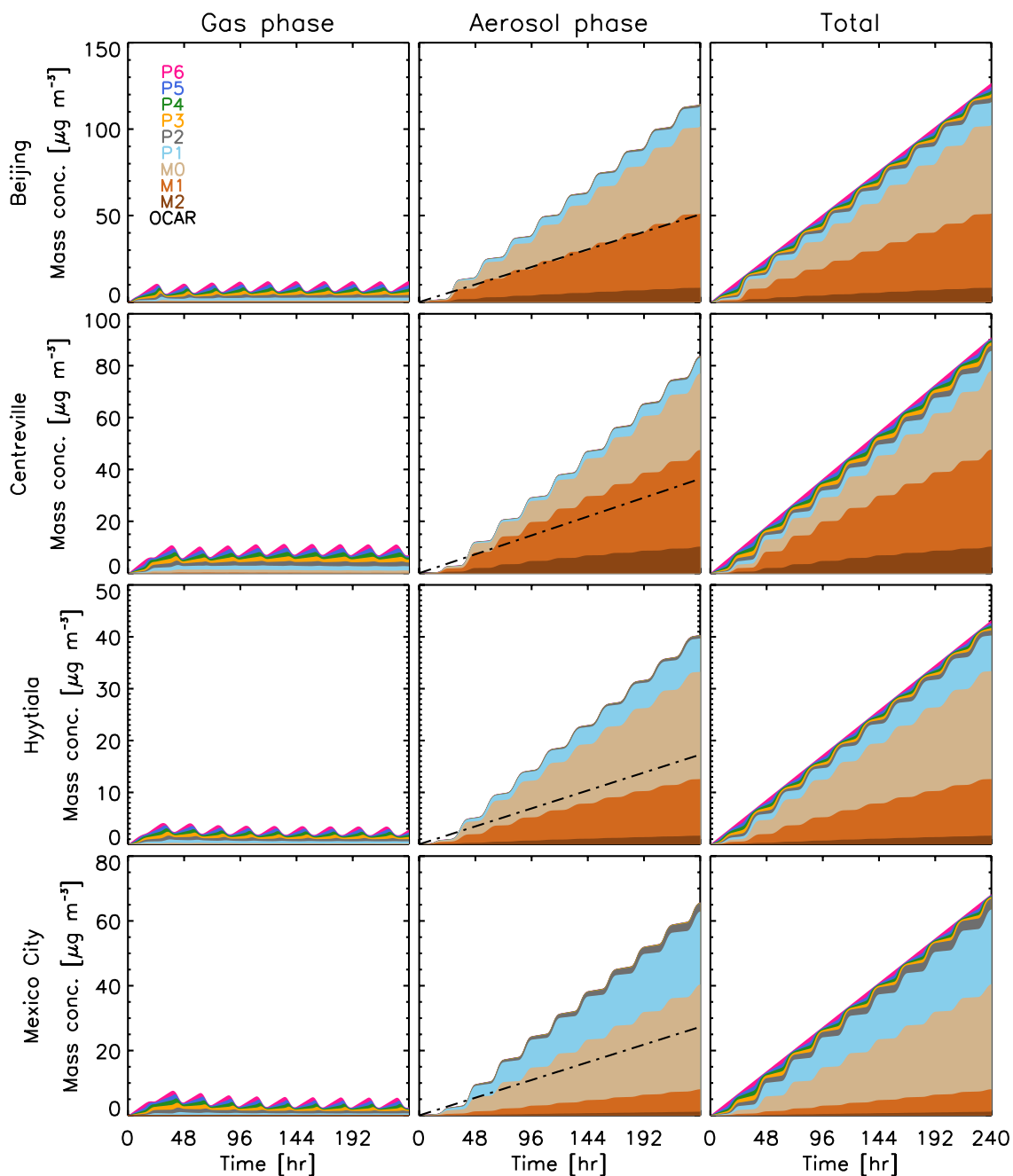


Figure 2.3 Same as Figure 2.2, for July.

---

### 2.5.3 Mixing state

The temporal evolution of total organic aerosol mass concentration per population is shown in Figure 2.4 (absolute amounts) and Figure 2.5 (relative amounts). The first and third columns are results from the new scheme with condensing and coagulating organics for January and July, respectively, while the second and fourth columns are results from the old scheme with only coagulating organics from January and July, respectively. The organic aerosol mass concentrations in Figure 2.4 correspond to the aerosol-phase concentrations in Figures 2.2 and 2.3 (middle column), except they are now separated by population, whereas in the earlier two figures they were separated by mass tracers representing volatility.

At a first glance, the population with the highest organic mass is BOC for January and July in both schemes. BOC is the population that contains OC, BC, and sulfate, and is the end result of coagulation of all populations in our idealized cases. However, in the old scheme, populations OCC and OCS also have significant amounts of organics. This is because in the new scheme the emitted populations are ACC, BC1 and OCC, and organics that are emitted in the OCC population can condense on and/or coagulate with other populations, including being lost by evaporation and then repartitioning to other populations. Thus, there is an additional loss mechanism of organics from those populations in the new scheme. In addition, there is competition between the ACC and BC1 populations in both schemes, and in the new scheme, aerosol-phase organics in the OCC population could either coagulate with the ACC population to form OCS, or they could coagulate with the BC1 population to form BOC. This competition determines how much OCS and BOC are formed, and it affects how much gas-phase organics from the OCC population could condense on the two populations and the distribution of organics among the populations. Since partitioning adds

a loss mechanism to OCC, part of the evaporated mass will go to BOC, making it larger, and a more efficient scavenger of other particles. As a result, most organics coagulate with and condense on the BOC population and/or the OCC population, and together with the emitted OCC population, hold the most organics and dominate the mass fractions.

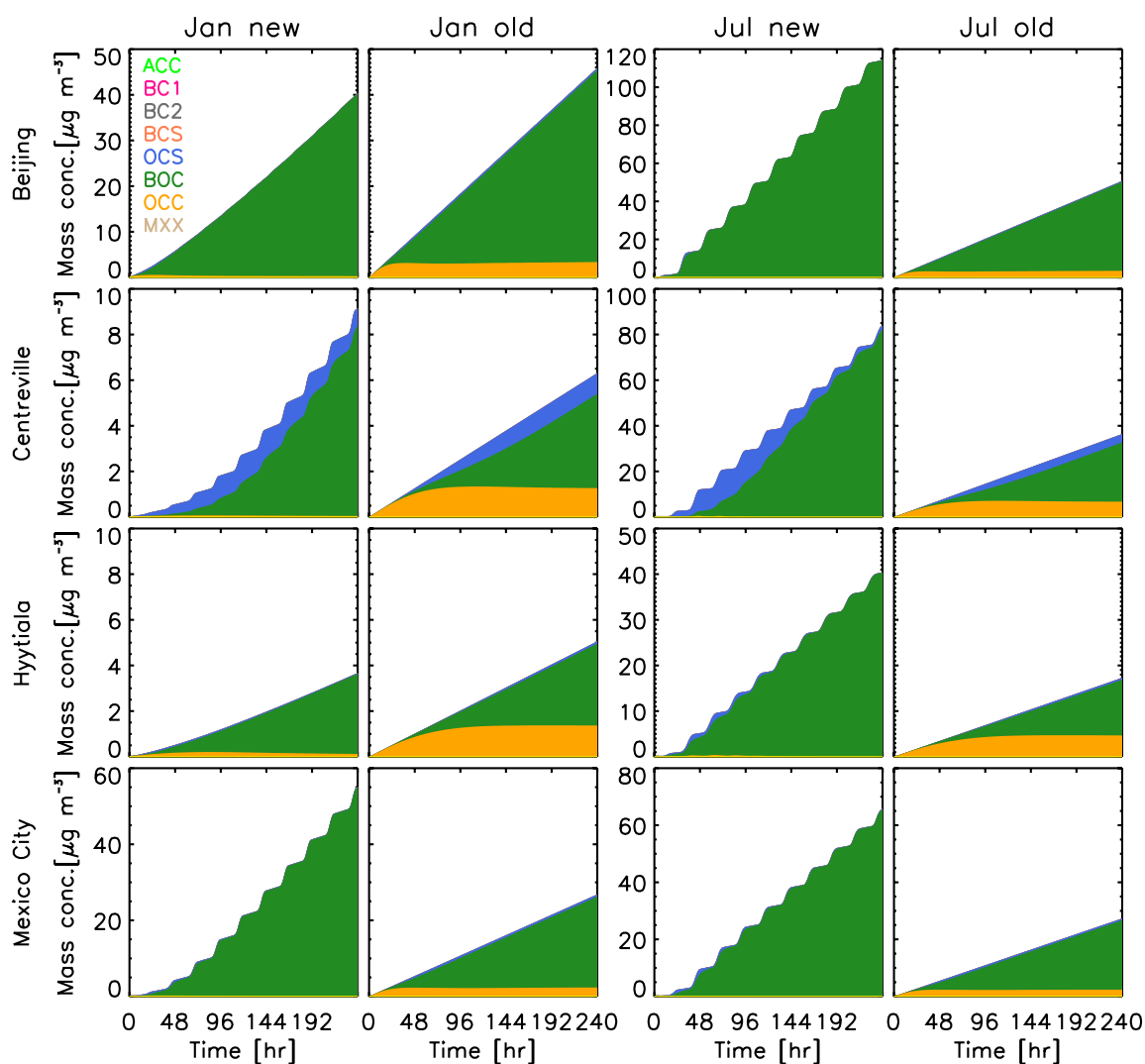


Figure 2.4 Temporal evolution of organic aerosol mass concentration in each organics-containing population from the new scheme (first column for January, third column for July), and the old scheme (second column for January, fourth column for July).

There is some similarity between the January and July results between the new and the old schemes (Figure 2.5). This similarity means that the distribution of organics among aerosol populations is not significantly affected by season. This is consistent with a study by Bauer et al. (2013), where they found that the mixing-state distribution is rather a characteristic of a region and not so much of a season, although the total (absolute) amounts by season may vary.

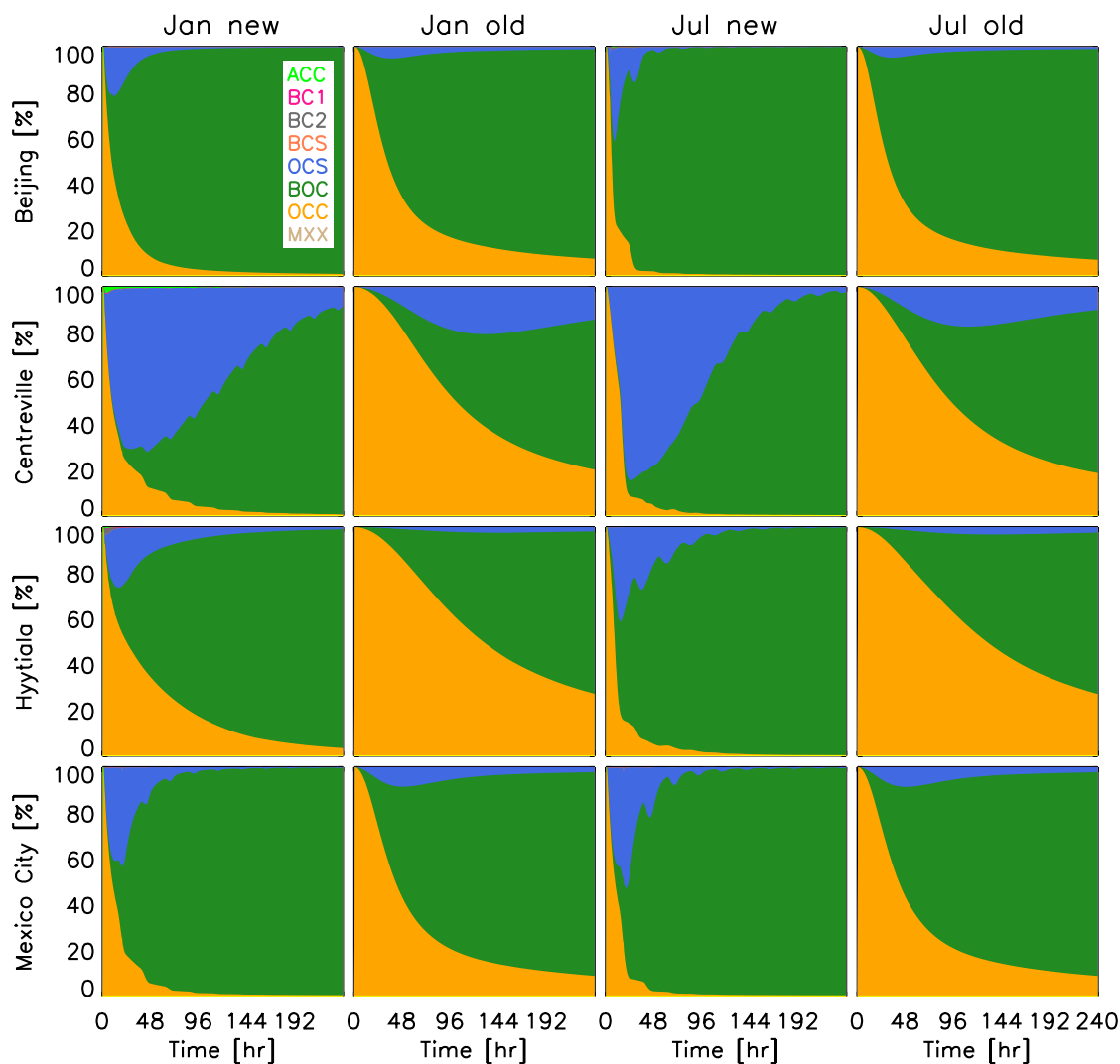


Figure 2.5 Temporal evolution of organic aerosol mass concentration fraction in each organics-containing population from the new scheme (first column for January, third column for July), and the old scheme (second column for January, fourth column for July).

By the end of the simulations, most locations have more organics present in the BOC population, except those in Centreville. The reason for this is sulfate; from the sulfate and black carbon emissions listed in Table 2.3, we can calculate the sulfate-to-black-carbon ratio in Centreville to be 2:1, higher than the corresponding ratios in all other locations. This high ratio helps the ACC population to survive the competition against BC1 for coagulation with OCC. This leads to higher OCS formation, which is available for gas-phase organics to condense on, thus coagulation and condensation both bring more organics in the OCS population during the first half of the simulation. These results show that the sulfate to black carbon ratio is important for the mixing state by delaying the inevitable BOC domination. Also, comparing the distribution fraction in Figure 2.5, volatile organics create rather different mixing states as those created by coagulation alone in the original scheme, meaning that the semi-volatility did alter the mixing state significantly.

#### 2.5.4 Size distribution

Another important factor on the evolution of aerosols is their size distribution. Shown in Figures 2.6 and 2.7 are the January size distributions from Mexico City and Centreville respectively. The first row shows number concentration, the second row surface area, and the third row volume. The first two columns are results from the new and old schemes after 24 hours of simulation, and the right two columns are after 120 hours. The total number concentration, surface area and volume from the eight populations are shown as dotted lines. Note also that these plots show the total aerosol size distribution per population, which includes the contribution of species other than organics.



The size distributions in July are very similar to January in all locations, and therefore only January is shown here. Beijing, Hyytiälä and Mexico City exhibit somewhat similar size distributions (with different absolute amounts), just as their mass fractions. The size distribution is dominated by OCC, OCS and BOC in the first 3 to 4 days, but later only by BOC. On the other hand, Centreville, similar to its mixing state, is different in its size distribution of different aerosol populations from the other three locations. Therefore, only the size distributions of Mexico City and Centreville are shown here.

In the new scheme for Mexico City after 24 hours of simulation, the number concentration has two modes. OCC has even smaller size than Aitken mode sulfate AKK does, as a result of the evaporation of organics, but its number concentration is higher. OCS and BOC have started to form from coagulation of OCC with ACC and BC1, and their diameter, number concentration, surface area and volume are very similar, almost overlapping, with BOC slightly smaller in diameter. After 120 hours of simulation, OCC's number concentration has decreased significantly, from  $4 \cdot 10^7 \text{ m}^{-3}$  to  $1 \cdot 10^7 \text{ m}^{-3}$ . This is because OCC is semi-volatile, it has evaporated and condensed onto other populations, and at the same time its loss due to coagulation with other populations has increased, due to the increase of their number concentration and decrease in size. OCS size grew very slightly, but BOC grew significantly, with peaks of surface area and volume both increasing approximately 1 order of magnitude. Its peak surface area increased from  $1.5 \cdot 10^5 \mu\text{m}^2\text{m}^{-3}$  to  $9 \cdot 10^5 \mu\text{m}^2\text{m}^{-3}$ , and its peak volume grew from approximately  $2 \cdot 10^4 \mu\text{m}^3\text{m}^{-3}$  to  $2 \cdot 10^5 \mu\text{m}^3\text{m}^{-3}$ . BOC's growing large surface area is another reason why it has so many organics and dominates the mass concentration: the greater the surface area, the more gas-phase species are able to condense. This matches the mixing-state results (Figure 2.5), where we saw after 24 hr that

ACC, OCC, and BOC have high mass fractions, whereas after 120 hours OCC and OCS are negligible, and more than 90% of the total organic aerosol mass is in the BOC population.

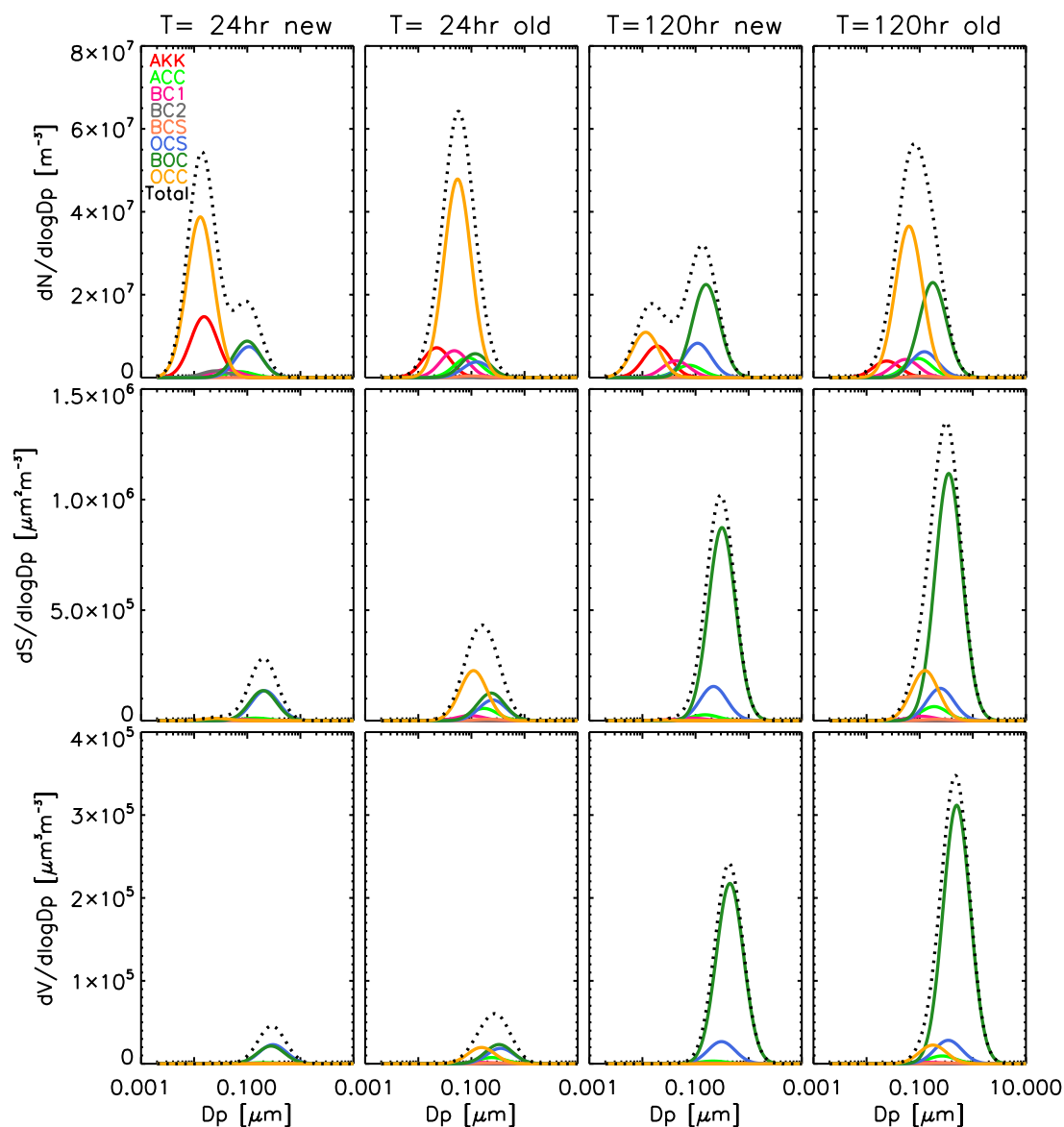


Figure 2.6 Organics-containing aerosol populations (except MXX) and AKK (Aitken mode sulfate) size distributions for Mexico City in January. Top row: number concentration. Middle row: surface area. Bottom row: volume. Total of all populations in dotted black lines.

In the old scheme, after 24 hours OCC has higher number concentration (peaking at  $5 \times 10^7 \text{ m}^{-3}$ ) and size than in the new scheme, and higher surface area and volume, due to its greater number

and diameter. OCS and BOC are both fewer in number (peaks are  $1 \cdot 10^7 \text{ m}^{-3}$  and  $1.5 \cdot 10^7 \text{ m}^{-3}$  lower in the old scheme) but slightly greater in diameter than they are in the new scheme. Later, after 120 h, OCC number concentration maximum decreases to  $3.5 \cdot 10^7 \text{ m}^{-3}$ , due to coagulation with ACC and BC1 to form more OCS and BOC. Therefore, OCS and BOC increased in number and size, with BOC seeing greater growth (the peak of number concentration increased from  $7 \cdot 10^6 \text{ m}^{-3}$  to  $2.3 \cdot 10^7 \text{ m}^{-3}$ , the peak of surface area increased from  $1.5 \cdot 10^5 \text{ } \mu\text{m}^2 \text{ m}^{-3}$  to  $1.1 \cdot 10^6 \text{ } \mu\text{m}^2 \text{ m}^{-3}$  and the peak of volume increased from  $3 \cdot 10^4 \text{ } \mu\text{m}^3 \text{ m}^{-3}$  to  $3.1 \cdot 10^5 \text{ } \mu\text{m}^3 \text{ m}^{-3}$ ). For OCS we calculated more modest increases of approximately 50% in number, surface area and volume concentration peaks: the number concentration from  $4 \cdot 10^6 \text{ m}^{-3}$  to  $7 \cdot 10^6 \text{ m}^{-3}$ , surface area from  $1 \cdot 10^5 \text{ } \mu\text{m}^2 \text{ m}^{-3}$  to  $1.5 \cdot 10^5 \text{ } \mu\text{m}^2 \text{ m}^{-3}$  and volume from  $2 \cdot 10^4 \text{ } \mu\text{m}^3 \text{ m}^{-3}$  to  $4 \cdot 10^4 \text{ } \mu\text{m}^3 \text{ m}^{-3}$ , as seen in the new scheme as well. However, BOC's growth in the old scheme is even greater than that in the new scheme. This slightly accelerated growth slows down at later hours (not shown), because BOC dominates faster in the new scheme than in the old one (Figure 2.4).

The Centreville size distributions tell a different story (Figure 2.7). In the early stages of the new scheme, OCS has greater number concentration and size than BOC does; OCS's peak number concentration is  $0.5 \cdot 10^7 \text{ m}^{-3}$ , more than double than that of BOC, while its peak surface area and volume are  $1 \cdot 10^5 \text{ } \mu\text{m}^2 \text{ m}^{-3}$  and  $2 \cdot 10^5 \text{ } \mu\text{m}^3 \text{ m}^{-3}$  respectively, whereas those of BOC are negligible. Later, OCS still outgrows BOC in number, but barely exceeds in surface area and is not greater in volume. BOC shifts to greater diameters; therefore, it has greater volume than OCS does after 120 hours. As for the old scheme, OCC does not decrease in number from 24 hours to 120 hours as it does in Mexico City, but its number increases from  $1.7 \cdot 10^7 \text{ m}^{-3}$  to  $2.5 \cdot 10^7 \text{ m}^{-3}$ . This means that in that period of time coagulation loss is less than the amount of OCC emitted, which is what was also seen earlier for the mass concentrations (Figure 2.2). At 120 hours, OCS

has again higher number concentration than BOC does, but only slightly (peak number concentration difference is approximately  $1 \cdot 10^6 \text{ m}^{-3}$ ) and not as much as in the case of Mexico City, and the latter's surface area and volume continue to be greater than those of the former due to its increasing diameter.

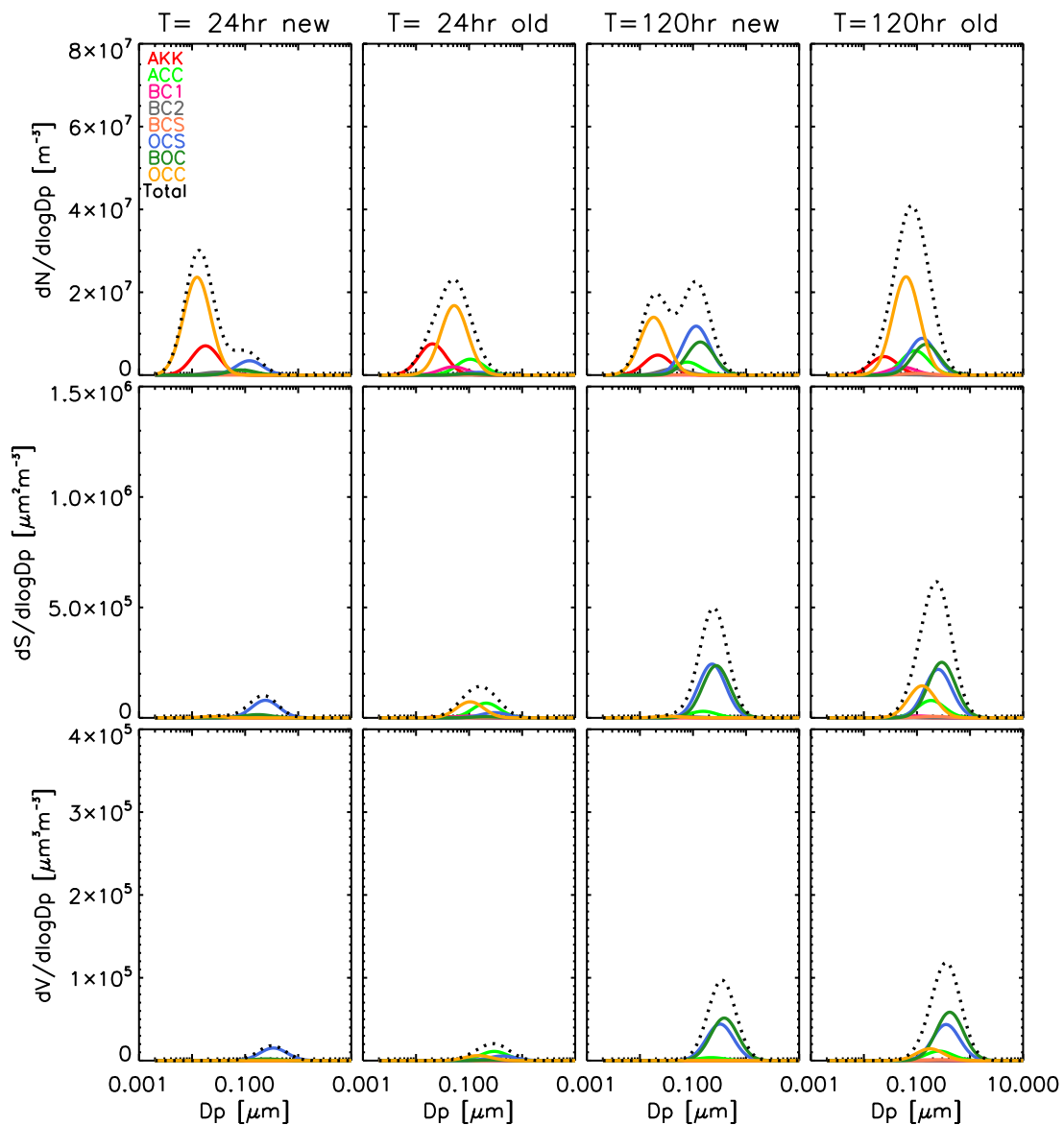


Figure 2.7 Same as Figure 2.6 for Centreville.

---

## 2.6 Conclusions

Organic aerosol volatility calculations were implemented into a new aerosol microphysics scheme, MATRIX-VBS. Results from idealized cases in Beijing, Centreville, Hyytiälä and Mexico City during summer and winter using the new scheme were compared against the original scheme and showed how the inclusion of semi-volatility of organics and their reactivity affected aerosol mass concentration, as well as their mixing state and size distribution. Emission factors,  $\cdot\text{OH}$  oxidation, temperature and total aerosol levels are the key factors determining organics' volatility distribution and mass concentration. The mixing state is affected by particle size and concentration, which determines coagulation and condensation pathways. Results from the new scheme showed different mixing-state distribution from the original scheme.

Going forward, the new scheme will be simplified, and we will reduce the number of tracers needed, in order to simplify the model and save computational resources, without losing the essential information needed for volatility. The simplified version of the box model will then be implemented in the NASA GISS ModelE Earth system model. While this study is purely theoretical, we will evaluate MATRIX-VBS after its implementation into GISS ModelE. We will gain even better understanding of how semi-volatile organics are altering aerosol mixing state, how meteorological conditions and pollution levels influence organics' volatility distribution, as well as their mixing state in the real world, and what implications these processes have on the climate system.

## CHAPTER 3

# Can semi-volatile organic aerosols lead to fewer cloud particles?

### Abstract

The impact of condensing organic aerosols on activated cloud number concentration is examined in a new aerosol microphysics box model, MATRIX-VBS. The model includes the volatility basis set (VBS) framework coupled with the aerosol microphysical scheme MATRIX (Multiconfiguration Aerosol Tracker of mIXing state) that resolves aerosol mass and number concentrations and aerosol mixing state. By including the condensation of organic aerosols, the new model produces fewer activated particles compared to the original model, which treats organic aerosols as nonvolatile. Parameters such as aerosol chemical composition, mass and number concentrations, and particle sizes that affect activated cloud number concentration are thoroughly tested via a suite of Monte Carlo simulations. Results show that by considering semi-volatile organics in MATRIX-VBS, there is a lower activated particle number concentration, except in cases with low cloud updrafts, in clean environments at above-freezing temperatures, and in polluted environments at high temperatures (310 K) and extremely low-humidity conditions.

---

### 3.1 Introduction

Atmospheric aerosols influence climate mainly via two pathways: aerosol–radiation interactions (the aerosol direct effect; Charlson et al., 1992), which affect the Earth’s radiative energy balance by absorbing and scattering terrestrial and solar radiation, and aerosol–cloud interactions (the aerosol indirect effect; Twomey, 1974; Albrecht, 1989), which affect cloud microphysics by activating and serving as seeds for cloud formation (Myhre et al., 2013; Seinfeld and Pandis, 2016). Aerosol activation as cloud condensation nuclei (CCN) is critical to the evolution and microphysics of clouds (Reutter et al., 2009). However, the relationship between aerosol mixing state and cloud microphysical properties remains a large uncertainty in aerosol–cloud interactions (Ghan et al., 1998; McFiggans et al., 2006; Ervens et al., 2007; Gibson et al., 2007; Medina et al., 2007; Cubison et al., 2008; Anttila, 2010).

Climate models calculate cloud droplet number concentration (CDNC) using aerosol activation schemes, whose main governing parameters include aerosol number, size, hygroscopicity, updraft velocity, and critical supersaturation. Physically based aerosol activation schemes (e.g., Abdul-Razzak and Ghan, 2000; Fountoukis and Nenes, 2005; Ming et al., 2006; Shipway and Abel, 2010) are commonly used in global climate models for fast diagnostics of nucleation and to estimate the aerosol indirect effect in long-term climate simulations (Ghan et al., 2011). Several studies examined the relationship between the aforementioned parameters and how they interact to activate particles. Ghan et al. (1998) examined sea salt’s influence on sulfate particle activation and introduced the competition effect. Since all CCN have to compete for available water vapor in order to activate, the competition limits the maximum supersaturation in in-cloud updrafts (Storelvmo et al., 2006). Ghan et al. (1998) concluded that activated number

concentration increases with increasing sea salt when sulfate is low and updraft is strong, and it decreases when sulfate is high and updraft is weak because maximum supersaturation is reduced. Another study (Reutter et al., 2009) explored how much CDNC depends on updraft velocity, size distribution, and hygroscopicity. They found that size distribution played a greater role than particle hygroscopicity in CDNC and discovered different CCN activation and cloud droplet formation regimes, which are determined by aerosol number concentration and updraft velocity.

Semi-volatile organic aerosols contribute significantly to the growth of particles to CCN sizes (Yu, 2011). More notably, as aerosol size increases, the range of organic volatilities involved in aerosol growth increases (Pierce et al., 2011; Yu, 2011). The inclusion of semi-volatile organics in models modifies CCN formation rates (Petters et al., 2006; Riipinen et al., 2011; Scott et al., 2015) as well as hygroscopicity (Petters and Kreidenweis, 2007), in addition to bulk aerosol mass, size distribution, and composition. By adding semivolatile organic partitioning to our existing microphysics model MATRIX (Multiconfiguration Aerosol Tracker of mIXing state; Bauer et al., 2008), which resolves aerosol mixing state, we were able to examine how semivolatile organics change bulk aerosol mass, size distribution, and composition. However, the effects of semi-volatile organic partitioning combined with aerosol mixing state on particle activation remain unexplored.

In our previous work, we demonstrated that including semi-volatile organics would lead to higher aerosol number concentration and smaller particles (Gao et al., 2017). As was the case for the original aerosol microphysics model MATRIX, our further-developed box model MATRIX-VBS (Gao et al., 2017) follows the same multimodal aerosol activation approach by Abdul-Razzak and Ghan (2000). The activation parameterization accounts for aerosol size distribution, composition, mixing state, and in-cloud updraft velocity. Curious about the change in activation



with the newly present semi-volatile organics and the governing parameters influencing it, we investigated the difference in activated number concentration in two box model setups: MATRIX (Bauer et al., 2008) and MATRIX-VBS (Gao et al., 2017).

## 3.2 Methods

### 3.2.1 Model Description

MATRIX-VBS (Gao et al., 2017) is an aerosol microphysics model that includes organic aerosol volatility in its calculations. It was developed by implementing VBS (volatility-basis set; Donahue et al., 2006) in the aerosol microphysics model MATRIX (Bauer et al., 2008), which is a box model that is also used in the NASA GISS ModelE Earth system model (Bauer et al., 2008, 2012; Schmidt et al., 2014). Since the publication of Gao et al., 2017, which included organic condensation on fine mode aerosols, we further developed the model which now allows semi-volatile organics in the system to condense on coarse mode dust and sea salt as well. We have also included nitrate radicals as an oxidant for organics in addition to the hydroxyl radical that was used in the original VBS scheme, even though it is a very minor oxidation pathway in the model (rate constant for the oxidation by  $\text{NO}_3^\bullet$  is  $1 \times 10^{-13} \text{ cm}^3 \text{ molecules}^{-1} \text{ s}^{-1}$ ; Atkinson, 1997).

As previously stated, we use Abdul-Razzak and Ghan (2000) activation parameterization, which calculates the activated particle number concentration depending on chemically-resolved number concentrations using Köhler Theory. The hygroscopicity parameters  $\kappa$  for each aerosol species presented in Table 3.1 were calculated from their solubility fraction. For organics, we assumed a linear increase of solubility with decreasing volatility (Jimenez et al., 2009). Since we use Pankow type partitioning (Pankow, 1994), water is not considered in the partitioning process.

In addition, we do not use different kappa/RH relationships per organic species, which was found to be important for biogenic SOA (Rastak et al., 2017).

Table 3.1 Hygroscopicity  $\kappa$  used for each organic aerosol volatility bin.

	$\text{Log}_{10}C^*$ [ $\mu\text{g m}^{-3}$ ]	soluble fraction [%]	$\kappa$
Sulfate	/	100	0.507
Black carbon	/	0	$5 \cdot 10^{-7}$
Non-volatile organic carbon	/	78	0.141
	-2	100	0.180
	-1	87.5	0.158
	0	75	0.135
	1	62.5	0.113
Semi-volatile organic carbon	2	50	0.090
	3	37.5	0.068
	4	25	0.045
	5	12.5	0.023
	6	0	0.000
Dust	/	13	0.14
Sea salt	/	100	1.335

### 3.2.2 Simulations

A Monte Carlo analysis with a range of chemical and meteorological conditions (Table 3.2) was performed to pinpoint which processes affect organics and the mixed aerosol population in general the most. Since global models need to resolve a wide range of conditions, from very clean to very polluted, and for a wealth of meteorological conditions, we simulated 630 possible atmospheric scenarios on Earth across the whole parameter space, e.g., temperature, RH, latitude, emissions levels, and updraft velocity, for 120 h (5 days) simulations with no deposition and dilution. Three types of environmental conditions were simulated: clean, moderate, and polluted, as defined by different levels of emissions that were determined using a probability distribution of the gridded emission fields in GISS ModelE for January present-day conditions. During this

development phase, biogenic SOAs from terpene oxidation in MATRIX-VBS are treated as nonvolatile, while only the anthropogenic aerosols are treated as semi-volatile.

Table 3.2 Parameters used in the Monte-Carlo simulations.

Parameter		Range	
T [K]		270, 280, 290, 300, 310	
RH [%]		0.1, 20, 40, 60, 80, 100	
Latitude		0, 30N/S, 60N/S, 90N/S	
Updraft velocity [m/s]		0.5, 1, 2	
Emissions of aerosols [μg/m³/s]	Sulfate (SO <sub>2</sub> in molecules/cm <sup>3</sup> )	10 <sup>5</sup> , 10 <sup>6</sup> , 5•10 <sup>6</sup>	
	Primary organics	5•10 <sup>-6</sup> , 5•10 <sup>-5</sup> , 5•10 <sup>-4</sup>	
	Nonvolatile biogenic organics from terpene source	1•10 <sup>-8</sup> , 5•10 <sup>-6</sup> , 1•10 <sup>-5</sup>	
	Black Carbon	10 <sup>-6</sup> , 10 <sup>-5</sup> , 10 <sup>-4</sup>	
Emissions of gases [molecules/cm <sup>3</sup> ]	VOCs (in sets)	Alkenes	5•10 <sup>2</sup> , 5•10 <sup>3</sup> , 5•10 <sup>4</sup>
		Paraffin	5•10 <sup>3</sup> , 10 <sup>4</sup> , 5•10 <sup>4</sup>
		Terpenes	10 <sup>4</sup> , 10 <sup>5</sup> , 10 <sup>6</sup>
		Isoprene	10 <sup>4</sup> , 10 <sup>5</sup> , 50 <sup>6</sup>
	NO <sub>x</sub>		10 <sup>5</sup> , 10 <sup>6</sup> , 10 <sup>7</sup>

### 3.3 Results and discussion

We found that activated number concentration is lower for most cases in the MATRIX-VBS model, which considers semi-volatile organic aerosols, compared to the MATRIX model. However, under low updrafts, in a clean environment at above-freezing temperatures, and in polluted environments at high temperatures (310 K) and extremely low humidity conditions (0 % RH) during aerosol formation, activated number concentration is higher in MATRIX-VBS than in MATRIX.

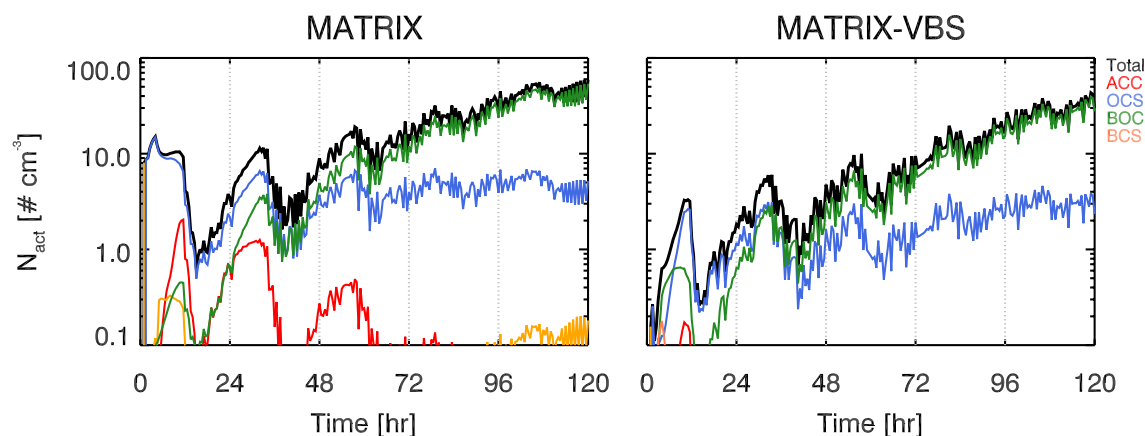


Figure 3.1. Activated number concentration of aerosol populations (see main text for details) for MATRIX (left) and MATRIX-VBS (right) for 290 K and 40% RH at 30°N latitude with medium emission levels and 0.5 m/s updraft velocity.

As an example, the activated number concentration for a case with temperature at 290 K, RH at 40 %, medium emission levels, and an updraft of 0.5 m s<sup>-1</sup> at 30 °N latitude is shown in Figure 3.1 for the two models. Mixing states of aerosols in MATRIX and MATRIX-VBS are represented as aerosol populations, which all contain SO<sub>4</sub>, NO<sub>3</sub>, NH<sub>4</sub> and H<sub>2</sub>O, in addition to the species that define the populations (Bauer et al., 2008, 2013). The four most dominant aerosol populations for the activated number concentration in MATRIX are ACC (SO<sub>4</sub>, NO<sub>3</sub>, NH<sub>4</sub>), OCS (organic carbon, SO<sub>4</sub>, NO<sub>3</sub>, NH<sub>4</sub>), BOC (black carbon, organic carbon, SO<sub>4</sub>, NO<sub>3</sub>, NH<sub>4</sub>), and BCS (black carbon, SO<sub>4</sub>, NO<sub>3</sub>, NH<sub>4</sub>). Only two dominant populations are calculated in MATRIX-VBS, OCS and BOC, as in Gao et al. (2017), since OCC evaporates and re-condenses on all particles, based on their calculated surface area and mass concentration. Since OCS and BOC have the largest surface area, they are calculated to have the strongest growth via organics condensation. Additionally, the competition among sulfate, organics, and black carbon determines the loss of ACC and the formation of BCS: OCC coagulates with ACC to form OCS, and this coagulation increases in MATRIX-VBS due to smaller OCC particles; therefore, there are fewer ACC particles left to coagulate with black carbon to form BCS. At the end of the 5-day simulation (Figure 3.1),

MATRIX-VBS has a total of approximately 30 activated particles  $\text{cm}^{-3}$ , whereas MATRIX has approximately 60 activated particles  $\text{cm}^{-3}$  under the same conditions.

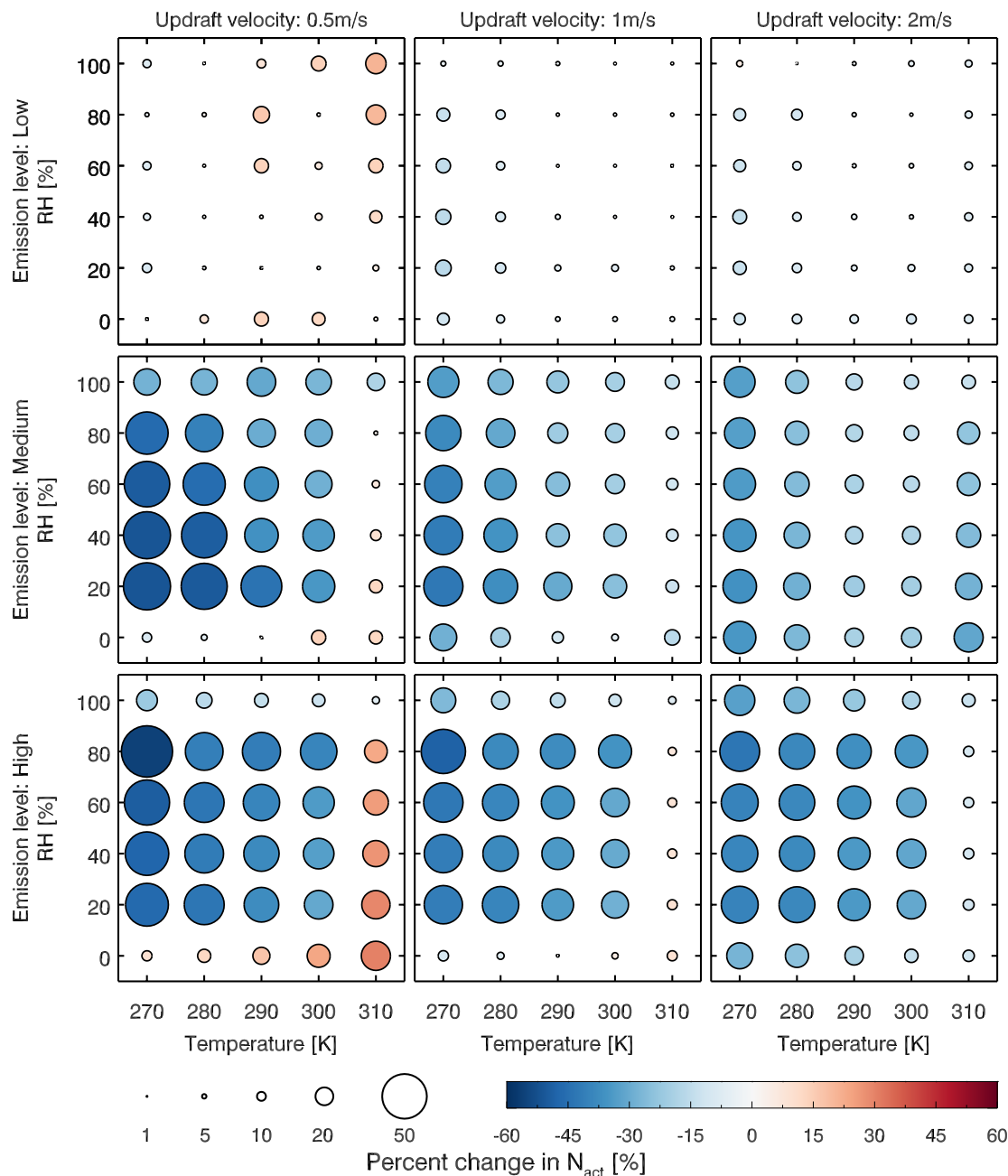


Figure 3.2 Fractional change of average activated number concentration (size and color of the circles) over the last 24 hours of a 5-day simulation between the two models with low (top row), medium (middle row) and high (bottom row) level emissions at updraft velocities of 0.5 (left column), 1 (middle column) and 2 (right column) m/s.

Figure 3.2 shows a more comprehensive look across all temperature and RH scenarios studied. The results show that for most scenarios, MATRIX-VBS has lower (blue circles) activated number concentration compared to MATRIX. However, some rare cases show the opposite behavior. These are for above-freezing temperatures in the low emission level under low-updraft (top left) scenarios, high temperature (310 K), and extremely low humidity (0 % RH) in the medium emission level under low-updraft (middle left) scenarios, as well as the high emission level under low-updraft (bottom left) and medium-updraft (bottom middle) scenarios. Note that low RH values do not mean that these correspond to cloud conditions. Aerosols form outside of clouds in our model, where RH can be very low. Activation will occur after aerosol formation though, when an air parcel starts rising with a given updraft velocity, in which air parcel supersaturation will develop and will cause aerosol activation.

Table 3.3 Minimum and maximum of fractional change in average activated number concentration over the last 24 hours between the two models with low, medium and high level emissions at updraft velocities of 0.5, 1 and 2 m/s.

Updraft velocity (m/s)	Fractional change in activated number concentration					
	0.5		1		2	
	min	max	min	max	min	max
Low emission level	-9%	+21%	-16%	+2%	-14%	+5%
Medium emission level	-51%	+14%	-42%	-5%	-36%	-13%
High emission level	-56%	+31%	-48%	+9%	-43%	-9%

Across all scenarios, the changes in activated number concentration between MATRIX-VBS and MATRIX range from  $-56\%$  to  $+31\%$  (Table 3.3). The range of the difference becomes more significant as emission levels increase, yet less significant as updraft velocity increases. Within most emission level–updraft velocity scenarios, as temperature increases, the fractional

change in activated number concentration between the two models decreases. Also, within most emission level–updraft velocity scenarios (Table 3.4, Figure 3.3), as temperature increases, there are fewer activated particles in MATRIX. We also observed the same behavior in MATRIX-VBS, higher temperature and fewer activated particles.

Table 3.4 Minimum and maximum of average activated number concentration over the last 24 hours of MATRIX and MATRIX-VBS with low, medium and high level emissions at updraft velocities of 0.5, 1 and 2 m/s.

Updraft velocity (m/s)		Activated number concentration					
		0.5		1		2	
		min	max	min	max	min	max
Low emission level	MATRIX	23	305	351	1160	963	2799
	MATRIX-VBS	24	283	338	1026	887	2473
Medium emission level	MATRIX	19	152	359	1233	1476	3711
	MATRIX-VBS	16	139	304	884	1021	2498
High emission level	MATRIX	3	60	199	1280	1925	5703
	MATRIX-VBS	3	63	185	1150	1677	4142

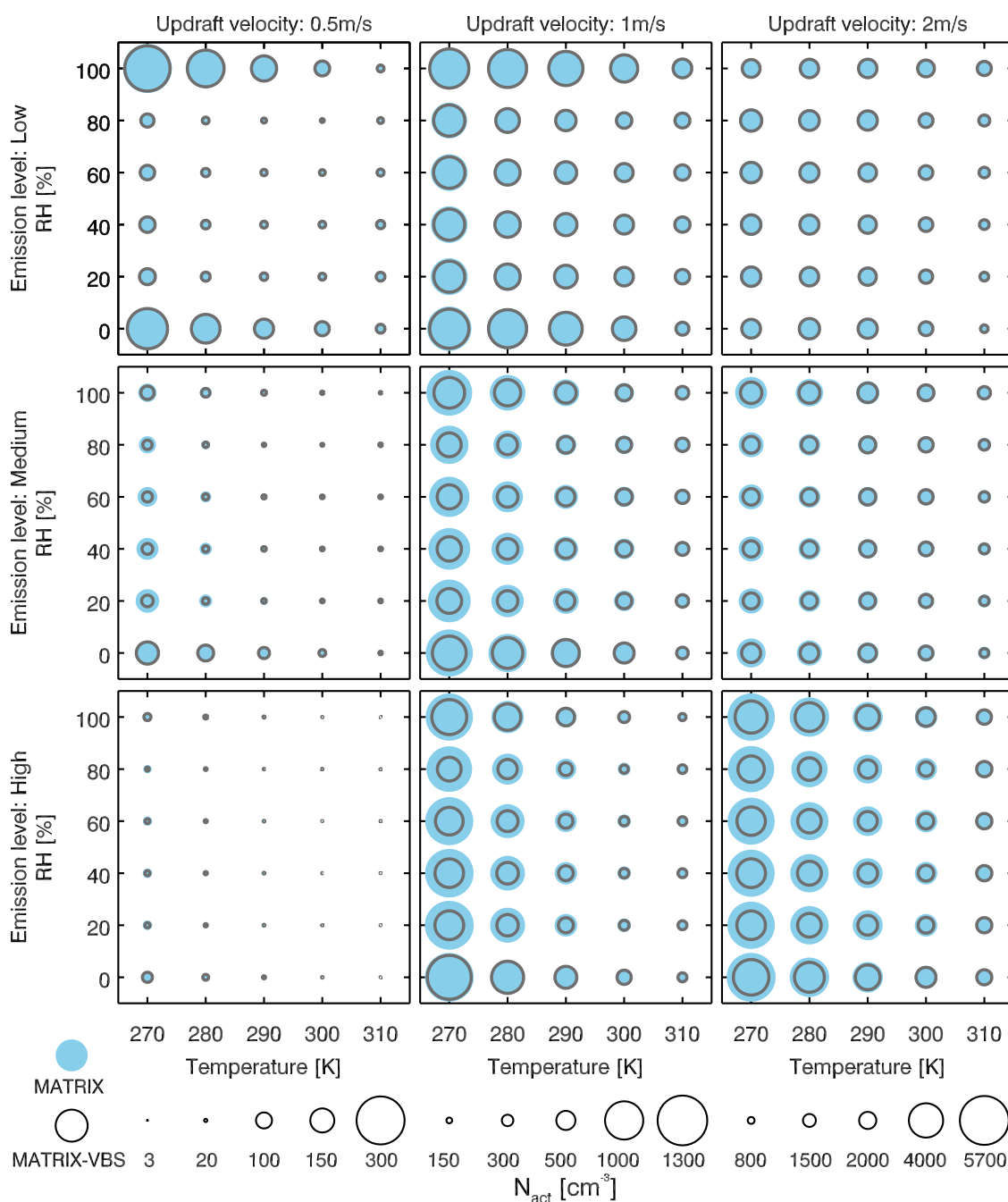


Figure 3.3 Average activated number concentration (circle size) during the last 24 hours of a 5-day simulation in MATRIX and MATRIX-VBS with low (top row), medium (middle row) and high (bottom row) emission levels at updraft velocities of 0.5 (left column), 1 (middle column) and 2 (right column) m/s. Note difference in scales per column.

In order to understand the cause of the difference in activation, we traced back to the key difference between the two models: partitioning of organics. The inclusion of organics partitioning



leads to changes in aerosol mixing state and size distribution, as discussed in Gao et al. (2017). Therefore, the change in activated number concentration could only be caused by changes in mass concentration, number concentration, and particle size. Since we use the Abdul-Razzak and Ghan (2000) parameterization, the activated number concentration is mainly a function of number concentration and dry particle diameter in our model. The parameterization is also a function of geometric standard deviation, which is constant per population in our model as it was in MATRIX (Bauer et al., 2008), as well as a function of aerosol composition and hygroscopicity, as mentioned in the model description, for which we assume a linear increase in solubility with decreasing volatility. The hygroscopicity of the aerosol populations changes with time, as the internal mixing of aerosol populations is altered by aerosol microphysics.

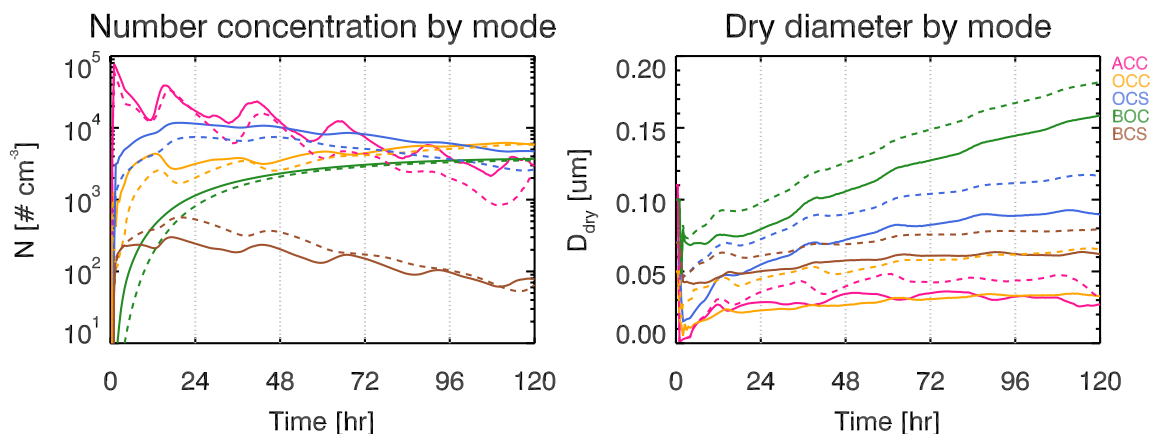


Figure 3.4 Number concentration (left column) and dry particle diameter (right column) by mode (color lines) for MATRIX (dashed lines) and MATRIX-VBS (solid lines) for the experiments with the same conditions as Figure 3.1.

As was the case in Gao et al. (2017), MATRIX-VBS has a higher aerosol number concentration (Figure 3.4 left) but smaller particles (Figure 3.4 right) compared to MATRIX in the case presented in Figure 3.1. Initially, we expected that smaller particles would be less likely to activate, so we performed a simple sensitivity test to confirm it. By changing dry particle diameter

---

of the particles in the activation scheme, the decreasing dry particle diameter indeed led to lower activated number concentration. However, a second sensitivity test with changing only number concentration showed that higher number concentration would actually lead to lower activated number concentration as well.

In the Abdul-Razzak and Ghan (2000) scheme, increasing number concentration decreases critical supersaturation, and lower critical supersaturation leads to higher minimum dry particle radius that is able to activate. Therefore, activation is suppressed since fewer particles exceed the threshold radius. The activated number concentration is calculated from the activation fraction and the number concentration. When the fraction is greater than the increase in number concentration, lower activated number concentration is achieved, as shown here.

As mentioned previously, within most of the scenarios, there is a decrease in fractional change as temperature increases, while both models experience a decrease in activated number concentration with increased temperature. This means the decrease in activated number concentration for MATRIX-VBS is not as significant as that for MATRIX. There are two factors that contribute to such a change. First, the heat and moisture diffusion term is dependent on temperature in the activation scheme (Abdul-Razzak and Ghan, 2000). Second, volatility of organics is temperature dependent. In MATRIX-VBS, when organic volatility is considered, the change is dampened. In other words, its number of activated particles is less sensitive to temperature change compared to MATRIX, leading to what we see in the circle plots, i.e., a greater change at lower temperatures.

The length of day and season changes the duration and intensity of gas-phase oxidation of semi-volatile gases, which is why we also looked at aerosol evolution driven by photochemistry

---

at different latitudes. Since the model uses January emissions, different seasons are simulated in the different hemispheres, while different day lengths are simulated at higher latitudes of the Southern Hemisphere compared to Northern Hemisphere tropical and high latitudes. As we inspected results across latitudes in the two hemispheres, we found varying activated number concentration in MATRIX-VBS compared to MATRIX and observed no evident trend. Such inconclusive and complex results may be due to gas phase chemistry and photochemical ageing of semi-volatile organic vapors, which would require further examination in a separate dedicated study.

### 3.4 Conclusions

With the inclusion of organic partitioning in an aerosol microphysics model, activated aerosol number concentration is decreased under most temperature and RH conditions, except when under low updrafts, in clean environments at most temperatures and RHs, and in polluted environments at high temperatures and extremely low-humidity conditions. Such changes are due to increased aerosol number concentration and smaller particles in the new model, as well as how number concentration and size are calculated in the chosen aerosol activation scheme, which determines how many particles are activated. Additionally, the temperature dependence of activated number concentration is decreased for most scenarios.

Our conclusion that fewer particles are activated at higher updrafts is in contrast to Connolly et al. (2014a), who found that fewer particles activated at low updrafts, using a different geometric standard deviation in the same parameterization of aerosol activation as the one we use. Such a difference can be due to the fact that the Abdul-Razzak and Ghan (2000) activation parameterization produces a different response when multiple modes are used, as shown by

---

Connolly et al. (2014b) and Simpson et al. (2014). Additionally, in our study, the geometric standard deviation remained constant per aerosol population. However, it is worth exploring in the future to use reduced geometric standard deviation in our calculations to directly compare with values used by Connolly et al. (2014a) and Crooks et al. (2018). In fact, in a comparison study, Ghan et al. (2011) found that the AbdulRazzak and Ghan (2000) scheme tends to have lower activation fractions and droplet concentrations compared to the Fountoukis and Nenes (2005) activation scheme.

Topping et al. (2013) showed that co-condensing organics lead to enhanced cloud droplet number concentration, which seems to contradict our results. However, it is important to note that contrary to Topping et al. (2013), our study is performed in a box model that does not resolve cloud droplet growth as the air mass rises and cools, which leads to additional condensation of organic vapors and water due to the temperature decline and contributes to cloud droplet growth due to additional water uptake. The simulations in this study, however comprehensive, are still highly idealized.

We would like to emphasize that our results do not imply that the Earth has fewer CCN than currently thought. Instead, they imply that if in a model, semi-volatile organics are simulated together with aerosol microphysics, a general decrease is to be expected, assuming our model captures all relevant contributory processes. We will investigate the effects of condensing organics in a global climate model in the future. The results presented here implicate that in the new model, most areas on Earth would experience fewer CCN on a typical day, but clean environments with above-freezing temperatures, or polluted environments on an extremely dry and hot day, would form more CCN under low-updraft-velocity conditions, compared to the old model. We expect

---

that implementing the improved box model on the global scale that includes a two-moment cloud microphysical scheme (Morrison and Gettelman, 2008; Gettelman and Morrison, 2015) would more accurately represent aerosol–cloud interactions, which will be our focus in a follow-up study. Thus it would offer us valuable insights into how the addition of process-level phenomena in aerosol microphysics, as applied here for the organics partitioning, would affect cloud microphysics in the global atmosphere and its implications for climate.

## **PART II**

### **Global Modeling**

## CHAPTER 4

# The global impact of organic aerosol volatility on particle microphysics and climate

### Abstract

We investigate the global performance of MATRIX-VBS, a new aerosol scheme that simulates organic partitioning in an aerosol microphysics model that has been developed in the box model framework in Gao et al. (2017). The scheme builds on its predecessor aerosol microphysics model MATRIX (Bauer et al., 2008), and it features the inclusion of organic partitioning between the gas and particle phases and the photochemical aging process using the volatility-basis set. The scheme's modular structure allows it to be used as a module in global models as well, and it has now been implemented in the Earth system model GISS ModelE (Miller et al., 2014a; Schmidt et al., 2014). To assess and evaluate the performance of the new model, we compared its mass concentration, number concentration, activated number concentration, and AOD, to the original scheme MATRIX, as well as against data from aircraft campaign ATom (Atmospheric Tomography Mission), ground measurement stations from AERONET (Aerosol Robotic Network), and satellite retrievals from MODIS (MODerate resolution Imaging Spectroradiometer) and CALIPSO (Cloud-Aerosol Lidar and Infrared Pathfinder Satellite Observations). Results show that organics are transported further away from sources, and their mass concentration increases aloft and decreases at the surface in MATRIX-VBS as compared to those in MATRIX. The surface mass concentration of organics agrees well with measurements but

there are discrepancies for vertical profiles aloft. In the new model, there is an increased number of particles and overall less activated ones (except for regions such as the highly polluted Eastern China) compared to those in the original MATRIX model. The difference in aerosol optical depth (AOD) between the two models can be due to smaller particles in the new model and the different aerosol compositions in the models. Compared to AERONET, MODIS and CALIPSO, both MATRIX and MATRIX-VBS overestimate AOD over source regions, with MATRIX-VBS having generally lower AOD, and underestimating biomass burning in the Amazon and Congo basins. Such result hint at the fact that by improving the representation of organic aerosols in the model did not necessarily improve its performance, even though it helped us understand aerosol processes better. Nevertheless, with future improvements on the representation of particle size distribution and more accurate volatility distribution for organic aerosol emissions, the model has the potential to perform better.

## 4.1 Introduction

It has been well-established that aerosols affect climate directly by absorbing and scattering solar radiation (aerosol–radiation interactions; Charlson et al., 1992) and indirectly by absorbing and scattering radiation (aerosol–cloud interactions, Twomey, 1974; Albrecht, 1989). By activating and acting as seeds for cloud formation, aerosols impact cloud microphysics (Myhre et al., 2013; Seinfeld and Pandis, 2016). Thanks to advances in measurement techniques, we know that organic aerosols are ubiquitous and a major component of atmospheric composition (Zhang et al., 2007), and our understanding of organic aerosol lifetime and its evolution has improved greatly (Jimenez et al., 2009; Shrivastava et al., 2017).



Primary organic aerosols are traditionally treated as nonvolatile in models, until Robinson et al. (2007) showed that organic aerosols are semi-volatile in nature and they can partition into the gas phase. Additionally, studies showed that organic aerosol formation is underestimated in models, and missing sources of secondary organic aerosols might be the cause (Heald et al., 2005; Volkamer et al., 2006; Hodzic et al., 2010; Spracklen et al., 2011). Measurements also show that most models underestimate organic aerosol concentrations (Tsigaridis et al., 2014). Recent studies tried to improve the organic aerosol representation in models and fill the gap between measurements and models by including semi-volatile primary organic aerosol (POA) and intermediate volatility organic compounds (IVOCs) as secondary organic aerosol (SOA) precursors (Lane et al., 2008; Shrivastava et al., 2008; Murphy and Pandis, 2009; Hodzic et al., 2010, 2016; Pye and Seinfeld, 2010; Tsimpidi et al., 2010, 2011, 2014, 2018; Jathar et al., 2011; Ahmadv et al., 2012; Athanasopoulou et al., 2013; Jo et al., 2013; Koo et al., 2014; Fountoukis et al., 2014; Ciarelli et al., 2017) using the volatility-basis set (VBS), an organic aerosol parameterization by Donahue et al. (2006) that resolves the volatility space of organic aerosols. However, when we include semi-volatile organics in models, they can alter aerosol concentration, composition, size distribution, CCN formation rates (Petters et al., 2006; Riipenen et al., 2011; Scott et al., 2015, Gao et al. 2018), hygroscopicity (Petters and Kreidenweis, 2007), and optics (Boucher et al., 2013; Myhre et al., 2013). In our study, we included semi-volatile organics in our model, and they also changed aerosol microphysics.

MATRIX-VBS was introduced as a box model previously by Gao et al. (2017, 2018). It was developed to include organic partitioning and its photochemical aging in an aerosol microphysics model MATRIX using the volatility basis set (VBS). This inclusion allowed organic

---

aerosols to not only coagulate with other aerosol populations, but also condense or evaporate, adding growth and loss pathways for different organic-containing populations.

During its box model stage, it was not feasible to compare and evaluate its simulation results against observational data, since the box model was missing critical processes such as transport, dilution and deposition. Now, the model scheme has been implemented in the global model GISS ModelE, and in order to evaluate its performance, we compare its simulations against the original model MATRIX, on which MATRIX-VBS is based, as well as observational data of vertical mass concentration for organic aerosols from the recently deployed aircraft campaign ATom (Atmospheric Tomography Mission), aerosol optical depth from ground measurement stations from AERONET (Aerosol Robotic Network), and satellite retrievals from MODIS (MODerate resolution Imaging Spectroradiometer) and CALIPSO (Cloud-Aerosol Lidar and Infrared Pathfinder Satellite Observations). Even though organic aerosols do not have a very strong signal in aerosol optical depth (AOD), AOD is the best globally observed aerosol property and a key step to link aerosol composition to forcing, which is the ultimate goal of this climate modeling work, even if not discussed here.

Available measurement data, such as those from AERONET stations used in this study as well as data from IMPROVE (Interagency Monitoring of Protected Visual Environments), are usually concentrated in the United States and Europe, with few stations in remote regions, such as boreal forests and marine regions in the Southern Hemisphere, and this presents a challenge when evaluating models, especially since remote regions are usually not understood well (Tsigaridis et al., 2014).

---

## 4.2 Model description

### 4.2.1 GISS ModelE

We use GISS ModelE Earth System Model version 2.1 (GISS-E2.1), which is an updated version of version 2 (GISS-E2; Miller et al., 2014a; Schmidt et al., 2014), which is NASA's climate model that includes the aerosol microphysics scheme MATRIX (Bauer et al. 2008; 2010; Bauer and Menon, 2012). Aside from updates such as corrections to radiative transfer, ocean mixing, and sea ice thermodynamics, the updated model has the same resolution of 2 degrees by 2.5 degrees horizontally with 40 vertical layers as GISS-E2, and the model top is at 0.1hPa.

A CMIP-class Earth System Model, GISS ModelE includes emissions of gaseous and aerosol species, interactive gas phase chemistry, aerosol processing, gas-aerosol interactions, dry and wet removal of atmospheric constituents, direct and indirect aerosol effects, cloud processes, radiative transfer and interaction with aerosols and gases, atmospheric circulation, dynamic vegetation, and optionally, oceanic circulation, among others. The basic structure of the model has been described in previous studies that simulate preindustrial, present, and future climate conditions (e.g. Miller et al., 2014a, Nazarenko et al., 2015), atmospheric composition studies (e.g. Bauer et al., 2010; Bauer and Menon, 2012; Bauer et al., 2013, Shindell et al., 2013, Tsigaridis et al., 2013, 2014), among others. GISS ModelE is open source and available to everyone.

### 4.2.2 MATRIX-VBS

As described in Gao et al. (2017, 2018), MATRIX-VBS is an aerosol microphysics model that includes the MATRIX (Multiconfiguration Aerosol Tracker of mIXing state) and VBS schemes. MATRIX is an aerosol microphysical scheme which resolves aerosol mass and number

concentrations, as well as aerosol mixing state. It represents new particle formation, growth via condensation (except organics) and coagulation among different aerosol populations, particle emissions, gas-particle mass transfer, and aerosol phase chemistry (Bauer et al., 2008). MATRIX can be used as a box model or a module in a global model.

The volatility-basis set VBS is an organic aerosol volatility framework that divides semi-volatile organic compounds into logarithmically-spaced classes of effective saturation concentrations, which are used for the partitioning between the gas and particulate phases (Donahue et al., 2006). VBS framework has been coupled with MATRIX in a box model (Gao et al., 2017, 2018), and the new scheme MATRIX-VBS (Gao et al., 2017) is implemented into the global model, GISS ModelE. The new MATRIX-VBS scheme advanced the representation of organic aerosols in MATRIX by making organics semi-volatile and able to condense onto and evaporate from aerosols, improving the traditional and simplistic treatment of organic aerosols as non-volatile.

### 4.3 Methodology

The development of the new model MATRIX-VBS was completed in the box model framework and is presented in Gao et al. (2017, 2018). The model has been implemented into GISS ModelE as an aerosol microphysics module, same as its predecessor, MATRIX. We performed two model experiments, one for MATRIX and one for MATRIX-VBS. The experiments were simulated and nudged to NCEP (National Center for Environmental Prediction) horizontal winds under transient conditions for 6 years. The experiments began in 2011, with the years 2011-2015 serving as a spinup. The year 2016 is analyzed in this study, as the available data from the ATom project are from summer 2016 and winter 2017 (but some satellite retrievals we

currently have do not extend to 2017). Natural and anthropogenic fluxes are taken from the CMIP6 inventory (Hoesly et al., 2018; van Marle et al., 2017), whereas sea salt and dust emissions are interactively calculated.

The ATom (Atom Science Team, 2018) project surveyed global cross-sections of aerosol composition in the remote troposphere, while flying ascents and descents and making vertical profiles (0.15 to 12 km) over the Pacific and Atlantic Oceans from approximately 80°N to approximately 65°S (Kupc et al., 2018). It is useful in identifying the aerosols in the remote troposphere from continental sources and quantifying the growth of particles into cloud activating sizes (Williamson et al., 2018). It did not chase plumes but used unbiased sampling, which is helpful for us to validate models on a global scale (Strode et al., 2018). Here, we use the ATom datasets currently available, which are two sets of data from summer 2016 (ATom-1) and winter 2017(ATom-2), to evaluate our simulated organic aerosol mass concentration.

To evaluate modeled aerosol optical depth, we use measurements from AERONET (Aerosol Robotic Network), MODIS (MODerate resolution Imaging Spectroradiometer), and CALIPSO (Cloud-Aerosol Lidar and Infrared Pathfinder Satellite Observations), as they provide column aerosol optical depth (AOD) and vertical profiles. AERONET observations (Holben et al., 1998) and MODIS Terra Collection 6 Level 3 (Platnick et al. 2015) provide column aerosol optical depth. CALIOP (Cloud-Aerosol Lidar with Orthogonal Polarization) Layer Product 3.0 from the CALIPSO mission (Winker et al., 2009) provides aerosol extinction profiles. Additionally, the CALIPSO aerosol extinction profiles were averaged according to Koffi et al. (2016).

## 4.4 Results and discussion

### 4.4.1 Organic aerosol mass

#### 4.4.1.1 Model version comparison

The annual mean burden of organic aerosols in MATRIX and MATRIX-VBS are shown in Figures 4.1.1, and their load differences are in Figure 4.1.2. The large scale spatial distributions are generally similar in the two models, but show significant differences on the regional scale. The high mass loads are over anthropogenic polluted areas, such as China, India, and the Eastern United States, over biomass burning areas, such as boreal forests in Russia, North America, as well as Congo and Amazon basins, with extensions over the oceans (e.g. the Atlantic Ocean, off the coast of Central Africa) due to transport from their continental organic aerosol sources. The emitted organics dilute in both models when they are transported from source regions downwind and over the oceans, but due to the difference in emissions, the mass concentration in remote regions are different in the two models.

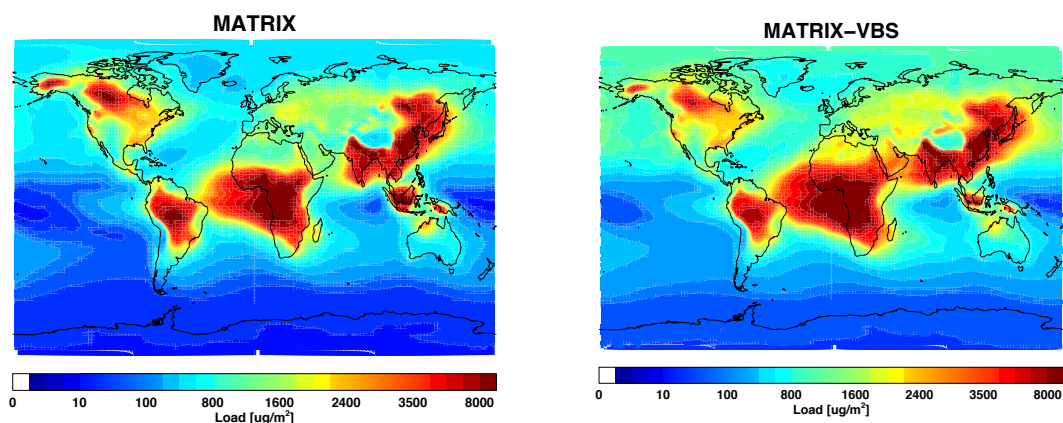


Figure 4.1.1 Annual mean mass load of organic aerosol in MATRIX ( $0.86 \mu\text{g}/\text{m}^2$ ) and MATRIX-VBS ( $1.09 \mu\text{g}/\text{m}^2$ ).

In MATRIX-VBS, organics can not only be diluted but also evaporate into the gas phase. The gases can become oxidized and condense again into the aerosol phase. This process allows the semi-volatile organics in MATRIX-VBS to travel further away from their sources, including to higher elevation. Therefore, there is higher organic aerosol concentration over remote regions in the Northern Hemisphere, such as the Sahara, the Middle East, and the Pacific Ocean. In contrast, in MATRIX, the organic aerosol spatial distribution is more distinctive, less extensively distributed and with higher concentrations near source regions.

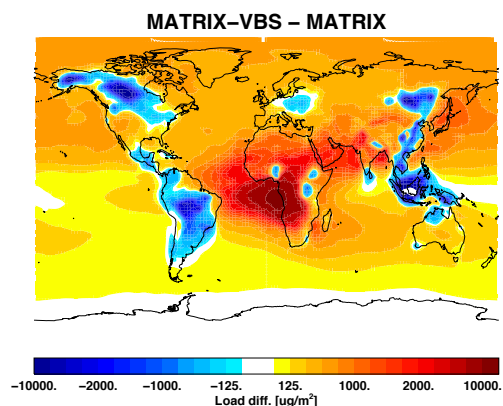


Figure 4.1.2 Difference in annual mean organic aerosol mass loads between MATRIX and MATRIX-VBS ( $0.22 \mu\text{g}/\text{m}^2$ ).

The differences between the two models is shown in Figure 4.1.2, where the organic aerosol load is higher in most regions in MATRIX-VBS except for North America, Central America, Amazon, Eastern Europe, East Africa, Southeast Asia, and Northeast China. Most prominently, the aerosol concentration is higher in Central Africa and its adjacent oceanic regions due to transport. Lower organics load in regions such as North America, Russia, and North Europe, can be caused by organics from biomass burning in boreal forests that do not oxidize much due to lower photochemical activity at high latitudes. There is also a more significant difference over the oceans in the high latitudes in the Northern Hemisphere, because even though organics are

---

transported to the Arctic in both models, semi-volatile organics in MATRIX-VBS can evaporate, transport further, and condense more readily into the aerosol phase under colder temperatures and after gaseous photochemical oxidation.

Additionally, the general difference in magnitudes of the mass loads between the models is also caused by the mass-based emission factor (Shrivastava et al., 2008) applied to POA emissions for the IVOC contribution in MATRIX-VBS, which makes its emissions 2.5 times that of the POA emissions in MATRIX, as mentioned in Chapter 2 for the box model, and more details on the emission factors for each volatility bin are shown in Table 2.2.

The zonal mean mass concentrations peak ( $1\mu\text{g}/\text{m}^2$ ) over the Northern Hemisphere mid-latitudes and tropics from the surface up to 750 hPa in MATRIX-VBS and up to 850 hPa in MATRIX (Figure 4.1.3). The zonal mean is lower in the mid-latitudes and tropics from the surface up to 850hPa, and it is higher aloft as well as at high latitudes in the Northern Hemisphere for MATRIX-VBS compared to that for MATRIX. The peak positive difference between MATRIX and MATRIX-VBS is close to the tropics at  $10^\circ\text{S}$  from 800 hPa to 650 hPa, and peak negative difference is at the surface from the tropics to the mid-latitudes in the Northern Hemisphere (Figure 4.1.4). There are more organics in MATRIX-VBS aloft and less at the surface because semi-volatile organics can evaporate, transport vertically and oxidize at higher altitudes, where there are also lower temperatures that help organics condense. Additionally, those organics at higher altitudes are less likely to be removed via deposition, since wet deposition occurs in and below clouds and dry deposition occurs at the surface layer.



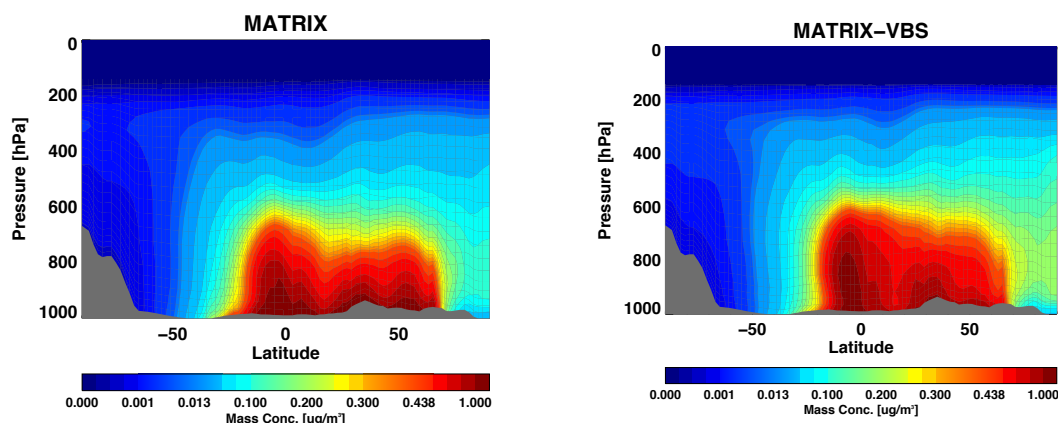


Figure 4.1.3 Annual mean zonal organic aerosol mass concentration in MATRIX and MATRIX-VBS.

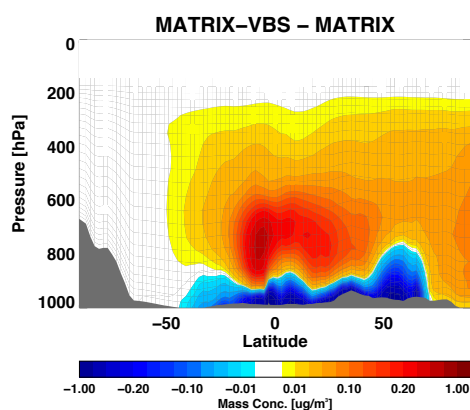


Figure 4.1.4 Difference in the annual mean zonal organic aerosol mass concentrations between MATRIX and MATRIX-VBS.

#### 4.4.1.2 Evaluation

In order to evaluate the difference in organic aerosol mass concentration between the two models, we compare it to the mass concentration measured from the ATom aircraft campaign, which profiled the global cross-sections of aerosol composition over the Pacific and Atlantic Oceans, as well as some over the Continental United States. Since ATom-1 is deployed from July 28 to August 22, 2016, and ATom-2 was deployed from January 26 to February 22, 2017, we

simulated and compared the modeled monthly mean organic aerosol mass concentrations in August 2016 (Figure 4.1.5) and February 2017 (Figure 4.1.7) between the two models, and we compared the two model results against ATom-1 (Figure 4.1.6) and ATom-2 (Figure 4.1.8) measurements for the two months simulated.

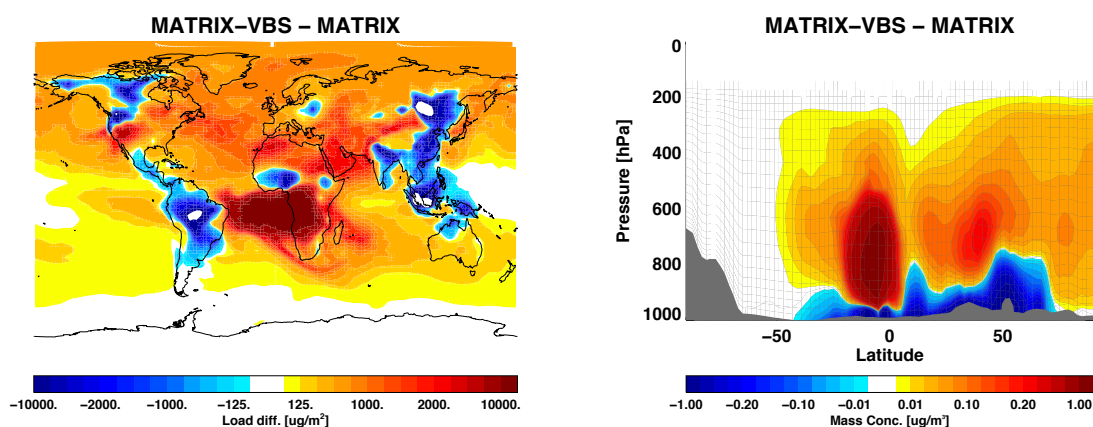


Figure 4.1.5 Difference in monthly mean spatial ( $0.46 \mu\text{g}/\text{m}^2$ ) and zonal organic aerosol mass loads between MATRIX and MATRIX-VBS for August 2016.

Shown in Figure 4.1.5, the difference in the monthly mean organic aerosol mass loads between the two models for August 2016 is similar to that for the annual mean organic aerosol mass load in 2016 (Figure 4.1.2). The main difference between the two comparisons is that the difference is more intensified in August 2016. Where there were higher annual mean loads in MATRIX-VBS, there is even higher load for the monthly mean in August, and where there were lower annual mean loads in MATRIX-VBS, there is an even lower load for the monthly mean of August.

The vertical difference between the annual mean and the August monthly mean is that there is higher concentration aloft in MATRIX-VBS. Whereas the annual mean difference peaks over  $10^\circ\text{S}$  from 800 hPa to 650 hPa, the monthly mean peak difference has a wider range, from 900 hPa to 650 hPa. There is also an additional intensified difference peak aloft over the mid-latitudes in

the Northern Hemisphere. These spatial and vertical differences between the annual and monthly mean mass loads can be explained by the different assumptions of volatility for organic emissions, such as biomass burning in Central Africa, as well as by the higher temperatures in the summer months for the Northern Hemisphere that changed the behavior of semi-volatile organics in the new model.

To see which model simulated the more accurate results, we compared them against ATom measurements (Figure 4.1.6 for ATom-1, Figure 4.1.8 for ATom-2). The ATom campaign flight routes are illustrated in the maps in the top row, with blue marks at airports. Each plot in the figure represents a measured region. The first column is over the Pacific Ocean, the second column over 120°W, the third column over the Continental United States, and the last column over the Atlantic Ocean. From top to bottom, each row represents a range of 30 degrees latitude, such as 60°N to 90°N, listed on the left margin of the figure.

The modeled August 2016 monthly mean and ATom-1 mass concentration profiles are shown in Figure 4.1.6. In general, both models agree well with the measurements at the surface, however, there are greater discrepancies aloft between models and against measurements. As discussed before, at high latitudes in the Northern Hemisphere, MATRIX-VBS has higher mass concentration than MATRIX does, however, neither model agrees well with measurements there.

So even though it can be explained that semi-volatile organics in MATRIX-VBS increased over high latitudes, it is not clearly evident from these measurements that this leads to a better match. Note that although we are simulating the year 2016 as needed, we used CMIP6 inventory that only provided emissions until 2015, including biomass burning, which can make a big difference in high altitudes during August due to boreal forest fires.

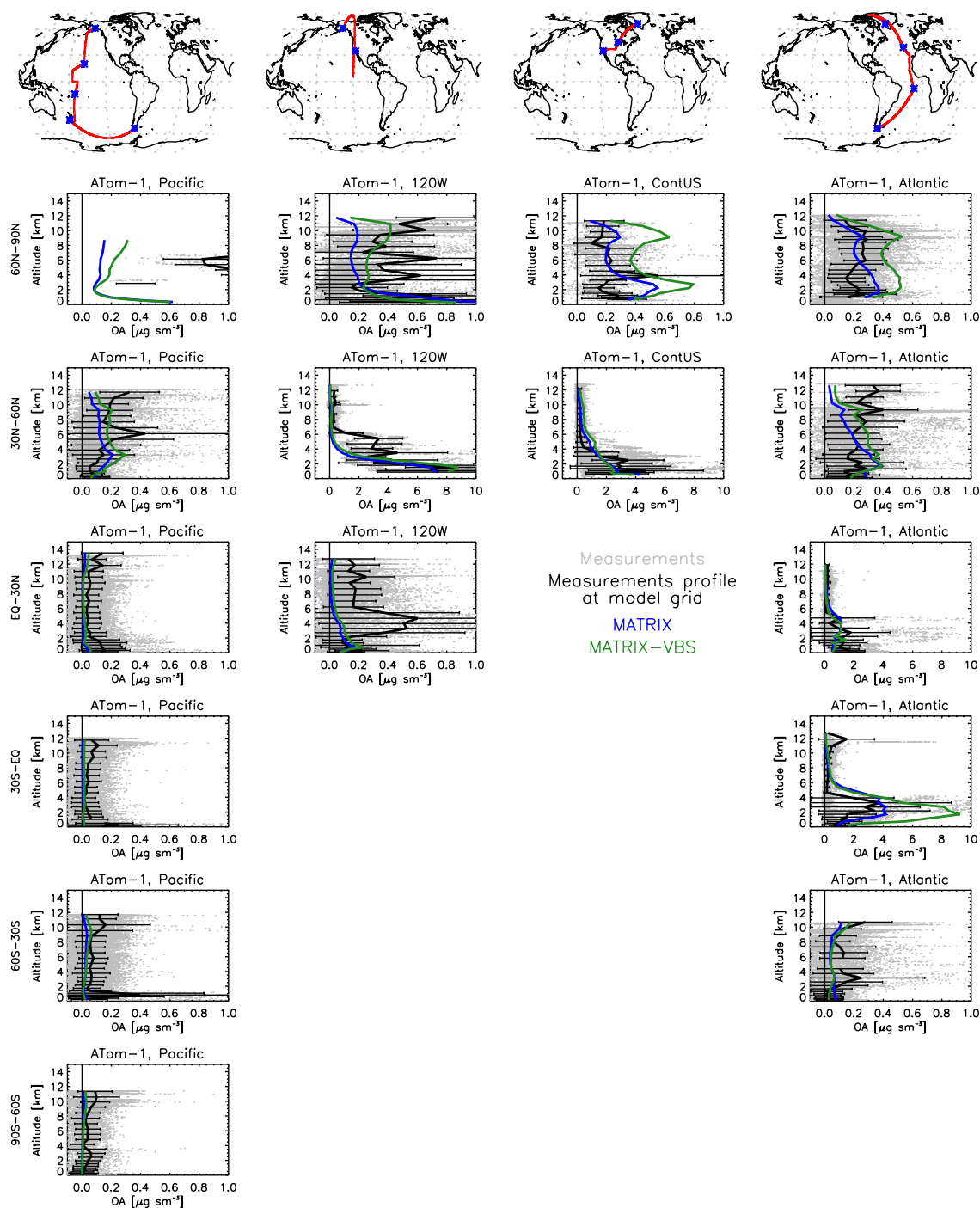


Figure 4.1.6 Vertical profiles of organic aerosol mass concentration for MATRIX (blue), MATRIX-VBS (green) for August 2016 and Atom-1 measurements (grey and averaged in black).

In other regions, both models compare similarly, except for 30°S-EQ over the Atlantic, where MATRIX performs extremely well with ATom, but MATRIX-VBS overestimates the peak concentration by more than double. This region will be examined further later in this chapter. Two regions that both models performed well against ATom are northern mid-latitudes over the Continental U.S. and EQ-30°N over the Atlantic. South Pacific Ocean regions have low concentrations that also agree well with ATom, which is expected as they are far from continental sources of organic aerosols.

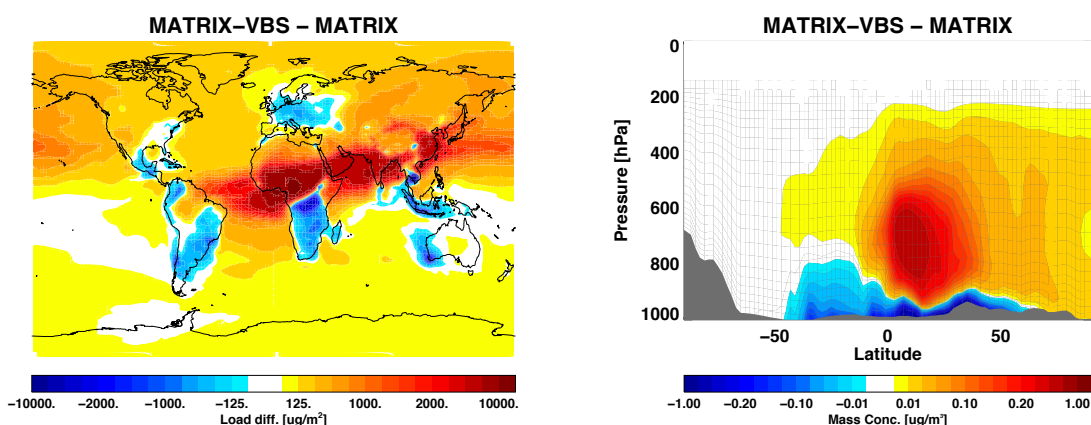


Figure 4.1.7 Difference in monthly mean spatial ( $0.25 \mu\text{g}/\text{m}^2$ ) and zonal organic aerosol mass loads between MATRIX and MATRIX-VBS for February 2017.

As for the winter, the difference between modeled February 2017 monthly mean is shown in Figure 4.1.7, and their comparison against ATom-2 mass concentration profiles are shown in Figure 4.1.8. The winter month organic aerosol mass concentration looks different from the annual and summer month mean mass concentrations. The signs in the difference have reversed over North America, East China, India, Central and South of Africa, as well as part of Amazon. These differences between the two seasons are due to the season change. Over the Northern Hemisphere, which is experiencing cold winter, has more readily condensed organics under cold temperatures, whereas over the Southern Hemisphere, which is experiencing hot summer, sees more evaporated

---

organics into the gas phase. This is also shown in the zonal mass loads in Figure 4.1.7, which shows a peak positive difference aloft from 850 hPa to 600 hPa near 15°N and a greater range of negative difference in the Southern Hemisphere from the surface up to 800 hPa. Compared to ATom-2, in general, both models underestimate mass concentration as compared to measurements, especially over the Pacific and Atlantic Oceans. There are still discrepancies of mass concentration over the northern high latitudes, but not as significant as it was in the summer as compared to ATom-1. At northern mid-latitudes over the Continental U.S. over 30°N-60°N the model continues to perform well.

Additionally, mass concentration of black carbon, nitrate, and sulfate are very similar between the two models. In both seasons, black carbon mass concentration from two models match ATom measurements very well, whereas nitrate is generally underestimated in the models, and sulfate is generally overestimated.

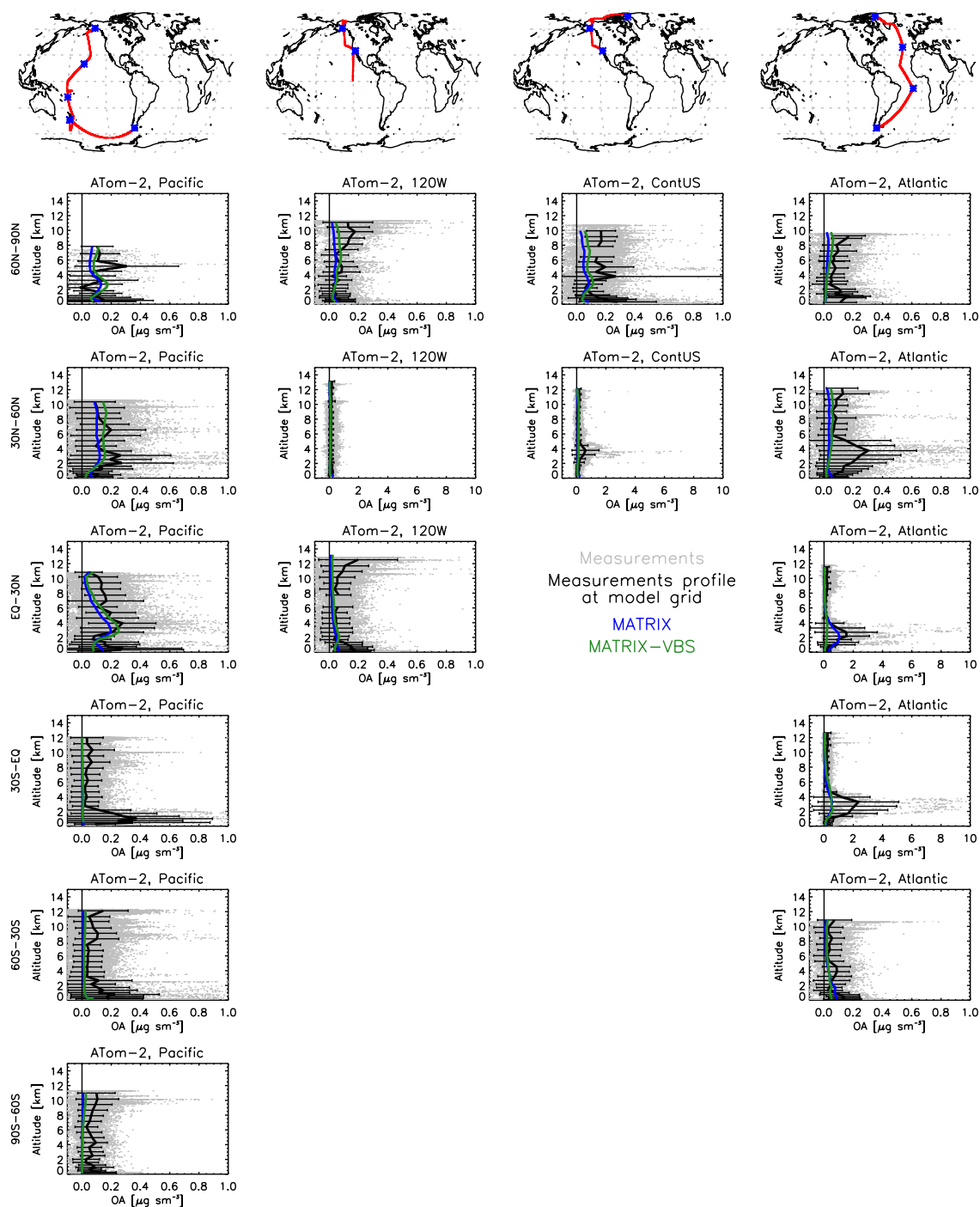


Figure 4.1.8 Vertical profiles of organic aerosol mass concentration for MATRIX (blue), MATRIX-VBS (green) for February 2017 and Atom-1 measurements (grey and averaged in black).

#### 4.4.2 Aerosol number concentration

The spatial distributions of near surface, lowest model layer, number concentration of organic-containing populations is very similar between the two models (Figure 4.2.1); however, their difference in magnitude is more pronounced (Figure 4.2.2). There is higher near surface number concentration in MATRIX-VBS than in MATRIX over continents and oceans, but lower near surface number concentration over high latitudes in the Southern Hemisphere and a few small regions, such as off the coast of Mexico and Hawaii. This difference is consistent with results from the box model simulations, where there was higher number concentration in MATRIX-VBS than in MATRIX (Gao et al., 2017, 2018). Zonally, the difference between number concentration of MATRIX-VBS and that of MATRIX is the same at the surface as discussed (zonal difference in Figure 4.2.2). Aloft, there are more particles in the mid-latitudes in MATRIX-VBS, due to the semi-volatile organics that partition, leading to higher aerosol number concentration.

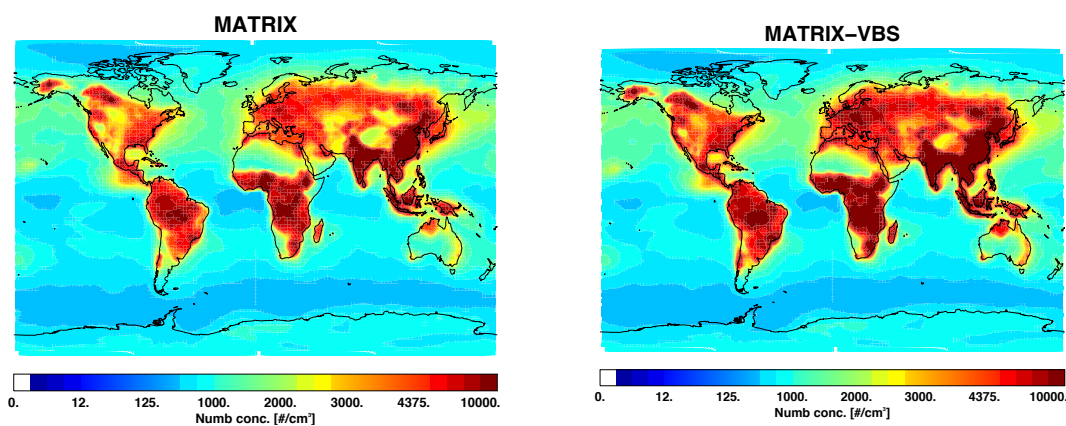


Figure 4.2.1 Total surface number concentration of organic-containing populations in MATRIX (4984 /cm<sup>3</sup>) and MATRIX-VBS (5636 /cm<sup>3</sup>).



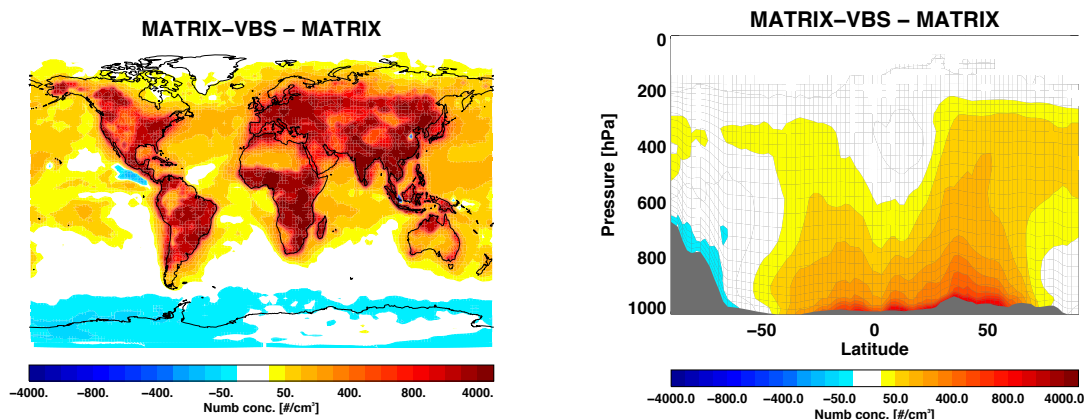


Figure 4.2.2 Difference in annual mean surface ( $652 \text{ /cm}^3$ ) and zonal number concentrations (MATRIX-VBS minus MATRIX) of organic-containing aerosol populations between the two models.

Taking a more detailed look at the number concentration for each of the organic-containing populations (Figure 4.2.3, for detailed aerosol composition descriptions of the aerosol populations, see Table 2.1 in Chapter 2), the decrease in MATRIX-VBS in high latitude in the Southern Hemisphere is due to ACC. Even though there are decreased number concentrations over most of the continental regions for ACC (East United States, Central America, Eastern South America, Africa, Europe, Southeast Asia), BC1, BC2, BOC, and BCS, they are overcompensated by the increased number concentration over the continents in OCC, OCS, and BOC. This is consistent with previous results that showed increased number concentration for OCC, OCS and BOC due to more emitted OCC that condense on and coagulate with ACC and BC1 (or BC2) to form OCS and BOC, respectively. The increase over the oceans is due to ACC, OCC, and OCS.

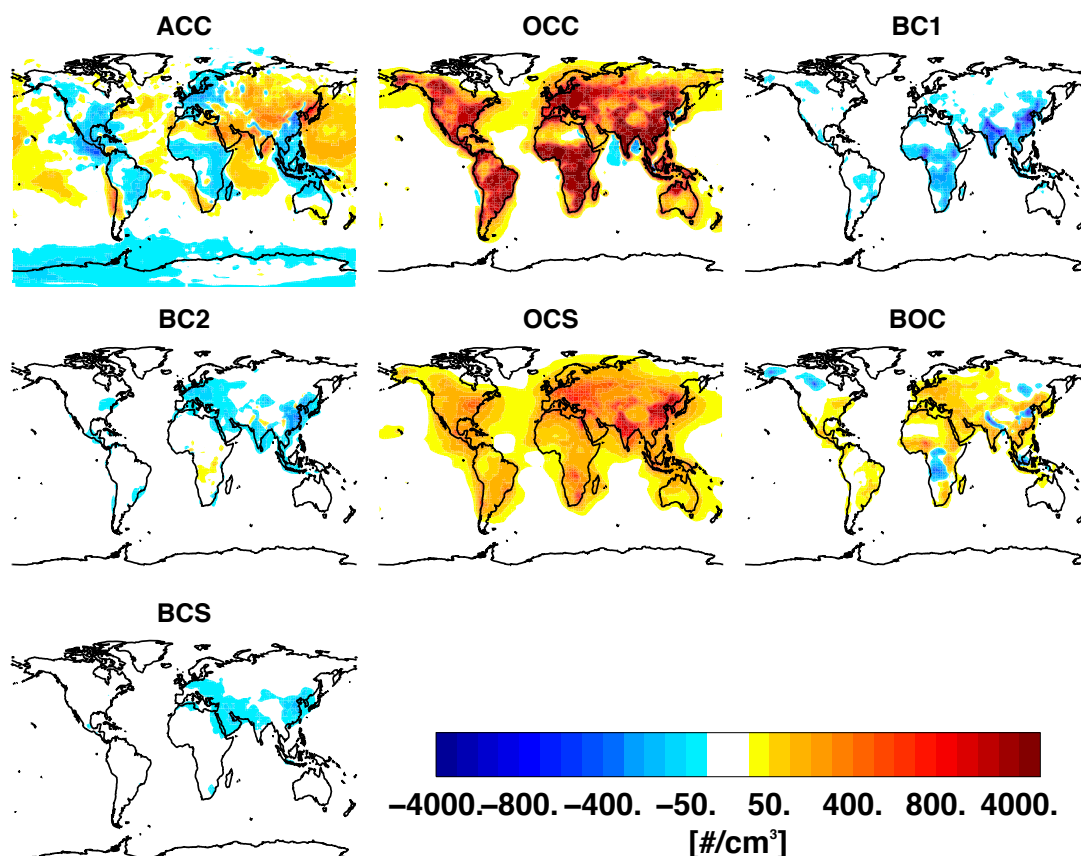


Figure 4.2.3 Annual mean surface number concentration differences (MATRIX-VBS minus MATRIX) in individual organic-containing aerosol populations: ACC (885 /cm<sup>3</sup>), OCC (1517 /cm<sup>3</sup>), BC1 (32 /cm<sup>3</sup>), BC2 (23 /cm<sup>3</sup>), OCS (231 /cm<sup>3</sup>), BOC (115 /cm<sup>3</sup>) and BCS (6 /cm<sup>3</sup>).

#### 4.4.3 Activated Number Concentration

Following the discussion in Chapter 3, we also looked at activated cloud number concentration at the surface (Figure 4.3.1). Consistent with our results from Chapter 3, most regions around the globe have less active number concentration, except for some regions such as East China and India, and high latitudes in the Southern Hemisphere (Figure 4.3.2). Our conclusion from Chapter 3 showed that polluted regions with high temperatures or low relative humidities

and cleaner regions with low updraft velocities would have higher activated number concentration in MATRIX-VBS than in MATRIX.

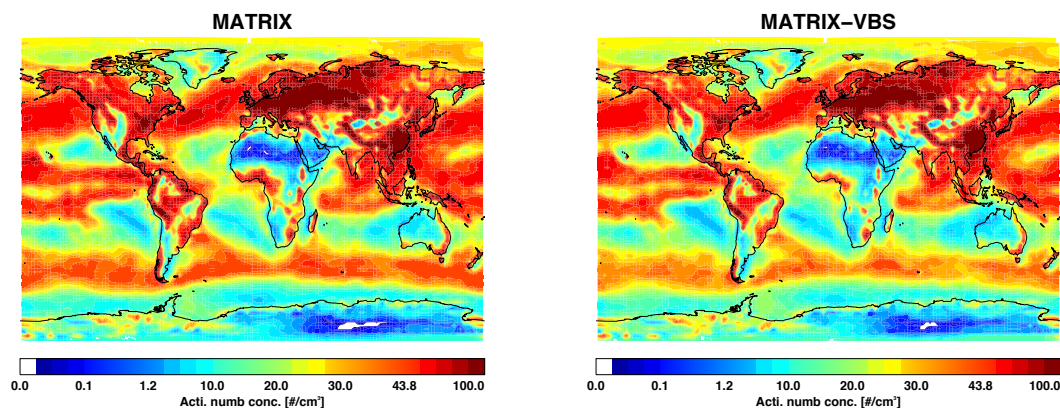


Figure 4.3.1 Annual mean total surface activated number concentration of organic-containing populations in MATRIX ( $36 / \text{cm}^3$ ) and MATRIX-VBS ( $33 / \text{cm}^3$ ).

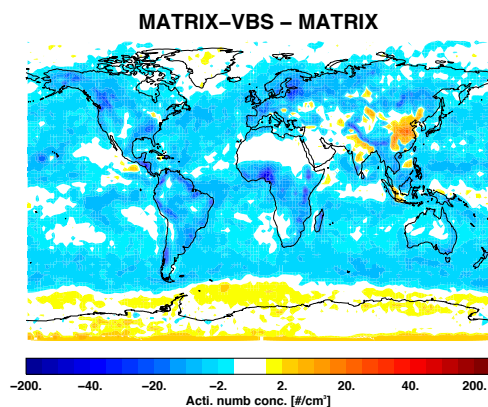


Figure 4.3.2 Difference in annual mean total surface activated number concentration (MATRIX-VBS minus MATRIX) between the two models ( $-3 / \text{cm}^3$ ).

Populations ACC, OCC, OCS, BOC, and BCS are dominating the activated number concentration due to their composition, size, and number concentration, as discussed in Chapter 3. Upon further inspection of each of these aerosol population in Figure 4.3.3, the increase in activated number concentration in MATRIX-VBS at high latitude over the Southern Hemisphere

is due to the ACC population, and over Eastern China and India are due to the regional increase in BOC and OCS populations. Even though BOC and OCS have increased activated number concentrations over Europe and Eastern United States, they are offset by those for ACC, OCC, and BCS populations. As previously discussed in Chapter 3, the number concentration increases in the OCC population, but the activated number concentration has decreased. However, the number concentration and activated number concentration for the OCS population both increased, and there is no consistency between the number concentration and activated number concentration for populations ACC and BOC, which means their sizes affect how many particles would activate. Size distribution of these aerosols will be examined later.

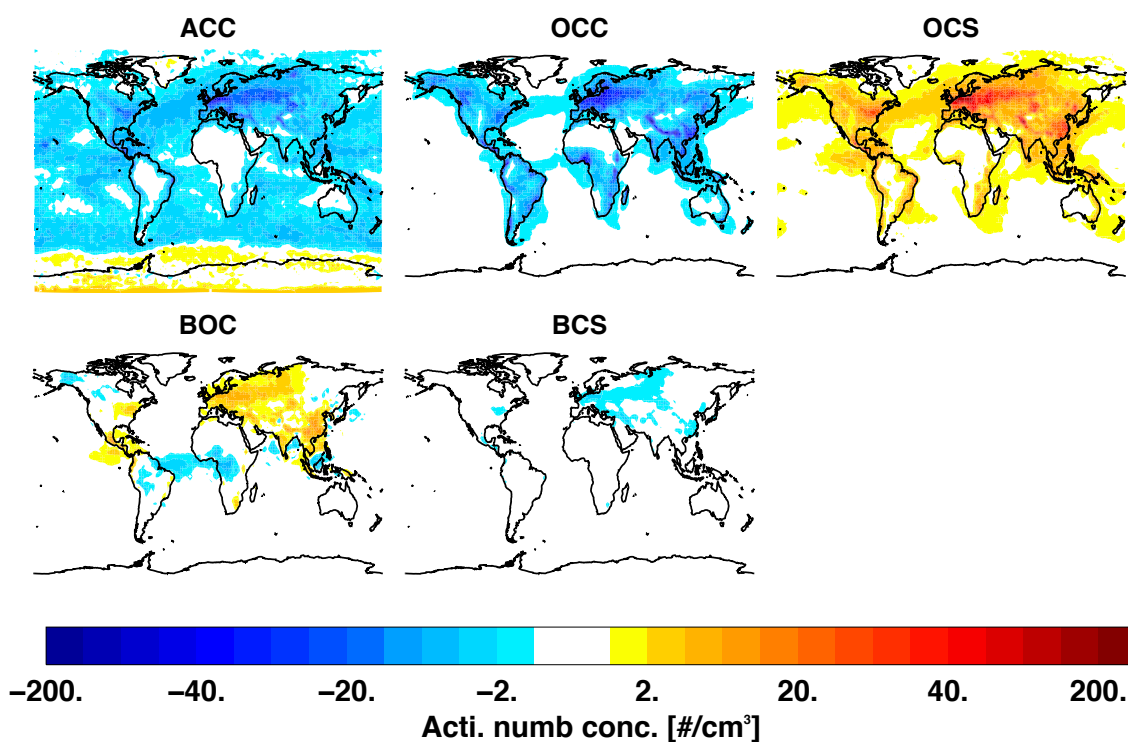


Figure 4.3.3 Annual mean surface activated number concentration differences (MATRIX-VBS minus MATRIX) in major organic-containing aerosol populations: ACC ( $-3.3 \text{ /cm}^3$ ), OCC ( $-2.6 \text{ /cm}^3$ ), OCS ( $2.8 \text{ /cm}^3$ ), BOC ( $0.2 \text{ /cm}^3$ ) and BCS ( $-0.2 \text{ /cm}^3$ ).

#### 4.4.4 Aerosol Optical Depth

The total annual mean clear sky AOD in MATRIX and MATRIX-VBS are shown in Figure 4.4.1. The difference between the two models are most prominent in polluted regions (Figure 4.4.2), such as biomass burning prominent regions Northwest of North America, Amazon basin, Africa, and anthropogenically polluted regions Eastern China, India, and Southeast Asia. To examine more closely the cause of the differences, we also compared the seasonal differences between the two models in Figure 4.4.3. We see that the major differences occur in seasonal biomass burning regions, especially prominent are the Africa plume in winter, boreal regions over North America and biomass burning in the Congo basin in the summer (North Hemisphere), and biomass burning in Indonesia in the fall (North Hemisphere). During those seasons, MATRIX-VBS has significantly lower (-0.5) AOD as compared to MATRIX.

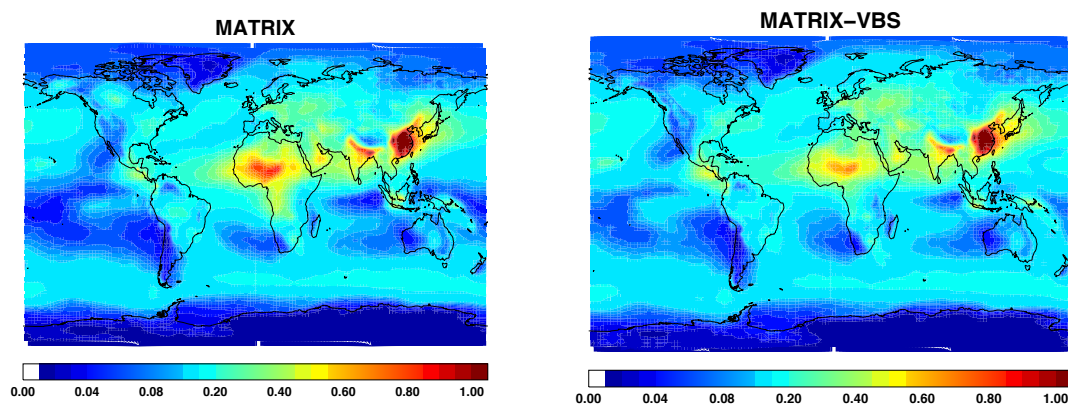


Figure 4.4.1 Annual mean total aerosol optical depth in MATRIX (0.159) and MATRIX-VBS (0.161).



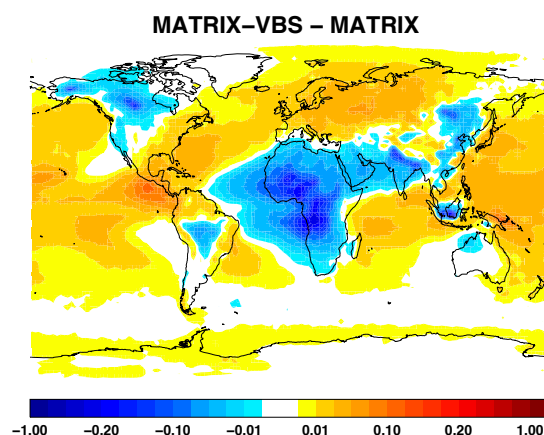


Figure 4.4.2 Difference in annual mean total aerosol optical depth between MATRIX and MATRIX-VBS (0.003).

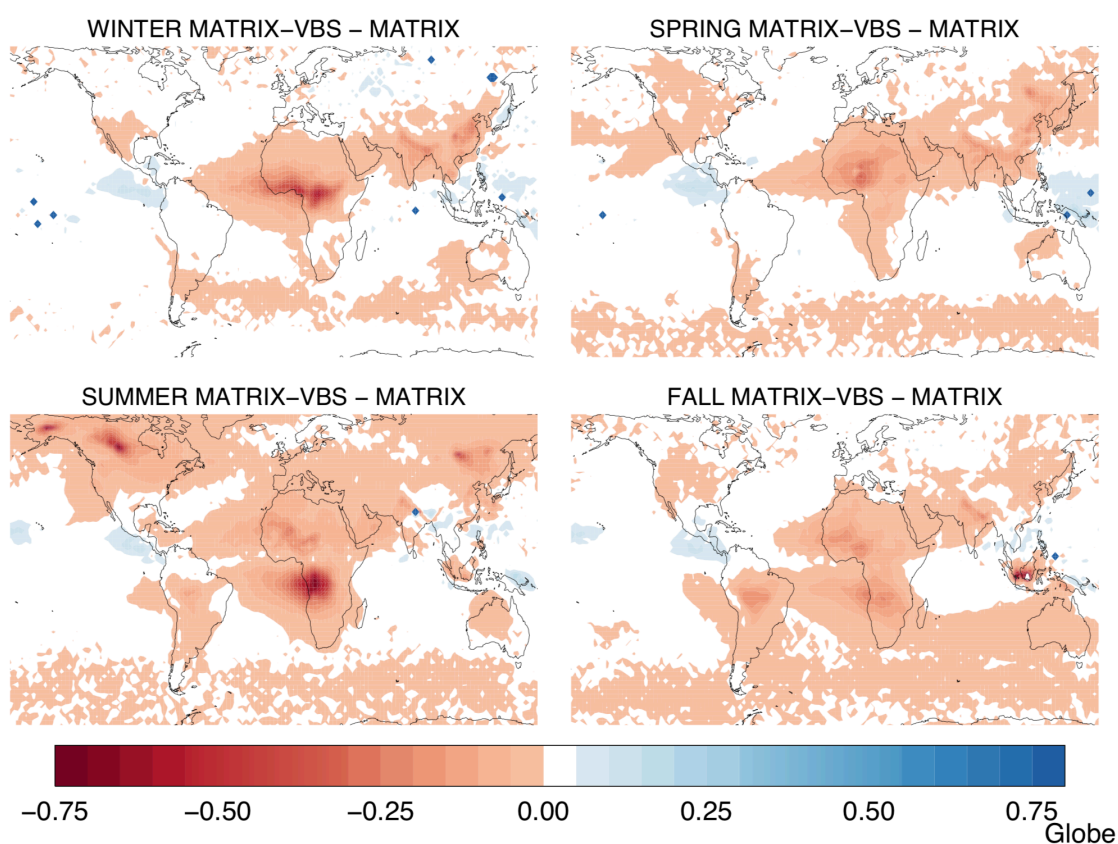


Figure 4.4.3 Difference in seasonal aerosol optical depth between MATRIX and MATRIX-VBS. Winter months are DJF, spring months are MAM, summer months are JJA, and fall months are SON.

To evaluate the model results, we compared them against seasonal AOD with retrievals from the MODIS satellite (Figure 4.4.4) and the ground-based AERONET (Figure 4.4.5) for the year 2016, same as the year simulated for our models. Compared to MODIS, both models overestimate AOD over anthropogenic polluted regions such as China and India as well as biomass burning regions such as central Africa. Over the oceans, both models underestimate AOD as compared to MODIS. Most strikingly, MATRIX-VBS does not capture the Congo basin biomass burning plume shown in MODIS as MATRIX does. Seasonally, MATRIX-VBS is underestimating the Congo basin plume in summer (JJA) and fall (SON), as well as the Amazon basin plume in the fall. A statistical analysis performed using seasonal mean MODIS and model data over the globe where MODIS reported data shows MATRIX correlate better with MODIS in all seasons (Table 4.1).

Table 4.1 Mean, standard deviation and correlation coefficient for seasonal mean AOD from MATRIX and MATRIX-VBS data against MODIS.

	MATRIX				MATRIX-VBS			
	Winter	Spring	Summer	Fall	Winter	Spring	Summer	Fall
Mean	0.25	0.19	0.27	0.22	0.20	0.17	0.19	0.17
Stdev	0.26	0.18	0.23	0.18	0.17	0.13	0.16	0.13
r	0.71	0.53	0.67	0.48	0.63	0.51	0.49	0.34
MODIS mean	0.28	0.21	0.28	0.24				

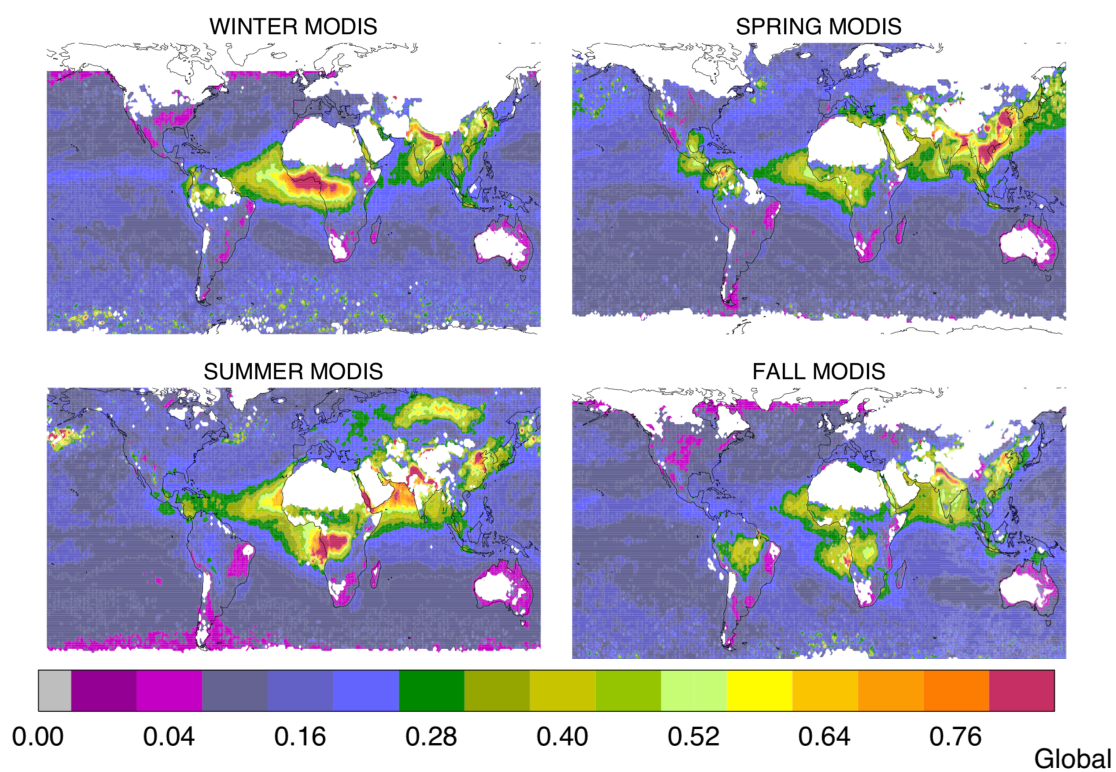


Figure 4.4.4 Seasonal column aerosol optical depth from MODIS.



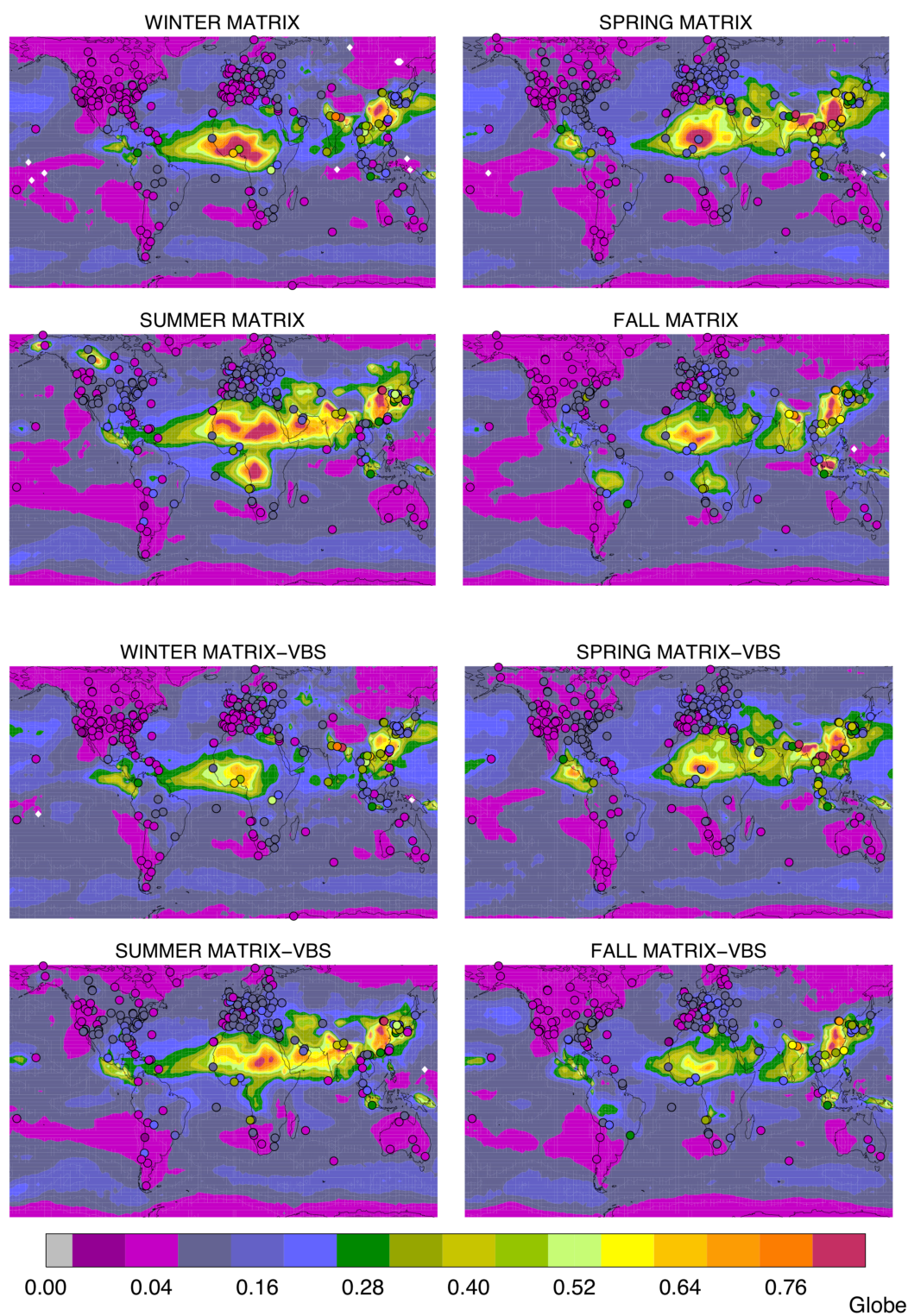


Figure 4.4.5 Seasonal aerosol optical depth for MATRIX (top) and MATRIX-VBS (bottom) with AERONET measurements over-plotted.

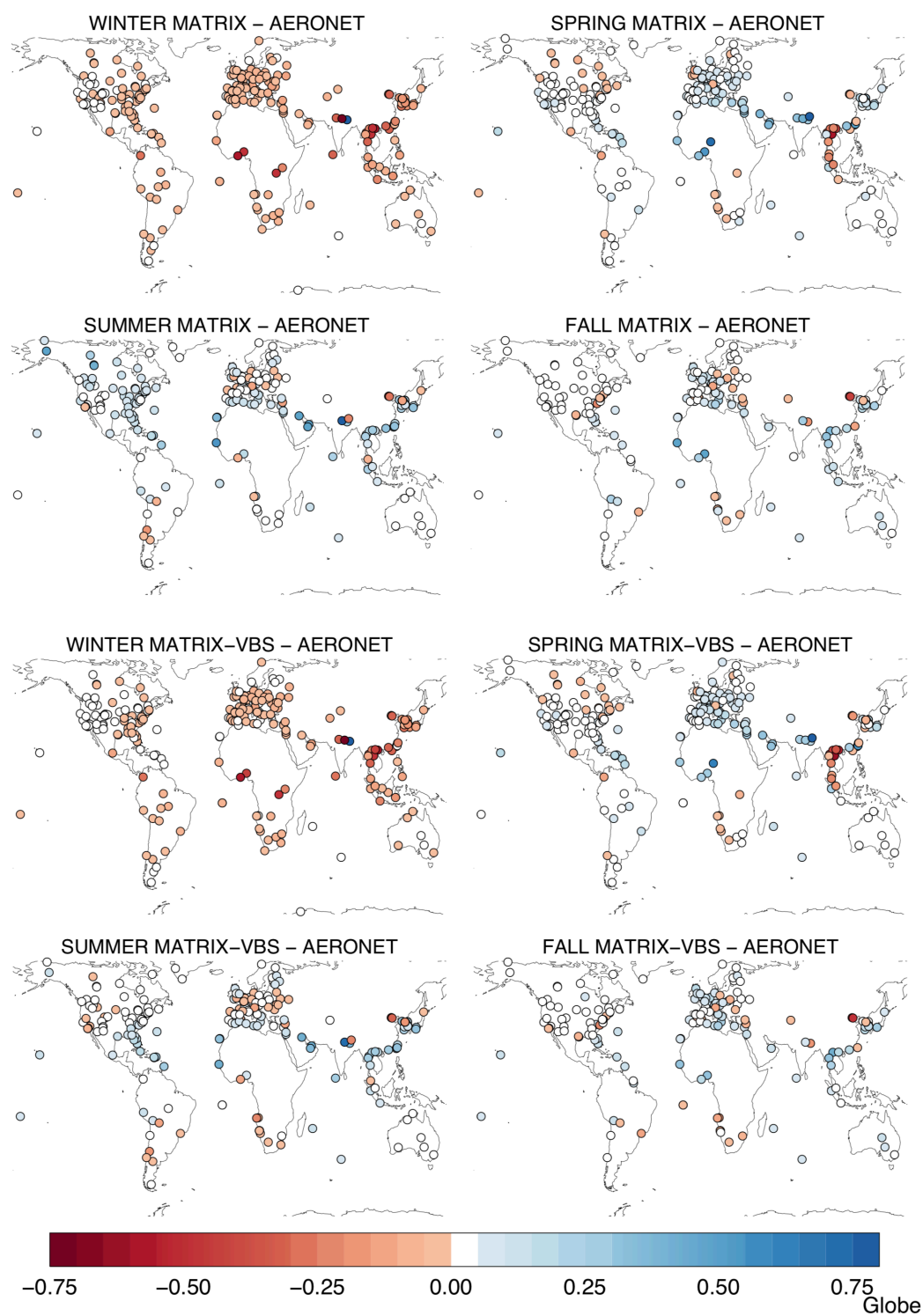


Figure 4.4.6 Seasonal difference in aerosol optical depth between the two models and AERONET measurements.

Table 4.2 Mean, standard deviation and correlation coefficient for seasonal mean AOD from MATRIX and MATRIX-VBS data against AERONET.

	MATRIX				MATRIX-VBS			
	Winter	Spring	Summer	Fall	Winter	Spring	Summer	Fall
Mean	0.14	0.17	0.22	0.15	0.15	0.17	0.18	0.14
Stdev	0.08	0.12	0.18	0.12	0.09	0.11	0.16	0.11
r	0.27	0.75	0.63	0.62	0.11	0.62	0.75	0.57
AERONET mean	0.09	0.01	0.16	0.11				

As for the comparison with station measurements from AERONET (Figure 4.4.5). Overall both model results show generally good agreement with the measurements, except for the highly polluted locations, which could also be caused by satellite products underestimating thick plumes. Figure 4.4.6 shows the seasonal difference between the modeled AOD and AOD from AERONET, except for winter (DJF), during which both models underestimate AOD as compared to AERONET, other seasons generally overestimate it or estimate it well. Another statistical analysis for seasonal mean AERONET and model data over stations where AERONET reported data shows that MATRIX-VBS correlates better with AERONET than MATRIX does only in the summer (JJA), and both models perform poorly in the winter (DJF) months (Table 4.2).

Even though there is an ample amount of AERONET stations, they are still not stationed in some of the most “interesting” remote regions for this study, which are areas with high organic aerosol amounts or large differences between the two models. Thus, it is difficult to evaluate, for instance, the missing biomass plume in MATRIX-VBS in the summer (JJA) and fall (SON), as observed by MODIS.

Nevertheless, we picked regions with the greatest difference of AOD between the two models, marked with boxes in Figure 4.4.7, one encompassing Central Alaska and the other Central Africa (Congo basin and its off-coast transport region). The CALIPSO extinction profiles in January, April, July, and October for both regions are shown in Figure 4.4.8. For both regions, both models compare well with CALIPSO, except for the month of July. In Alaska, MATRIX significantly overestimates aerosol extinction, whereas MATRIX-VBS still overestimates aerosol extinction but to a much lower extent compared to MATRIX, the difference is approximately a factor of 3. This discrepancy could be due to the fact that we use 2015 emissions to simulate the year 2016. In Central Africa, while MATRIX still overestimates aerosol extinction by approximately a factor of 1.5, MATRIX-VBS underestimates it, up to 3 km altitude, by approximately a third. It also interesting that with regard to aerosol population, aerosol extinction is dominated by OCC and BOC populations in MATRIX, whereas in MATRIX-VBS, the aerosol extinction from OCC population is almost negligible and only the BOC population dominates. This hints at the effect of aerosol composition on AOD as well.

There is one AERONET station inside or near each of the examined regions shown in Figure 4.4.7, one is Ascension Island ( $8^{\circ}\text{S}$ ,  $14.5^{\circ}\text{W}$ ) off the coast of Africa, outside the boxed region in Central Africa, whose primary organic aerosol source is biomass burning from the Congo Basin, and the other is Bonanza Creek in the boreal forest biome of Central Alaska ( $64.74^{\circ}\text{N}$ ,  $148.32^{\circ}\text{W}$ ), inside the boxed region in Alaska, whose primary organic aerosol source is boreal forest fires.

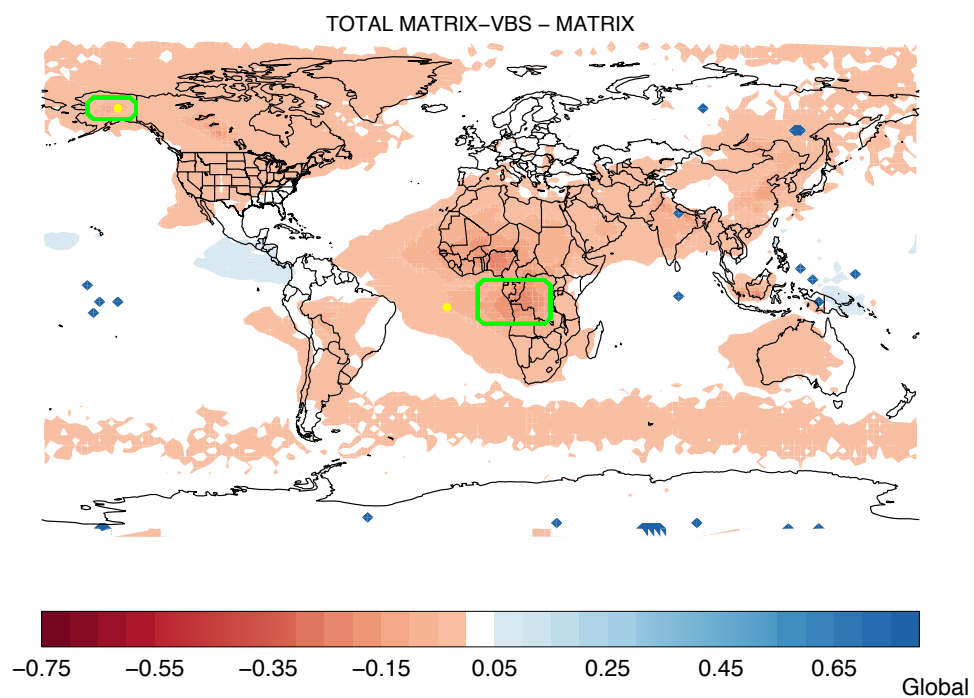


Figure 4.4.7 Difference in total annual clear sky AOD between the two models, showing green boxes over regions studied for CALIPSO and yellow circles over AERONET stations Bonanza Creek in Alaska and Ascension Island off the coast of Central Africa.

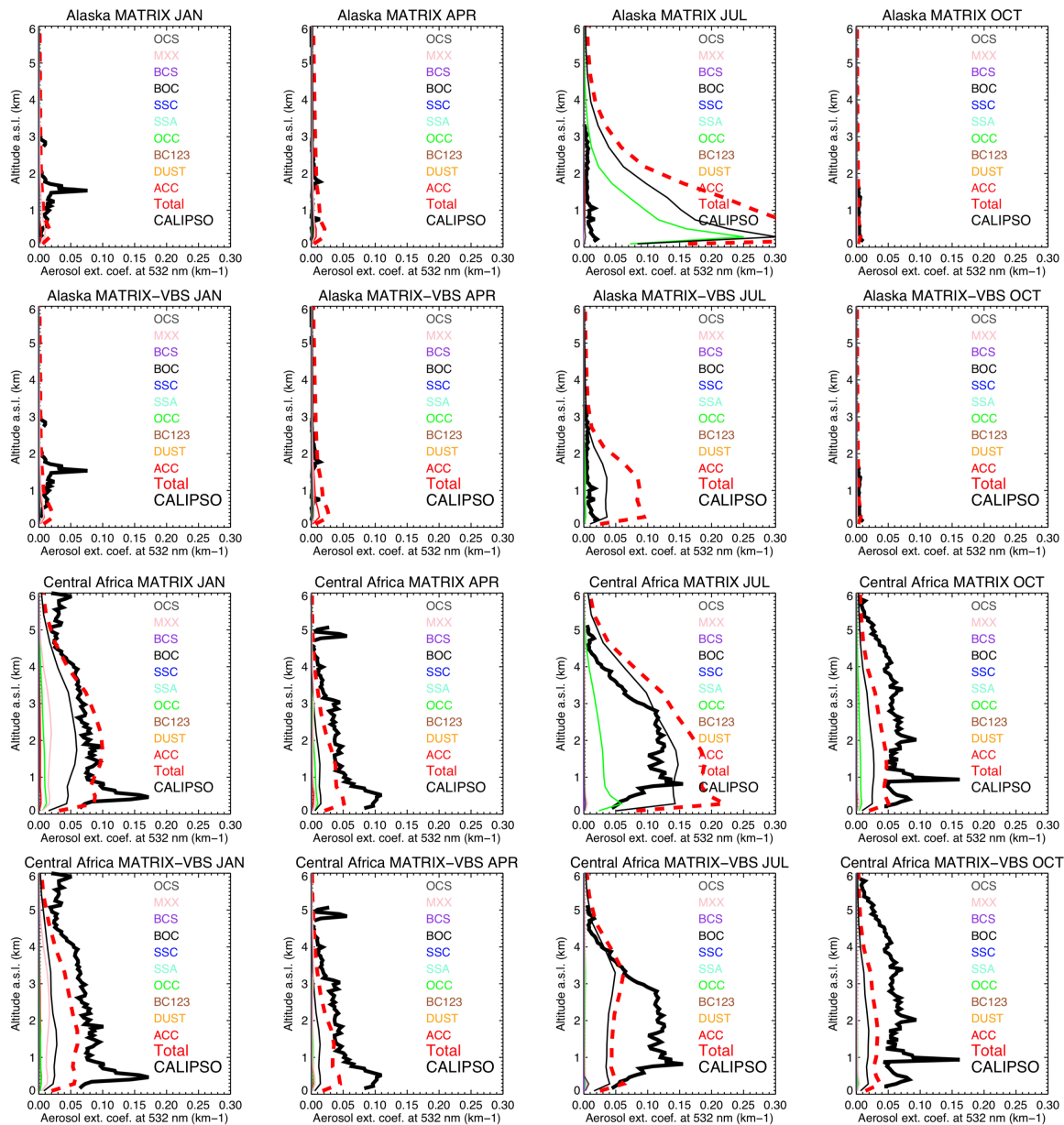


Figure 4.4.8 Height profile plots of aerosol extinction from CALIPSO and the two models.

The time series of AOD from both models, MODIS, CALIPSO, and AERONET in both stations are shown in Figure 4.4.9. For Ascension Island, both models generally agree well with measurements, except for the month of August, when MATRIX is on the high end of observations range, and MATRIX-VBS is underestimating AOD compared to measurements. For Bonanza



Creek, both models overestimate AOD from May until August, with MATRIX peaking at 1.0 and MATRIX-VBS peaking at 0.3, whereas measurements stayed under 0.1.

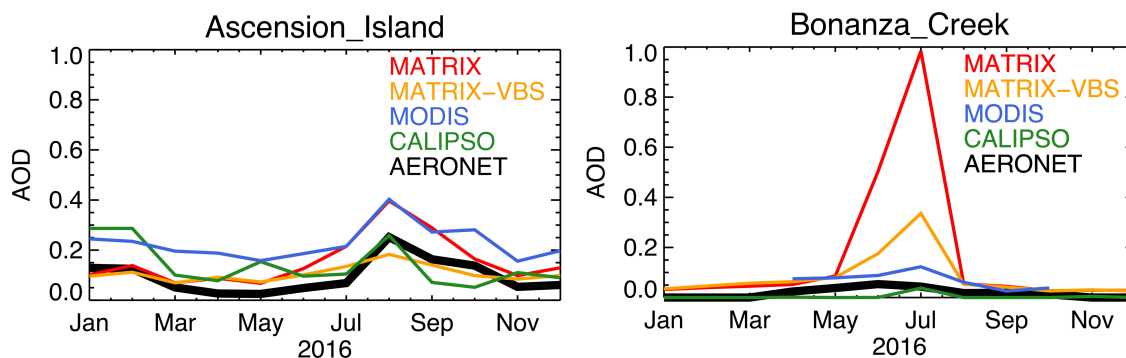


Figure 4.4.9 Time series of AOD from AERONET stations Ascension Island and Bonanza Creek for MATRIX, MATRIX-VBS, MODIS, CALIPSO, AERONET.

To understand the difference, we examined the mass, number, and size in these two stations. For Ascension Island, the summer mass concentration can be compared to ATom-1, in Figure 4.1.6 (for 30°S-EQ band over the Atlantic). MATRIX does well when compared to measurement whereas MATRIX-VBS overestimates the mass concentration, with a peak that overestimates more than double the peak measured concentration. For Bonanza Creek, we can refer to Figure 4.1.6 (for 60°N-90°N band over 120°W) and see that both models underestimate mass concentration aloft, with MATRIX-VBS higher than MATRIX and performing better compared to measurement. Shown in Figure 4.4.10 is the size distribution for the two stations. There are more, but smaller particles in MATRIX-VBS compared to those in MATRIX in both cases. This could mean that even though there are higher mass concentration and number concentration in MATRIX-VBS for both locations, they lead to lower AOD in the model. What really determined AOD could be the size and the composition of the particles. There are smaller particles in MATRIX-VBS, and from the comparisons with the CALIPSO profiles we can see that the

controlling aerosol population for aerosol extinction changed from OCC and BOC in MATRIX to just BOC in MATRIX-VBS.

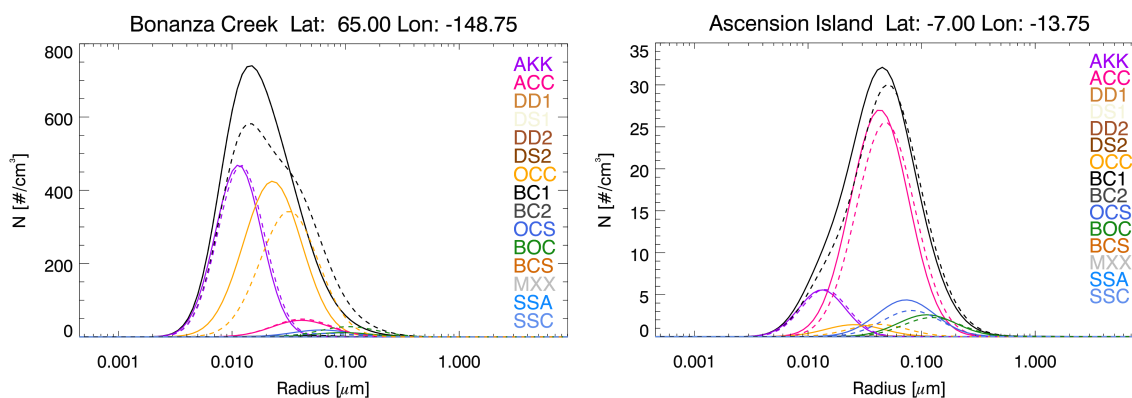


Figure 4.4.10 Size distributions of near surface aerosols in Ascension Island and Bonanza Creek for MATRIX-VBS (solid lines) and MATRIX (dashed lines).

## 4.5 Conclusions

The newly developed aerosol microphysics model MATRIX-VBS has been implemented in the Earth system model GISS ModelE. Its simulations of mass concentration, number concentration, activated aerosol number concentration and aerosol optical depth were compared to its original model version MATRIX and evaluated against aircraft and ground measurements and satellite retrievals.

Results showed a generally similar spatial distribution of mass load for both models, but with different amounts. The difference in spatial distribution of organic aerosols is that those in MATRIX-VBS experienced longer transport and are more uniformly distributed, in other words, there are higher concentrations in MATRIX-VBS where low concentrations are calculated in MATRIX. There is also increased mass concentration aloft and decreased at the surface.

For the summer month of August, the difference in mass load between the two models is very similar to the that of the annual mean. Compared to the summer ATom measurements, both



models agree well with measurements at the surface, but for most regions, the profiles aloft do not match very well for both models, mostly underestimate organic aerosol mass concentration. A few regions capture the vertical profiles well, such as mid-latitudes over the Continental United States and low latitudes over the Atlantic Ocean. Both models do not capture the vertical profiles at high latitudes in the Northern Hemisphere well, even though we understand the increase in mass concentration observed there for MATRIX-VBS. However, it is possible that mass-based emission factor and its distribution among different volatility bins may not be applicable in all regions, thus affecting organic aerosol lifetime in the atmosphere and its transport. It is also somewhat unexpected that there are higher than modeled mass concentrations over the Southern Pacific Ocean, since it is so remote and far from the source regions. However, it could be because our model does not have oceanic OA sources, which leads to an underestimation of OA concentration. In contrast, for the winter month of February, the difference in mass load between the two models are the opposite of that in the summer month and the annual mean due to season change, which affect emissions and organic volatility. Compared against winter ATom measurements, both models still generally underestimate the organic aerosol mass concentration, especially over the oceans.

As for number concentration and activated number concentration, results are in good agreement with our previous studies - there is higher aerosol number concentration in organic-containing aerosol populations in MATRIX-VBS as compared to that in MATRIX, and generally lower activated number concentration in MATRIX-VBS with a few exceptional regions such as the highly polluted China. As discussed in our previous study, activated number concentration depends on number concentration as well as size, which will be included in future work.

Lastly, comparisons of AOD showed lower AOD in MATRIX-VBS as compared to MATRIX. Both models overestimate AOD over source regions compared to AERONET and

MODIS data, which can be caused by underestimation of thick plumes by satellite products. Both models also do not compare well against AERONET data in the winter (DJF). By comparing the AOD vertical profiles in two biomass regions against CALIPSO data, we learned that both models perform well except for the month of July. Results from two remote locations in boreal Alaska and Ascension Island show that there is an increased number of particles and a decrease in their sizes in MATRIX-VBS as compared to MATRIX. So for the two locations, we found increased mass and number concentration as well as decreased particle size in MATRIX-VBS and lower AOD. Additionally, composition of the particles plays a role in this change too, from the comparisons with the CALIPSO vertical profiles, we found a shift of dominating aerosol population for aerosol extinction from OCC and BOC in the original model to only BOC in the new model, which need to be considered further to improve our understanding of the impact of composition on AOD and climate forcing.

Nevertheless, more questions and challenges remain. This study showed that compared to observations, MATRIX-VBS is not performing as well as MATRIX does. MATRIX-VBS is missing or underestimating biomass burning in the Amazon and Congo basins, which could be due to their smaller sized particles and change in aerosol composition or even emissions, which will be further explored in future studies. It is also worth exploring the volatility distribution for organic aerosol emissions, perhaps the mass-based emission factors are not valid globally for all air mass types and climate zones. Additionally, particle size distribution needs to be fully evaluated for MATRIX-VBS because, as shown in this study, it affects not only activated number concentration but also AOD, both of which influence our climate. Finally, one major challenge of the organic aerosol evaluation is the lack of measurements available over regions of significant interest, which are usually in the remote parts of the world. Additional future field campaigns in these regions will be crucial and helpful in shedding light on model performance.

## **PART III**

### **Concluding Material**

# CHAPTER 5

## Summary and future work

A new model, MATRIX-VBS, was developed by implementing organic aerosol volatility calculations in an aerosol microphysics model in a box model framework. Results from four test cases in different environments showed the impact of semi-volatile organics on the mixing state, mass concentration and size distribution. The number concentrations for organic-containing aerosol populations have increased in the new model, and aerosol sizes have decreased.

A suite of Monte-Carlo simulations was performed to create a range of meteorological and environmental conditions found in the atmosphere. Results showed that by including semi-volatile organics, there is lower activated particle number concentration in the new scheme compared to that in the original scheme MATRIX, except in environments with low cloud updrafts, in clean regions at above freezing temperatures, and in polluted regions at high temperature (310 K) and extremely low humidity conditions. For particle activation, both MATRIX and MATRIX-VBS use the Abdul-Razzak and Ghan (2000) scheme, which calculates the activated particle number concentrations from the chemically resolved number concentrations using Köhler Theory, yet the two models simulate different aerosol number concentration and particle sizes, which would ultimately decide how many particles could activate under certain conditions.

Next, MATRIX-VBS was implemented into the global model, and we examined the mass, number, and activated particle number concentrations in the two models, also comparing them against limited available measurements, which include organic aerosol mass concentration data

---

from aircraft campaign ATom (Atmospheric Tomography Mission), and aerosol optical depth data from ground measurement stations from AERONET (Aerosol Robotic Network), and satellite retrievals from MODIS (MODerate resolution Imaging Spectroradiometer) and CALIPSO (Cloud-Aerosol Lidar and Infrared Pathfinder Satellite Observations).

On the global scale, conclusions drawn from simulated mass, number, and activated number concentrations are consistent with those from the box model. MATRIX-VBS has a more wide-spread spatial distribution of organic aerosol load as well as higher mass concentration aloft and lower concentration at the surface as compared to MATRIX. Aircraft measurements showed higher mass concentration, which means the models are still underestimating organics in many regions, especially at high latitudes in the Northern Hemisphere and remote Southern Pacific Ocean. As in the box model, activated number concentrations are lower in MATRIX-VBS as compared to that for MATRIX, except for regions such as highly polluted eastern China.

MATRIX-VBS has generally lower AOD compared to MATRIX, which can be due to the decreased particle sizes and changed aerosol composition. Both models overestimate AOD compared to ground measurement and satellite retrievals in near source regions, and they underestimate AOD in the winter (DJF) according to ground measurements from AERONET stations. MATRIX-VBS also underestimate AOD over the Amazon and Congo basin biomass burning regions. Comparisons of vertical profiles against CALIPSO showed generally good agreements, except for the July month. Overall, MATRIX-VBS moved further away from observations than MATRIX.

Evaluation against measurements has its challenges. While there are increased efforts in new field campaigns and measurements, one critical challenge in the evaluation process remains

in the limitations of measurements: the regions with the greatest unknowns and differences between model versions, such as the biomass burning plume in the Congo basin, measurements are not available, making it difficult to evaluate. This is also evident as discussed during the evaluation and inter-comparison of organic aerosol in global models by Tsigaridis et al. (2014). Therefore, additional field campaigns in remote regions mentioned in this study would be very helpful in our understanding of aerosols in the real world and evaluating model performance.

From the initial evaluation of MATRIX-VBS against MATRIX and measurement, I found that results from the new model have not improved the representation of organic aerosols in the real world. Nevertheless, the new aerosol scheme did help us better understand organic aerosol processes. Going forward, better representations of existing governing parameters and conditions are needed to improve the new scheme, which would affect aerosol mass, number, size and mixing state, thus influencing radiative forcing and the climate. Results from this study point to the need for more investigation on both particle microphysics and organic aerosol volatility. More specifically, we need to improve the representations of aerosol microphysics, particularly the particle size distribution, as well as the representation of organic aerosol volatility, specifically by including biogenic SOA volatility and adjusting the distribution of mass-based emission factors among volatility bins.

As discussed throughout this study, size distribution is critical to aerosol microphysics and its impact on climate, since it directly links to aerosol optical properties and CCN concentrations. However, the problem exists in that there is currently no diameter threshold for aerosols to completely evaporate (decrease number concentration) when they become too small. This is potentially a problem when organics evaporate into extremely small sizes and remain in the model,

---

which would produce the increased number concentration and smaller diameters that we see in our results. Whether what we see is realistic or not calls for comparison against measurements. Therefore, evaluating aerosol size distribution on the global scale is critical since it could possibly explain the decreased AOD in the new model as well as the behavior of activated cloud number concentration. Data from the ATom aircraft campaign as well from AMS (Aerosol Mass Spectrometry) ground station measurements could help us understand the evolution of particle size in the real world.

Meanwhile, organic aerosol volatility needs further exploration in the model as well. As shown in the global study, one key conclusion was that the inconsistency of model simulated organic aerosol mass concentration with measurements can be due to the volatility distribution for organic aerosol emissions. More specifically, mass-based emission factors we applied may not be valid globally. This calls for the possibility of implementing regional emission factors that have different volatility distribution for certain climate zones to better simulate organic aerosol emissions. Additionally, only organics of anthropogenic origin are semi-volatile in MATRIX-VBS, biogenic SOA are still treated as non-volatile and are produced with a constant yield from terpenes emissions. Since studies have shown that emissions of its precursors, namely BVOC such as isoprene and terpenes from vegetation dominate the global VOC source (Guenther et al., 2012), I would like to include biogenic SOA as semi-volatile and investigate how its addition could make an impact on climate. Lastly, with these improvements, it would be very interesting to simulate different future emission scenarios in MATRIX-VBS and investigate the climate impacts that organic aerosol volatility makes in a changing world.

## **PART IV**

### **Bibliography**



## Bibliography

Aan de Brugh, J. M. J., Schaap, M., Vignati, E., Dentener, F., Kahanert, M., Sofiev, M., Huijnen, V., and Krol, M. C.: The European aerosol budget in 2006, *Atmos. Chem. Phys.*, 11, 1117–1139, doi:10.5194/acp-11-1117-2011, 2011.

Abdul-Razzak, H. and Ghan, S. J.: A parameterization of aerosol activation, 2. Multiple aerosol types, *J. Geophys. Res.*, 105(D5), 6837–6844, <https://doi.org/10.1029/1999JD901161>, 2000.

Adams, P. J. and Seinfeld, J. H.: Predicting global aerosol size distributions in general circulation models, *J. Geophys. Res.*, 107, 4370, doi:10.1029/2001JD001010, 2002.

Ahmadov, R., McKeen, S. A., Robinson, A. L., Bahreini, R., Middlebrook, A. M., de Gouw, J. A., Meagher, J., Hsie, E. Y., Edgerton, E., Shaw, S., and Trainer, M.: A volatility basis set model for summertime secondary organic aerosols over the eastern United States in 2006, *J. Geophys. Res.-Atmos.*, 117, D06301, <https://doi.org/10.1029/2011jd016831>, 2012.

Aitken, J. A.: On some nuclei of cloudy condensation, *Trans. R. Soc. Edinburgh*, XXXIX, 1897.

Albrecht, B. A.: Aerosols, cloud microphysics, and fractional cloudiness, *Science*, 245, 1227–1230, 1989.

Andreae, M. O., Jones, C. D., and Cox, P. M.: Strong present-day aerosol cooling implies a hot future, *Nature*, 435, 1187–1190, doi:10.1038/nature03671, 2005.

Anttila, T.: Sensitivity of cloud droplet formation to the numerical treatment of the particle mixing state, *J. Geophys. Res.*, 115, D21205, doi:10.1029/2010JD013995, 2010.

Athanasopoulou, E., Vogel, H., Vogel, B., Tsimpidi, A. P., Pandis, S. N., Knöche, C., and Fountoukis, C.: Modeling the meteorological and chemical effects of secondary organic aerosols during an EUCAARI campaign, *Atmos. Chem. Phys.*, 13, 625–645, doi:10.5194/acp-13-625-2013, 2013.

Atkinson, R.: Gas-phase tropospheric chemistry of volatile organic compounds: 1. Alkanes and alkenes, *J. Phys. Chem. Ref. Data*, 26, 215–290, 1997.

ATom Science Team: NASA Ames Earth Science Project Office (ESPO), available at: <https://espo.nasa.gov/atom/content/ATom>, 2018

Bauer, S. E., Wright, D. L., Koch, D., Lewis, E. R., McGraw, R., Chang, L.-S., Schwartz, S. E., and Ruedy, R.: MATRIX (Multiconfiguration Aerosol TRacker of mIXing state): an aerosol microphysical module for global atmospheric models, *Atmos. Chem. Phys.*, 8, 6003–6035, doi:10.5194/acp-8-6003-2008, 2008.

Bauer, S. E., Menon, S., Koch, D., Bond, T. C., and Tsigaridis, K.: A global modeling study on carbonaceous aerosol microphysical characteristics and radiative effects, *Atmos. Chem. Phys.*, 10, 7439–7456, doi:10.5194/acp-10-7439-2010, 2010.

Bauer, S. E., and Menon, S.: Aerosol direct, indirect, semidirect, and surface albedo effects from sector contributions based on the IPCC AR5 emissions for preindustrial and present-day conditions, *J. Geophys. Res.*, 117, D01206, doi:10.1029/2011JD016816, 2012.

Bauer, S. E., Ault, A. and Prather, K. A.: Evaluation of aerosol mixing state classes in the GISS modelE-MATRIX climate model using single-particle mass spectrometry measurements, *J. Geophys. Res. Atmos.*, 118, 9834–9844, doi:10.1002/jgrd.50700, 2013.

Bellouin, N., Mann, G. W., Woodhouse, M. T., Johnson, C., Carslaw, K. S., and Dalvi, M.: Impact of the modal aerosol scheme GLOMAP-mode on aerosol forcing in the Hadley Centre Global Environmental Model, *Atmos. Chem. Phys.*, 13, 3027–3044, doi:10.5194/acp-13-3027-2013, 2013.

Bergman, T., Kerminen, V.-M., Korhonen, H., Lehtinen, K. J., Makkonen, R., Arola, A., Mielonen, T., Romakkaniemi, S., Kulmala, M., and Kokkola, H.: Evaluation of the sectional aerosol microphysics module SALSA implementation in ECHAM5- HAM aerosol-climate model, *Geosci. Model Dev.*, 5, 845–868, doi:10.5194/gmd-5-845-2012, 2012.

Bergström, R., Denier van der Gon, H. A. C., Prévôt, A. S. H., Yttri, K. E., and Simpson, D.: Modelling of organic aerosols over Europe (2002–2007) using a volatility basis set (VBS) framework: application of different assumptions regarding the formation of secondary organic aerosol, *Atmos. Chem. Phys.*, 12, 8499–8527, doi:10.5194/acp-12-8499-2012, 2012.

Binkowski, F. S. and Shankar, U.: The Regional Particulate Matter Model: 1. Model description and preliminary results, *J. Geophys. Res.*, 100, 26191–26209, 1995.

Boucher, O., Randall, D., Artaxo, P., Bretherton, C., Feingold, G., Forster, P., Kerminen, V.-M., Kondo, Y., Liao, H., Lohmann, U., Rasch, P., Satheesh, S.K., Sherwood, S., Stevens, B., and Zhang, X.Y.: Clouds and Aerosols. In: *Climate Change 2013: The Physical Science Basis. Contribution of Working Group I to the Fifth Assessment Report of the Intergovernmental Panel on Climate Change*, edited by: Stocker, T. F., Qin, D., Plattner, G.-K., Tignor, M., Allen, S. K., Boschung, J., Nauels, A., Xia, Y., Bex, V., and Midgley, P. M., Cambridge University Press, Cambridge, UK and New York, NY, USA, 571–657 pp., doi:10.1017/CBO9781107415324, 2013.

Carslaw, K. S., Boucher, O., Spracklen, D. V., Mann, G. W., Rae, J. G. L., Woodward, S., and Kulmala, M.: A review of natural aerosol interactions and feedbacks within the Earth system, *Atmos. Chem. Phys.*, 10, 1701–1737, doi:10.5194/acp-10-1701-2010, 2010.

Charlson, R. J., Schwartz, S. E., Hales, J. M., Cess, R. D., Coakley, J. A., Hansen, J. E., and Hofmann, D. J.: Climate Forcing by Anthropogenic Aerosols, *Science*, 255, 423–430, 1992.

Ciarelli, G., El Haddad, I., Bruns, E., Aksoyoglu, S., Mohler, O., Baltensperger, U., and Prevot, A. S. H.: Constraining a hybrid volatility basis-set model for aging of wood-burning emissions using smog chamber experiments: a box-model study based on the VBS scheme of the CAMx model (v5.40), *Geosci. Model Dev.*, 10, 2303–2320, <https://doi.org/10.5194/gmd-10-2303-2017>, 2017.

Connolly, P. J., Topping, D. O., Malavelle, F., and McFiggans, G.: A parameterisation for the activation of cloud drops including the effects of semivolatile organics, *Atmos. Chem. Phys.*, 14, 22892302, <https://doi.org/10.5194/acp1422892014>, 2014.

Connolly P.J, McFiggans G.B., Wood R., Tsiamis A.: Factors determining the most efficient spray distribution for marine cloud brightening. *Phil. Trans. R. Soc. A* 372: 20140056. <http://dx.doi.org/10.1098/rsta.2014.0056>, 2014b.

Crooks, M., Connolly, P., and McFiggans, G.: A parameterisation for the co-condensation of semi-volatile organics into multiple aerosol particle modes, *Geosci. Model Dev.*, 11, 3261–3278, <https://doi.org/10.5194/gmd-11-3261-2018>, 2018.

Cubison, M. J., Ervens, B., Feingold, G., Docherty, K. S., Ulbrich, I. M., Shields, L., Prather, K., Hering, S., and Jimenez, J. L.: The influence of chemical composition and mixing state of Los Angeles urban aerosol on CCN number and cloud properties, *Atmos. Chem. Phys.*, 8, 5649–5667, <https://doi.org/10.5194/acp-8-5649-2008>, 2008.

Dockery, D. W., Pope, C. A., Xu, X. P., Spengler, J. D., Ware, J. H., Fay, M. E., Ferris, B. G., and Speizer, F. E.: An association between air pollution and mortality in 6 United States cities, New England J. Medicine, 329, 1753–1759, 1993.

Donahue, N. M., Robinson, A. L., Stanier, C. O., and Pandis, S. N.: Coupled partitioning, dilution, and chemical aging of semivolatile organics, *Environ. Sci. Technol.*, 40, 2635–2643, doi:10.1021/es052297c, 2006.

Donahue, N. M., Epstein, S. A., Pandis, S. N. and Robinson, A. L.: A two-dimensional volatility basis set: 1. organic-aerosol mixing thermodynamics, *Atmos. Chem. Phys.*, 11(7), 3303–3318, doi:10.5194/acp-11-3303-2011, 2011.

Donahue, N. M., Kroll, J. H., Pandis, S. N., and Robinson, A. L.: A two-dimensional volatility basis set – Part 2: Diagnostics of organic-aerosol evolution, *Atmos. Chem. Phys.*, 12, 615–634, <https://doi.org/10.5194/acp-12-615-2012>, 2012.

Dusek, U., Frank, G. P., Hildebrandt, L., Curtius, J., Schneider, J., Walter, S., Chand, D., Drewnick, F., Hings, S., Jung, D., Borrmann, S., and Andreae, M. O.: Size matters more than chemistry for cloud-nucleating ability of aerosol particles, *Science*, 312(5778), 1375–1378, 2006.

Epstein, S. A., Riipinen, I., and Donahue, N. M.: A Semi-Empirical Correlation between Enthalpy of Vaporization and Saturation Concentration for Organic Aerosol, *Environ. Sci. Technol.*, 44, 743–748, doi:10.1021/es902497z, 2010.

Ervens, B., Cubison, M., Andrews, E., Feingold, G., Ogren, J. A., Jimenez, J. L., DeCarlo, P., and Nenes, A.: Prediction of cloud condensation nucleus number concentration using measurements of aerosol size distributions and composition and light scattering enhancement due to humidity, *J. Geophys. Res.*, 112, D10S32, doi:10.1029/2006jd007426, 2007.

Fierce, L., Riemer, N., and Bond, T. C.: Toward reduced representation of mixing state for simulating aerosol effects on climate. *Bulletin of the American Meteorological Society*, 98(5), 971–980. <https://journals.ametsoc.org/doi/abs/10.1175/BAMS-D-16-0028.1>, 2017.

Fountoukis, C. and Nenes, A.: Continued development of a cloud droplet formation parameterization for global climate models, *J. Geophys. Res.*, 110, D11212, doi:10.1029/2004JD005591, 2005.

Fountoukis, C., Racherla, P. N., Denier van der Gon, H. A. C., Polymeneas, P., Charalampidis, P. E., Pilinis, C., Wiedensohler, A., Dall'Osto, M., O'Dowd, C., and Pandis, S. N.: Evaluation of a three-dimensional chemical transport model (PMCAMx) in the European domain during the EUCAARI May 2008 campaign, *Atmos. Chem. Phys.*, 11, 10331–10347, doi:10.5194/acp-11-10331-2011, 2011.

Fountoukis, C., Megaritis, A. G., Skyllakou, K., Charalampidis, P. E., Pilinis, C., Denier van der Gon, H. A. C., Crippa, M., Canonaco, F., Mohr, C., Prévôt, A. S. H., Allan, J. D., Poulain, L., Petäjä, T., Tiitta, P., Carbone, S., Kiendler-Scharr, A., Nemitz, E., O'Dowd, C., Swietlicki, E., and Pandis, S. N.: Organic aerosol concentration and composition over Europe: insights from comparison of regional model predictions with aerosol mass spectrometer factor analysis, *Atmos. Chem. Phys.*, 14, 9061–9076, doi:10.5194/acp-14-9061-2014, 2014.

Gao, C. Y., Tsigaridis, K., and Bauer, S. E.: MATRIX-VBS (v1.0): implementing an evolving organic aerosol volatility in an aerosol microphysics model, *Geosci. Model Dev.*, 10, 751–764, <https://doi.org/10.5194/gmd-10-751-2017>, 2017.

Gao, C. Y., Bauer, S. E., and Tsigaridis, K.: Can semi-volatile organic aerosols lead to fewer cloud particles?, *Atmos. Chem. Phys.*, 18, 14243–14251, <https://doi.org/10.5194/acp-18-14243-2018>, 2018.

Gery, M.W., Whitten, G. Z., Killus, J. P., and Dodge, M. C.: A photochemical kinetics mechanism for urban and regional scale computer modeling, *J. Geophys. Res.*, 94, 12925–12956, doi:10.1029/JD094iD10p12925, 1989.

Gettelman, A. and Morrison, H.: Advanced Two-Moment Bulk Microphysics for Global Models, Part I: Off-Line Tests and Comparison with Other Schemes, *J. Climate*, 28, 1268–1287, <https://doi.org/10.1175/JCLI-D-14-00102.1>, 2015.

Ghan, S. J., Guzman, G., and Abdul-Razzak, H.: Competition between sea salt and sulfate particles as cloud condensation nuclei, *Journal 25. of the atmospheric sciences*, 55, 3340-3347, 1998.

Ghan, S. J., Laulainen, N., Easter, R. C., Wagener, R., Nemesure, S., Chapman, E., Zhang, Y., and Leung, R.: Evaluation of aerosol direct radiative forcing in MIRAGE, *J. Geophys. Res.*, 106, 5295–5316, 2001a.

Ghan, S. J., Easter, R. C., Hudson, J., and Breon, F.-M.: Evaluation of aerosol indirect radiative forcing in MIRAGE, *J. Geophys. Res.*, 106, 5317–5334, 2001b.

Ghan, S. J., Abdul-Razzak, H., Nenes, A., Ming, Y., Liu, X., Ovchinnikov, M., Shipway, B., Meskhidze, N., Xu, J., and Shi, X.: Droplet nucleation: physically-based parameterizations and comparative evaluation, *J. Adv. Model. Earth Syst.*, 3, M10001, doi:10.1029/2011MS000074, 2011.

Gibson, E.R., Gierlus, K.M., Hudson, P.K., Grassian, V.H.: Generation of internally mixed insoluble and soluble aerosol particles to investigate the impact of atmospheric aging and heterogeneous processing on the CCN activity of mineral dust aerosol, *Aerosol Sci. Technol.*, 41, 914–924, 2007.

Griffin, R. J., Dabdub, D., and Seinfeld, J. H.: Estimate of global atmospheric organic aerosol from oxidation of biogenic hydrocarbons, *Geophys. Res. Lett.*, 26, 2721–2724, 1999.

Guenther, A., Hewitt, C. N., Erickson, D., Fall, R., Geron, C., Graedel, T., Harley, P., Klinger, L., Lerdau, M., McKay, W. A., Pierce, T., Scholes, B., Steinbrecher, R., Tallamraju, R., Taylor, J., and Zimmerman, P.: A Global Model of Natural Volatile Organic Compound Emissions, *J. Geophys. Res.*, 100, 8873–8892, 1995.

Guenther, A. B., Jiang, X., Heald, C. L., Sakulyanontvittaya, T., Duhl, T., Emmons, L. K., and Wang, X.: The Model of Emissions of Gases and Aerosols from Nature version 2.1 (MEGAN2.1): an extended and updated framework for modeling biogenic emissions, *Geosci. Model Dev.*, 5, 1471–1492, doi:10.5194/gmd-5-1471-2012, 2012.

Hansen, J., Sato, M., Ruedy, R., Nazarenko, L., Lacis, A., Schmidt, G. A., Russell, G., Aleinov, I., Bauer, M., Bauer, S., Bell, N., Cairns, B., Canuto, V., Chandler, M., Cheng, Y., Del Genio, A., Faluvegi, G., Fleming, E., Friend, A., Hall, T., Jackman, C., Kelley, M., Kiang, N., Koch, D., Lean, J., Lerner, J., Lo, K., Menon, S., Miller, R., Minnis, P., Novakov, T., Oinas, V., Perlwitz, J., Perlwitz, Ju., Rind, D., Romanou, A., Shindell, D., Stone, P., Sun, S., Tausnev, N., Thresher, D., Wielicki, B., Wong, T., Yao, M., and Zhang, S.: Efficacy of Climate Forcings, *J. Geophys. Res.*, 110, D18104, doi:10.1029/2005JD005776, 2005.

Heald, C. L., Jacob, D. J., Park, R. J., Russell, L. M., Huebert, B. J., Seinfeld, J. H., Liao, H. and Weber, R. J.: A large organic aerosol source in the free troposphere missing from current models, *Geophys. Res. Lett.*, 32(18), 1–4, doi:10.1029/2005GL023831, 2005.

Healy, R. M., Riemer, N., Wenger, J. C., Murphy, M., West, M., Poulain, L., Wiedensohler, A., O'Connor, I. P., McGillicuddy, E., Sodeau, J. R., and Evans, G. J.: Single particle diversity and mixing state measurements, *Atmos. Chem. Phys.*, 14, 6289–6299, <https://doi.org/10.5194/acp-14-6289-2014>, 2014.

Hodzic, A., Jimenez, J. L., Madronich, S., Canagaratna, M. R., Decarlo, P. F., Kleinman, L. and Fast, J.: Modeling organic aerosols in a megacity: Potential contribution of semi-volatile and intermediate-volatility primary organic compounds to secondary organic aerosol formation, *Atmos. Chem. Phys.*, 10(12), 5491–5514, doi:10.5194/acp-10-5491-2010, 2010.

Hodzic, A., Kasibhatla, P. S., Jo, D. S., Cappa, C. D., Jimenez, J. L., Madronich, S., and Park, R. J.: Rethinking the global secondary organic aerosol (SOA) budget: stronger production, faster removal, shorter lifetime, *Atmos. Chem. Phys.*, 16, 7917–7941, doi:10.5194/acp-16-7917-2016, 2016.

Hoesly, R. M., Smith, S. J., Feng, L., Klimont, Z., Janssens-Maenhout, G., Pitkanen, T., Seibert, J. J., Vu, L., Andres, R. J., Bolt, R. M., Bond, T. C., Dawidowski, L., Kholod, N., Kurokawa, J.-I., Li, M., Liu, L., Lu, Z., Moura, M. C. P., O'Rourke, P. R., and Zhang, Q.: Historical (1750–2014) anthropogenic emissions of reactive gases and aerosols from the Community Emissions Data System (CEDS), *Geosci. Model Dev.*, 11, 369–408, <https://doi.org/10.5194/gmd-11-369-2018>, 2018.

Hoffmann, T., Odum, J. R., Bowman, F., Collins, D., Klockow, D., Flagan, R. C., and Seinfeld, J. H.: Formation of Organic Aerosols from the Oxidation of Biogenic Hydrocarbons, *J. Atmos. Chem.*, 26, 189–222, 1997.

Holben, B. N., Eck, T. F., Slutsker, I., Tanre, D., Buis, J. P., Setzer, A., et al.: AERONET – A federated instrument network and data archive for aerosol characterization, *Remote Sens. Environ.*, 66(1), 1–16, 1998.

Jacobson, M. Z.: Development and application of a new air pollution modeling system – II. Aerosol module structure and design, *Atmos. Environ.*, 31, 131–144, 1997a.

Jacobson, M. Z.: Development and application of a new air pollution modeling system – III, *Atmos. Environ.*, 31, 587–608, 1997b.

Jacobson, M. Z.: Strong radiative heating due to the mixing state of black carbon in atmospheric aerosols, *Nature*, 409, 695–697, 2001.

Jathar, S. H., Farina, S. C., Robinson, a. L. and Adams, P. J.: The influence of semi-volatile and reactive primary emissions on the abundance and properties of global organic aerosol, *Atmos. Chem. Phys.*, 11(15), 7727–7746, doi:10.5194/acp-11-7727-2011, 2011.

Jimenez, J. L., Canagaratna, M. R., Donahue, N. M., Prevot, a S. H., Zhang, Q., Kroll, J. H., DeCarlo, P. F., Allan, J. D., Coe, H., Ng, N. L., Aiken, a C., Docherty, K. S., Ulbrich, I. M., Grieshop, a P., Robinson, a L., Duplissy, J., Smith, J. D., Wilson, K. R., Lanz, V. a, Hueglin, C.,

Sun, Y. L., Tian, J., Laaksonen, a, Raatikainen, T., Rautiainen, J., Vaattovaara, P., Ehn, M., Kulmala, M., Tomlinson, J. M., Collins, D. R., Cubison, M. J., Dunlea, E. J., Huffman, J. a, Onasch, T. B., Alfarra, M. R., Williams, P. I., Bower, K., Kondo, Y., Schneider, J., Drewnick, F., Borrmann, S., Weimer, S., Demerjian, K., Salcedo, D., Cottrell, L., Griffin, R., Takami, a, Miyoshi, T., Hatakeyama, S., Shimono, a, Sun, J. Y., Zhang, Y. M., Dzepina, K., Kimmel, J. R., Sueper, D., Jayne, J. T., Herndon, S. C., Trimborn, a M., Williams, L. R., Wood, E. C., Middlebrook, a M., Kolb, C. E., Baltensperger, U. and Worsnop, D. R.: Evolution of organic aerosols in the atmosphere., *Science*, 326(5959), 1525–1529, doi:10.1126/science.1180353, 2009.

Jo, D. S., Park, R. J., Kim, M. J., and Spracklen, D. V.: Effects of chemical aging on global secondary organic aerosol using the volatility basis set approach, *Atmos. Environ.*, 81, 230–244, 2013.

Kanakidou, M., Seinfeld, J. H., Pandis, S. N., Barnes, I., Dentener, F. J., Facchini, M. C., Van Dingenen, R., Ervens, B., Nenes, A., Nielsen, C. J., Swietlicki, E., Putaud, J. P., Balkanski, Y., Fuzzi, S., Horth, J., Moortgat, G. K., Winterhalter, R., Myhre, C. E. L., Tsigaridis, K., Vignati, E., Stephanou, E. G., and Wilson, J.: Organic aerosol and global climate modelling: a review, *Atmos. Chem. Phys.*, 5, 1053–1123, <https://doi.org/10.5194/acp-5-1053-2005>, 2005.

Kirkby, J., Duplissy, J., Sengupta, K., Frege, C., Gordon, H., Williamson, C., Heinritzi, M., Simon, M., Yan, C. and Almeida, J.: Ion-induced nucleation of pure biogenic particles, *Nature*, 533(7604), 521–526, doi:10.1038/nature17953, 2016.

Koch, D., Bauer, S. E., Del Genio, A., Faluvegi, G., McConnell, J. R., Menon, S., Miller, R. L., Rind, D., Ruedy, R., Schmidt, G. A., and Shindell, D.: Coupled Aerosol-Chemistry-Climate Twentieth-Century Transient Model Investigation: Trends in Short-Lived Species and Climate Responses, *J. Climate*, 24, 2693–2714, doi:10.1175/2011JCLI3582.1, 2011.

Koffi, B., Schulz, M., Bréon, F.-M., Dentener, F., Steensen, B. M., Griesfeller, J., Winker, D., Balkanski, Y., Bauer, S. E., Bellouin, N., Bernsten, T., Bian, H., Chin, M., Diehl, T., Easter, R., Ghan, S., Hauglustaine, D. A., Iversen, T., Kirkevåg, A., Liu, X., Lohmann, U., Myhre, G., Rasch, P., Seland, O., Skeie, R. B., Steenrod, S. D., Stier, P., Tackett, J., Takemura, T., Tsigaridis, K., Vuolo, M. R., Yoon, J., and Zhang, K.: Evaluation of the aerosol vertical distribution in global aerosol models through comparison against CALIOP measurements: AeroCom phase II results, *J. Geophys. Res.-Atmos.*, 121, 7254–7283, <https://doi.org/10.1002/2015JD024639>, 2016.

Koo, B., Knipping, E., and Yarwood, G.: 1.5-Dimensional volatility basis set approach for modeling organic aerosol in CAMx and CMAQ, *Atmos. Environ.*, 95, 158–164, <https://doi.org/10.1016/j.atmosenv.2014.06.031>, 2014.

Kupc, A., Williamson, C., Wagner, N. L., Richardson, M., and Brock, C. A.: Modification, calibration, and performance of the Ultra-High Sensitivity Aerosol Spectrometer for particle size distribution and volatility measurements during the Atmospheric Tomography Mission (ATom)

airborne campaign, *Atmos. Meas. Tech.*, 11, 369–383, <https://doi.org/10.5194/amt-11-369-2018>, 2018.

Lamarque, J. F., Bond, T. C., Eyring, V., Granier, C., Heil, A., Klimont, Z., Lee, D., Liousse, C., Mieville, A., Owen, B., Schultz, M. G., Shindell, D., Smith, S. J., Stehfest, E., Van Aardenne, J., Cooper, O. R., Kainuma, M., Mahowald, N., McConnell, J. R., Naik, V., Riahi, K. and Van Vuuren, D. P.: Historical (1850–2000) gridded anthropogenic and biomass burning emissions of reactive gases and aerosols: Methodology and application, *Atmos. Chem. Phys.*, 10(15), 7017–7039, doi:10.5194/acp-10-7017-2010, 2010.

Lane, T. E., Donahue, N. M., and Pandis, S. N.: Simulating secondary organic aerosol formation using the volatility basis-set approach in a chemical transport model, *Atmos. Environ.*, 42, 7439–7451, 2008.

Lathi  re, J., Hauglustaine, D. A., De Noblet-Ducoudr  , N., Krinner, G. and Folberth, G. A.: Past and future changes in biogenic volatile organic compound emissions simulated with a global dynamic vegetation model, *Geophys. Res. Lett.*, 32(20), L20818, doi:10.1029/2005GL024164, 2005.

Lee, Y. H. and Adams, P. J.: Evaluation of aerosol distributions in the GISS-TOMAS global aerosol microphysics model with re- mote sensing observations, *Atmos. Chem. Phys.*, 10, 2129–2144, doi:10.5194/acp-10-2129-2010, 2010.

Liu, D., Allan, J., Whitehead, J., Young, D., Flynn, M., Coe, H., McFiggans, G., Fleming, Z. L., and Bandy, B.: Ambient black carbon particle hygroscopic properties controlled by mixing state and composition, *Atmos. Chem. Phys.*, 13, 2015–2029, <https://doi.org/10.5194/acp-13-2015-2013>, 2013.

Liu, X., Penner, J. E., and Herzog, M.: Global modeling of aerosol dynamics: model description, evaluation, and interactions between sulfate and nonsulfate aerosols, *J. Geophys. Res.*, 110, D18206, doi:10.1029/2004JD005674, 2005.

Liu, X., Easter, R. C., Ghan, S. J., Zaveri, R., Rasch, P., Shi, X., Lamarque, J.-F., Gettelman, A., Morrison, H., Vitt, F., Conley, A., Park, S., Neale, R., Hannay, C., Ekman, A. M. L., Hess, P., Mahowald, N., Collins, W., Iacono, M. J., Bretherton, C. S., Flanner, M. G., and Mitchell, D.: Toward a minimal representation of aerosols in climate models: description and evaluation in the Community Atmosphere Model CAM5, *Geosci. Model Dev.*, 5, 709–739, doi:10.5194/gmd-5-709-2012, 2012.

Lurmann, F. W., Wexler, A. S., Pandis, S. N., Musarra, S., Kumar, N., and Seinfeld, J. H.: Modelling urban and regional aerosols II. Application to California’s south coast air basin, *Atmos. Environ.*, 31, 2695–2715, 1997. <sup>[1]</sup><sub>SEP</sub>

Mann, G. W., Carslaw, K. S., Spracklen, D. V., Ridley, D. A., Manktelow, P. T., Chipperfield, M. P., Pickering, S. J., and Johnson, C. E.: Description and evaluation of GLOMAP-mode: a modal global aerosol microphysics model for the UKCA composition-climate model, *Geosci.*



---

Model Dev., 3, 519–551, doi:10.5194/gmd-3-519-2010, 2010.

Mann, G. W., Carslaw, K. S., Reddington, C. L., Pringle, K. J., Schulz, M., Asmi, A., Spracklen, D. V., Ridley, D. A., Woodhouse, M. T., Lee, L. A., Zhang, K., Ghan, S. J., Easter, R. C., Liu, X., Stier, P., Lee, Y. H., Adams, P. J., Tost, H., Lelieveld, J., Bauer, S. E., Tsigaridis, K., van Noije, T. P. C., Strunk, A., Vignati, E., Bellouin, N., Dalvi, M., Johnson, C. E., Bergman, T., Kokkola, H., von Salzen, K., Yu, F., Luo, G., Petzold, A., Heintzenberg, J., Clarke, A., Ogren, J. A., Gras, J., Baltensperger, U., Kaminski, U., Jennings, S. G., O'Dowd, C. D., Harrison, R. M., Beddows, D. C. S., Kulmala, M., Viisanen, Y., Ulevicius, V., Mihalopoulos, N., Zdimal, V., Fiebig, M., Hansson, H.-C., Swietlicki, E., and Henzing, J. S.: Intercomparison and evaluation of global aerosol microphysical properties among AeroCom models of a range of complexity, *Atmos. Chem. Phys.*, 14, 4679–4713, <https://doi.org/10.5194/acp-14-4679-2014>, 2014.

Marcolli, C., Luo, B., and Peter, T.: Mixing of the organic aerosol fractions: liquids as the thermodynamically stable phases, *J. Phys. Chem. A*, 108, 2216–2224, 2004.

McFiggans, G., Artaxo, P., Baltensperger, U., Coe, H., Facchini, M. C., Feingold, G., Fuzzi, S., Gysel, M., Laaksonen, A., Lohmann, U., Mentel, T. F., Murphy, D. M., O'Dowd, C. D., Snider, J. R., and Weingartner, E.: The effect of physical and chemical aerosol properties on warm cloud droplet activation, *Atmos. Chem. Phys.*, 6, 2593–2649, <https://doi.org/10.5194/acp-6-2593-2006>, 2006.

McGraw, R.: Description of Aerosol Dynamics by the Quadrature Method of Moments, *Aerosol Sci. Technol.*, 27(2), 255–265, doi:10.1080/02786829708965471, 1997.

Medina, J., Nenes, A., Sotiropoulou, R.-E. P., Cottrell, L. D., Ziemba, L. D., Beckman, P. J., and Griffin, R. J.: Cloud condensation nuclei closure during the International Consortium for Atmospheric Research on Transport and Transformation 2004 campaign: Effects of size-resolved composition, *J. Geophys. Res.*, 112, D10S31, doi:10.1029/2006jd007588, 2007.

Menon, S. and Rotstayn, L.: The radiative influence of aerosol effects on liquid-phase cumulus and stratiform clouds based on sensitivity studies with two climate models, *Clim. Dynam.*, 27, 345–356, 2006.

Metzger, A., Verheggen, B., Dommen, J., Duplissy, J., Prevot, A. S. H., Weingartner, E., Riipinen, I., Kulmala, M., Spracklen, D. V., Carslaw, K. S., and Baltensperger, U.: Evidence for the role of organics in aerosol particle formation under atmospheric conditions, *P. Natl. Acad. Sci. USA*, 107, 6646–6651, doi:10.1073/pnas.0911330107, 2010.

Mezuman, K., Bauer, S. E., and Tsigaridis, K.: Evaluating secondary inorganic aerosols in three dimensions, *Atmos. Chem. Phys.*, 16, 10651–10669, doi:10.5194/acp-16-10651-2016, 2016.

Miller, R. L., Schmidt, G. A., Nazarenko, L. S., Tausnev, N., Bauer, S. E., Del Genio, A. D., Kelley, M., Lo, K. K., Ruedy, R., Shindell, D. T., Aleinov, I., Bauer, M., Bleck, R., Canuto, V., Chen, Y.-H., Cheng, Y., Clune, T. L., Faluvegi, G., Hansen, J. E., Healy, R. J., Kiang, N. Y., Koch, D., Lacis, A., LeGrande, A. N., Lerner, J., Menon, S., Oinas, V., Pérez García-Pando, C.,

- Perlwitz, J. P., Puma, M., Rind, D., Romanou, A., Russell, G., Sato, M., Sun, S., Tsigaridis, K., Unger, N., Voulgarakis, A., Yao, M.-S., and Zhang, J.: CMIP5 historical simulations (1850–2012) with GISS ModelE2, *J. Adv. Model. Earth Syst.*, 6, 441–477, doi:10.1002/2013MS000266, 2014a.
- Miller, R. L., Knippertz, P., García-Pando, C. P., Perlwitz, J. P., and Tegen, I.: Impact of dust radiative forcing upon climate, in: *Mineral Dust: A Key Player in the Earth System*, edited by: Knippertz, P. and Stuut, J. W., Springer Science Business Media, Dordrecht, the Netherlands, 2014b.
- Ming, Y., Ramaswamy, V., Donner, L. J., and Phillips, V. T. J.: A new parameterization of cloud droplet activation applicable to general circulation models, *J. Atmos. Sci.*, 63, 1348–1356, 2006.
- Moffet, R. C. and Prather, K. A.: In-situ measurements of the mixing state and optical properties of soot with implications for radiative forcing estimates, *P. Natl. Acad. Sci. USA*, 106, 11872–11877, 2009.
- Morrison, H. and Gettelman, A.: A new two-moment bulk stratiform cloud microphysics scheme in the Community Atmosphere Model, version 3 (CAM3). Part I: Description and numerical tests, *J. Climate*, 21, 3642–3659, <https://doi.org/10.1175/2008JCLI2105.1>, 2008.
- Murphy, B. N. and Pandis, S. N.: Simulating the formation of semivolatile primary and secondary organic aerosol in a regional chemical transport model, *Environ. Sci. Technol.*, 43(13), 4722–4728, doi:10.1021/es803168a, 2009.
- Murphy, B. N., Donahue, N. M., Fountoukis, C. and Pandis, S. N.: Simulating the oxygen content of ambient organic aerosol with the 2D volatility basis set, *Atmos. Chem. Phys.*, 11(15), 7859–7873, doi:10.5194/acp-11-7859-2011, 2011.
- Murphy, B. N., Donahue, N. M., Robinson, A. L., and Pandis, S. N.: A naming convention for atmospheric organic aerosol, *Atmos. Chem. Phys.*, 14, 5825–5839, doi:10.5194/acp-14-5825-2014, 2014.
- Myhre, G., Shindell, D., Bréon, F.-M., Collins, W., Fuglestad, J., Huang, J., Koch, D., Lamarque, J.-F., Lee, D., Mendoza, B., Nakajima, T., Robock, A., Stephens, G., Takemura T., and Zhang, H.: Anthropogenic and Natural Radiative Forcing, in: *Climate Change 2013: The Physical Science Basis. Contribution of Working Group I to the Fifth Assessment Report of the Intergovernmental Panel on Climate Change*, edited by: Stocker, T. F., Qin, D., Plattner, G.-K., Tignor, M., Allen, S. K., Boschung, J., Nauels, A., Xia, Y., Bex, V., and Midgley, P. M., Cambridge University Press, Cambridge, UK and New York, NY, USA, 659–740, doi:10.1017/CBO9781107415324, 2013.
- Nazarenko, L., Schmidt, G. A., Miller, R. L., Tausnev, N., Kelley, M., Ruedy, R., Russell, G. L., Aleinov, I., Bauer, M., Bauer, S., Bleck, R., Canuto, V., Cheng, Y., Clune, T. L., Del Genio, A. D., Faluvegi, G., Hansen, J. E., Healy, R. J., Kiang, N. Y., Koch, D., Lacis, A. A., Le Grande, A. N., Lerner, J., Lo, K. K., Menon, S., Oinas, V., Perlwitz, J., Puma, M. J., Rind, D., Romanou, A.,

- Sato, M., Shindell, D. T., Sun, S., Tsigaridis, K., Unger, N., Voulgarakis, A., Yao, M. S., and Zhang, J.: Future climate change under RCP emission scenarios with GISS ModelE2, *J. Adv. Model. Earth Sy.*, 7, 244–267, 2015.
- Odum, J. R., Hoffmann, T., Bowman, F., Collins, D., Flagan, R. C., and Seinfeld, J. H.: Gas/Particle partitioning and secondary organic aerosol yields, *Environ. Sci. Technol.*, 30, 2580–2585, 1996.
- Odum, J. R., Jungkamp, T. P. W., Griffin, R. J., Flagan, R. C., and Seinfeld, J. H.: The atmospheric aerosol-forming potential of whole gasoline vapor, *Science*, 276, 96–99, 1997.
- Orellana, M. V., Matrai, P. A., Leck, C., Rauschenberg, C. D., Lee, A. M., and Coz, E.: Marine microgels as a source of cloud condensation nuclei in the high Arctic, *P. Natl. Acad. Sci.*, 108, 13612–13617, doi:10.1073/pnas.1102457108, 2011.
- Ovadnevaite, J., Ceburnis, D., Martucci, G., Bialek, J., Monahan, C., Rinaldi, M., Facchini, M. C., Berresheim, H., Worsnop, D. R., and O'Dowd, C.: Primary marine organic aerosol: A dichotomy of low hygroscopicity and high CCN activity, *Geophys. Res. Lett.*, 38, L21806, doi:10.1029/2011GL048869, 2011.
- Paasonen, P., Asmi, A., Petäjä, T., Kajos, M. K., Äijälä, M., Junninen, H., Holst, T., Abbatt, J. P. D., Arneth, A., Birmili, W., van der Gon, H. D., Hamed, A., Hoffer, A., Laakso, L., Laaksonen, A., Richard Leaitch, W., Plass-Dülmer, C., Pryor, S. C., Räisänen, P., Swietlicki, E., Wiedensohler, A., Worsnop, D. R., Kerminen, V.-M. and Kulmala, M.: Warming-induced increase in aerosol number concentration likely to moderate climate change, *Nat. Geosci.*, 6(6), 438–442, doi:10.1038/ngeo1800, 2013.
- Pankow, J. F.: An absorption model of gas/particle partitioning of organic compounds in the atmosphere, *Atmos. Environ.*, 28, 185–188, 1994.
- Petters, M. D., Prenni, A. J., Kreidenweis, S. M., DeMott, P. J., Matsunaga, A., Lim, Y. B., and Ziemann, P. J.: Chemical aging and the hydrophobic-hydrophilic conversion of carbonaceous aerosol, *Geophys. Res. Lett.*, 33, L24806, doi:10.1029/2006GL027249, 2006.
- Petters, M. D. and Kreidenweis, S. M.: A single parameter representation of hygroscopic growth and cloud condensation nucleus activity, *Atmos. Chem. Phys.*, 7, 1961–1971, doi:10.5194/acp-7-1961-2007, 2007.
- Pierce, J. R., Riipinen, I., Kulmala, M., Ehn, M., Petäjä, T., Junninen, H., Worsnop, D. R., and Donahue, N. M.: Quantification of the volatility of secondary organic compounds in ultrafine particles during nucleation events, *Atmos. Chem. Phys.*, 11, 9019–9036, doi:10.5194/acp-11-9019-2011, 2011.
- Platnick, S., Hubanks, P., Meyer, K., and King, M. D.: MODIS Atmosphere L3 Daily Product, Goddard Space Flight Center, USA, [https://doi.org/dx.doi.org/10.5067/MODIS/MOD08\\_D3.006](https://doi.org/dx.doi.org/10.5067/MODIS/MOD08_D3.006), 2015.

Pye, H. O. T. and Seinfeld, J. H.: A global perspective on aerosol from low-volatility organic compounds, *Atmos. Chem. Phys.*, 10(9), 4377–4401, doi:10.5194/acp-10-4377-2010, 2010.

Raes, F., Liao, H., Chen, W. T., and Seinfeld, J. H.: Atmospheric chemistry-climate feedbacks, *J. Geophys. Res.-Atmos.*, 115, D12121, doi:10.1029/2009jd013300, 2010.

Rastak, N., Pajunoja, A., Navarro, J. C. A., Ma, J., Song, M., Partridge, D. G., Kirkevåg, A., Leong, Y., Hu, W. W., Taylor, N. F., Lambe, A., Cerully, K., Bougiatioti, A., Liu, P., Krejci, R., Petaja, T., Percival, C., Davidovits, P., Worsnop, D. R., Ekman, A. M. L., Nenes, A., Martin, S., Jimenez, J. L., Collins, D. R., Topping, D. O., Bertram, A. K., Zuend, A., Virtanen, A., and Riipinen, I.: Microphysical explanation of the RH-dependent water affinity of biogenic organic aerosol and its importance for climate, *Geophys. Res. Lett.*, 44, 5167–5177, doi:10.1002/2017gl073056, 2017.

Reutter, P., Su, H., Trentmann, J., Simmel, M., Rose, D., Gunthe, S. S., Wernli, H., Andreae, M. O., and Pöschl, U.: Aerosol- and updraft-limited regimes of cloud droplet formation: influence of particle number, size and hygroscopicity on the activation of cloud condensation nuclei (CCN), *Atmos. Chem. Phys.*, 9, 7067–7080, <https://doi.org/10.5194/acp-9-7067-2009>, 2009.

Riccobono, F., Schobesberger, S., Scott, C. E., Dommen, J., Ortega, I. K., Rondo, L., Almeida, J., Amorim, A., Bianchi, F., Breitenlechner, M., David, A., Downard, A., Dunne, E. M., Duplissy, J., Ehrhart, S., Flagan, R. C., Franchin, A., Hansel, A., Junninen, H., Kajos, M., Keskinen, H., Kupc, A., Kürten, A., Kvashin, A. N., Laaksonen, A., Lehtipalo, K., Makhmutov, V., Mathot, S., Nieminen, T., Onnela, A., Petäjä, T., Praplan, A. P., Santos, F. D., Schallhart, S., Seinfeld, J. H., Sipilä, M., Spracklen, D. V., Stozhkov, Y., Stratmann, F., Tomé, A., Tsagkogeorgas, G., Vaattovaara, P., Viisanen, Y., Vrtala, A., Wagner, P. E., Weingartner, E., Wex, H., Wimmer, D., Carslaw, K. S., Curtius, J., Donahue, N. M., Kirkby, J., Kulmala, M., Worsnop, D. R., and Baltensperger, U.: Oxidation products of biogenic emissions contribute to nucleation of atmospheric particles, *Science*, 344, 717–721, 2014.

Riipinen, I., Pierce, J. R., Yli-Juuti, T., Nieminen, T., Häkkinen, S., Ehn, M., Junninen, H., Lehtipalo, K., Petäjä, T., Slowik, J., Chang, R., Shantz, N. C., Abbatt, J., Leaitch, W. R., Kerminen, V.-M., Worsnop, D. R., Pandis, S. N., Donahue, N. M., and Kulmala, M.: Organic condensation: a vital link connecting aerosol formation to cloud condensation nuclei (CCN) concentrations, *Atmos. Chem. Phys.*, 11, 3865–3878, doi:10.5194/acp-11-3865-2011, 2011.

Rinne, J., Bäck, J., and Hakola, H.: Biogenic volatile organic compound emissions from Eurasian taiga: current knowledge and future directions, *Boreal Env. Res.*, 14, 807–826, 2009.

Robinson, A. L., Donahue, N. M., Shrivastava, M. K., Weitkamp, E. a, Sage, A. M., Grieshop, A. P., Lane, T. E., Pierce, J. R. and Pandis, S. N.: Rethinking organic aerosols: semivolatile emissions and photochemical aging., *Science*, 315(5816), 1259–1262, doi:10.1126/science.1133061, 2007.

Samet, J. M., Dominici, F., Curriero, F. C., Coursac, I., and Zeger, S. L.: Fine particulate air pollution and mortality in 20 US cities, 1987–1994, *New England J. Medicine*, 343, 1742–1749, 2000.

Sanderson, M. G., Jones, C. D., Collins, W. J., Johnson, C. E., and Derwent, R. G.: Effect of climate change on isoprene emissions and surface ozone levels, *Geophys. Res. Lett.*, 30(4), 1936, doi:10.1029/2003GL017642, 2003.

Sandu, A. and Sander, R.: Technical note: Simulating chemical systems in Fortran90 and Matlab with the Kinetic PreProcessor KPP-2.1, *Atmos. Chem. Phys.*, 6, 187–195, doi:10.5194/acp-6-187-2006, 2006.

Schmidt, G. A., Kelley, M., Nazarenko, L., Ruedy, R., Russell, G. L., Aleinov, I., Bauer, M., Bauer, S. E., Bhat, M. K., Bleck, R., Canuto, V., Chen, Y., Cheng, Y., Clune, T. L., Del Genio, A., de Fainchtein, R., Faluvegi, G., Hansen, J. E., Healy, R. J., Kiang, N. Y., Koch, D., Lacis, A. A., LeGrande, A. N., Lerner, J., Lo, K. K., Matthews, E. E., Menon, S., Miller, R. L., Oinas, V., Oloso, A. O., Perlwitz, J. P., Puma, M. J., Putman, W. M., Rind, D., Romanou, A., Sato, M., Shindell, D. T., Sun, S., Syed, R. A., Tausnev, N., Tsigaridis, K., Unger, N., Voulgarakis, A., Yao, M.-S., and Zhang, J.: Configuration and assessment of the GISS ModelE2 contributions to the CMIP5 archive, *J. Adv. Model. Earth Syst.*, 6, 141–184, doi:10.1002/2013MS000265, 2014.

Schwarz, J. P., Gao, R. S., Spackman, J. R., Watts, L. A., Thomson, D. S., Fahey, D. W., Ryerson, T. B., Peischl, J., Holloway, J. S., Trainer, M., Frost, G. J., Baynard, T., Lack, D. A., de Gouw, J. A., Warneke, C., and Del Negro, L. A.: Measurement of the mixing state, mass, and optical size of individual black carbon particles in urban and biomass burning emissions, *Geophys. Res. Lett.*, 35, L13810, doi:10.1029/2008GL033968, 2008.

Scott, C. E., Spracklen, D. V., Pierce, J. R., Riipinen, I., D'Andrea, S. D., Rap, A., Carslaw, K. S., Forster, P. M., Artaxo, P., Kulmala, M., Rizzo, L. V., Swietlicki, E., Mann, G. W., and Pringle, K. J.: Impact of gas-to-particle partitioning approaches on the simulated radiative effects of biogenic secondary organic aerosol, *Atmos. Chem. Phys.*, 15, 12989–13001, doi:10.5194/acp-15-12989-2015, 2015.

Seinfeld, J. H. and Pandis, S. N.: *Atmospheric Chemistry and Physics: From Air Pollution to Climate Change*, third edition, John Wiley & Sons Inc., Hoboken, New Jersey, 2016.

Shindell, D. T., Grenfell, J. L., Rind, D., Grewe, V. and Price, C.: Chemistry-climate interactions in the Goddard Institute for Space Studies general circulation model: 1. Tropospheric chemistry model description and evaluation, *J. Geophys. Res.*, 106(D8), 8047, doi:10.1029/2000JD900704, 2001.

Shindell, D. T., Faluvegi, G., and Bell, N.: Preindustrial-to-presentday radiative forcing by tropospheric ozone from improved simulations with the GISS chemistry-climate GCM, *Atmos. Chem. Phys.*, 3, 1675–1702, doi:10.5194/acp-3-1675-2003, 2003.

Shindell, D. T., Faluvegi, G., Bauer, S. E., Koch, D. M., Unger, N., Menon, S., Miller, R. L., Schmidt, G. A., and Streets, D. G.: Climate response to projected changes in shortlived species under an A1B scenario from 2000–2050 in the GISS climate model, *J. Geophys. Res.*, 112, D20103, doi:10.1029/2007JD008753, 2007.

Shindell, D. T., Lamarque, J.-F., Schulz, M., Flanner, M., Jiao, C., Chin, M., Young, P. J., Lee, Y. H., Rotstayn, L., Mahowald, N., Milly, G., Faluvegi, G., Balkanski, Y., Collins, W. J., Conley, A. J., Dalsøren, S., Easter, R., Ghan, S., Horowitz, L., Liu, X., Myhre, G., Nagashima, T., Naik, V., Rumbold, S. T., Skeie, R., Sudo, K., Szopa, S., Takemura, T., Voulgarakis, A., Yoon, J.-H., and Lo, F.: Radiative forcing in the ACCMIP historical and future climate simulations, *Atmos. Chem. Phys.*, 13, 2939–2974, doi:10.5194/acp-13-2939-2013, 2013.

Shipway, B. J. and Abel, S. J.: Analytical estimation of cloud droplet nucleation based on an underlying aerosol population, *Atmos. Res.*, 96, 344–355, 2010.

Shrivastava, M. K., Lane, T. E., Donahue, N. M., Pandis, S. N., and Robinson, A. L.: Effects of gas particle partitioning and aging of primary emissions on urban and regional organic aerosol concentrations, *J. Geophys. Res.-Atmos.*, 113, D18301, doi:10.1029/2007JD009735, 2008.

Shrivastava, M., Cappa, C., Fan, J., Goldstein, A., Guenther, A., Jimenez, J., Kuang, C., Laskin, A., Martin, S., Ng, N., Petaja, T., Pierce, J., Rasch, P., Roldin, P., Seinfeld, J., Shilling, J., Smith, J., Thornton, J., Volkamer, R., Wang, J., Worsnop, D., Zaveri, R., Zelenyuk, A., and Zhang, Q.: Recent advances in understanding secondary organic aerosol: Implications for global climate forcing, *Rev. Geophys.*, 55, 509–559, <https://doi.org/10.1002/2016RG000540>, 2017.

Simpson, E., Connolly, P., and McFiggans, G.: An investigation into the performance of four cloud droplet activation parameterisations, *Geosci. Model Dev.*, 7, 1535–1542, <https://doi.org/10.5194/gmd-7-1535-2014>, 2014.

Spracklen, D. V., Pringle, K. J., Carslaw, K. S., Chipperfield, M. P., and Mann, G. W.: A global off-line model of size- resolved aerosol microphysics: I. Model development and prediction of aerosol properties, *Atmos. Chem. Phys.*, 5, 2227–2252, doi:10.5194/acp-5-2227-2005, 2005a.

Spracklen, D. V., Jimenez, J. L., Carslaw, K. S., Worsnop, D. R., Evans, M. J., Mann, G. W., Zhang, Q., Canagaratna, M. R., Allan, J., Coe, H., McFiggans, G., Rap, a. and Forster, P.: Aerosol mass spectrometer constraint on the global secondary organic aerosol budget, *Atmos. Chem. Phys.*, 11(23), 12109–12136, doi:10.5194/acp-11-12109-2011, 2011.

Stieb, D. M., Judek, S., and Burnett, R. T.: Meta-analysis of timeseries studies of air pollution and mortality: Effects of gases and particles and their influence of cause of death, age and season, *J. Air & Manage. Assoc.*, 52, 470–484, 2002.

Stier, P., Feichter, J., Kinne, S., Kloster, S., Vignati, E., Wilson, J., Ganzeveld, L., Tegen, I., Werner, M., Balkanski, Y., Schulz, M., Boucher, O., Minikin, A., and Petzold, A.: The aerosol-climate model ECHAM5-HAM, *Atmos. Chem. Phys.*, 5, 1125–1156, doi:10.5194/acp-5-1125-2005, 2005.

Storelvmo, T., Kristjánsson, J. E., Ghan, S. J., Kirkevåg, A., Seland, Ø., and Iversen, T.: Predicting cloud droplet number concentration in Community Atmosphere Model (CAM)-Oslo, *J. Geophys. Res.*, 111, doi:10.1029/2005JD006300, d24208, 2006.

Strode, S. A., Liu, J., Lait, L., Commane, R., Daube, B., Wofsy, S., Conaty, A., Newman, P., and Prather, M.: Forecasting carbon monoxide on a global scale for the ATom-1 aircraft mission: insights from airborne and satellite observations and modeling, *Atmos. Chem. Phys.*, 18, 10955–10971, <https://doi.org/10.5194/acp-18-10955-2018>, 2018.

Topping, D., Connolly, P., and McFiggans, G.: Cloud droplet number enhanced by co-condensation of organic vapours, *Nature Geosci.*, 6, 443–446, 2013.

Tröstl, J., Chuang, W., Gordon, H., Heinritzi, M., Yan, C., Molteni, U., Ahlm, L., Frege, C., Bianchi, F. and Wagner, R.: The role of low-volatility organic compounds in initial particle growth in the atmosphere, *Nature*, 533(7604), 527–531, doi:10.1038/nature18271, 2016.

Tsigradis, K., Koch, D., and Menon, S.: Uncertainties and importance of sea spray composition on aerosol direct and indirect effects, *J. Geophys. Res.-Atmos.*, 118, 220–235, doi:10.1029/2012jd018165, 2013.

Tsigradis, K., Daskalakis, N., Kanakidou, M., Adams, P. J., Artaxo, P., Bahadur, R., Balkanski, Y., Bauer, S. E., Bellouin, N., Benedetti, A., Bergman, T., Berntsen, T. K., Beukes, J. P., Bian, H., Carslaw, K. S., Chin, M., Curci, G., Diehl, T., Easter, R. C., Ghan, S. J., Gong, S. L., Hodzic, A., Hoyle, C. R., Iversen, T., Jathar, S., Jimenez, J. L., Kaiser, J. W., Kirkevåg, A., Koch, D., Kokkola, H., H Lee, Y., Lin, G., Liu, X., Luo, G., Ma, X., Mann, G. W., Mihalopoulos, N., Morcrette, J. J., Müller, J. F., Myhre, G., Myriokefalitakis, S., Ng, N. L., O'donnell, D., Penner, J. E., Pozzoli, L., Pringle, K. J., Russell, L. M., Schulz, M., Sciare, J., Seland, Shindell, D. T., Sillman, S., Skeie, R. B., Spracklen, D., Stavrakou, T., Steenrod, S. D., Takemura, T., Tiitta, P., Tilmes, S., Tost, H., Van Noije, T., Van Zyl, P. G., Von Salzen, K., Yu, F., Wang, Z., Wang, Z., Zaveri, R. A., Zhang, H., Zhang, K., Zhang, Q. and Zhang, X.: The AeroCom evaluation and intercomparison of organic aerosol in global models, *Atmos. Chem. Phys.*, 14(19), 10845–10895, doi:10.5194/acp-14-10845-2014, 2014.

Tsigradis, K., and Kanakidou, M.: The present and future of secondary organic aerosol direct forcing on climate. *Curr. Clim. Change Rep.*, 4, no. 2, 84–98, doi:10.1007/s40641-018-0092-3, 2018.

Tsimpidi, A. P., Karydis, V. A., Zavala, M., Lei, W., Molina, L., Ulbrich, I. M., Jimenez, J. L. and Pandis, S. N.: Evaluation of the volatility basis-set approach for the simulation of organic aerosol formation in the Mexico City metropolitan area, *Atmos. Chem. Phys.*, 10(2), 525–546, doi:10.5194/acp-10-525-2010, 2010.

Tsimpidi, A. P., Karydis, V. A., Zavala, M., Lei, W., Bei, N., Molina, L. and Pandis, S. N.: Sources and production of organic aerosol in Mexico City: Insights from the combination of a chemical transport model (PMCAMx-2008) and measurements during MILAGRO, *Atmos. Chem. Phys.*, 11(11), 5153–5168, doi:10.5194/acp-11-5153-2011, 2011.

Tsimpidi, a. P., Karydis, V. a., Pozzer, a., Pandis, S. N. and Lelieveld, J.: ORACLE (v1.0): module to simulate the organic aerosol composition and evolution in the atmosphere, *Geosci. Model Dev.*, 7(6), 3153–3172, doi:10.5194/gmd-7-3153-2014, 2014.

Tsimpidi, A. P., Karydis, V. A., Pozzer, A., Pandis, S. N., and Lelieveld, J.: ORACLE 2-D (v2.0): an efficient module to compute the volatility and oxygen content of organic aerosol with a global chemistry–climate model, *Geosci. Model Dev.*, 11, 3369–3389, <https://doi.org/10.5194/gmd-11-3369-2018>, 2018.

Turpin, B. J. and Lim, H. J.: Species contributing to PM<sub>2.5</sub> mass concentrations: revisiting common assumptions for estimating organic mass, *Aerosol Sci. Technol.*, 35, 602–610, 2001.

Twomey, S. A.: Pollution and the Planetary albedo, *Atmos. Environ.*, 8, 1251–1256, 1974.

van Marle, M. J. E., Kloster, S., Magi, B. I., Marlon, J. R., Daniau, A.-L., Field, R. D., Arneth, A., Forrest, M., Hantson, S., Kehrwald, N. M., Knorr, W., Lasslop, G., Li, F., Mangeon, S., Yue, C., Kaiser, J. W., and van der Werf, G. R.: Historic global biomass burning emissions for CMIP6 (BB4CMIP) based on merging satellite observations with proxies and fire models (1750–2015), *Geosci. Model Dev.*, 10, 3329–3357, <https://doi.org/10.5194/gmd-10-3329-2017>, 2017.

Volkamer, R., Jimenez, J. L., San Martini, F., Dzepina, K., Zhang, Q., Salcedo, D., Molina, L. T., Worsnop, D. R., and Molina, M. J.: Secondary organic aerosol formation from anthropogenic air pollution: Rapid and higher than expected, *Geophys. Res. Lett.*, 33, L17811, doi:10.1029/2006GL026899, 2006.

Wichmann, H. E. and Peters, A.: Epidemiological Evidence for the effects of ultrafine particle exposure, *Phi. T. Roy. A*, 358, 2751–2769, 2000.

Williamson, C., Kupc, A., Wilson, J., Gesler, D. W., Reeves, J. M., Erdesz, F., McLaughlin, R., and Brock, C. A.: Fast time response measurements of particle size distributions in the 3–60 nm size range with the nucleation mode aerosol size spectrometer, *Atmos. Meas. Tech.*, 11, 3491–3509, <https://doi.org/10.5194/amt-11-3491-2018>, 2018.

Wilson, J., Cuvelier, C., and Raes, F.: A modeling study of global mixed aerosol fields, *J. Geophys. Res.*, 106, 34081–34108, 2001.

Winker, D. M., Vaughan, M. A., Omar, A. H., Hu, Y., Powell, K. A., Liu, Z., Hunt, W. H., and Young, S. A.: Overview of the CALIPSO Mission and CALIOP Data Processing Algorithms, *J. Atmos. Oceanic Technol.*, 26, 2310–2323, 2009.

Yu, F.: A secondary organic aerosol formation model considering successive oxidation aging and kinetic condensation of organic compounds: Global scale implications, *Atmos. Chem. Phys.*, 11(3), 1083–1099, doi:10.5194/acp-11-1083-2011, 2011.

Yu, F. and Luo, G.: Simulation of particle size distribution with a global aerosol model: contribution of nucleation to aerosol and CCN number concentrations, *Atmos. Chem. Phys.*, 9,



---

7691–7710, doi:10.5194/acp-9-7691-2009, 2009. <sup>[L]</sup><sub>SEP</sub>

Zhang, K., O'Donnell, D., Kazil, J., Stier, P., Kinne, S., Lohmann, U., Ferrachat, S., Croft, B., Quaas, J., Wan, H., Rast, S., and Feichter, J.: The global aerosol-climate model ECHAM-HAM, version 2: sensitivity to improvements in process representations, *Atmos. Chem. Phys.*, 12, 8911–8949, doi:10.5194/acp-12-8911-2012, 2012.

Zhang, Q., Jimenez, J. L., Canagaratna, M. R., Allan, J. D., Coe, H., Ulbrich, I., Alfarra, M. R., Takami, a., Middlebrook, a. M., Sun, Y. L., Dzepina, K., Dunlea, E., Docherty, K., DeCarlo, P. F., Salcedo, D., Onasch, T., Jayne, J. T., Miyoshi, T., Shimo, a., Hatakeyama, S., Takegawa, N., Kondo, Y., Schneider, J., Drewnick, F., Borrmann, S., Weimer, S., Demerjian, K., Williams, P., Bower, K., Bahreini, R., Cottrell, L., Griffin, R. J., Rautiainen, J., Sun, J. Y., Zhang, Y. M. and Worsnop, D. R.: Ubiquity and dominance of oxygenated species in organic aerosols in anthropogenically-influenced Northern Hemisphere midlatitudes, *Geophys. Res. Lett.*, 34(13), 1–6, doi:10.1029/2007GL029979, 2007.

Zhang, Q. J., Beekmann, M., Drewnick, F., Freutel, F., Schneider, J., Crippa, M., Prevot, A. S. H., Baltensperger, U., Poulain, L., Wiedensohler, A., Sciare, J., Gros, V., Borbon, A., Colomb, A., Michoud, V., Doussin, J. F., Denier Van Der Gon, H. A. C., Haeffelin, M., Dupont, J. C., Siour, G., Petetin, H., Bessagnet, B., Pandis, S. N., Hodzic, A., Sanchez, O., Honoré, C. and Perrussel, O.: Formation of organic aerosol in the Paris region during the MEGAPOLI summer campaign: Evaluation of the volatility-basis-set approach within the CHIMERE model, *Atmos. Chem. Phys.*, 13(11), 5767–5790, doi:10.5194/acp-13-5767-2013, 2013.